AD-A079 920 MASSACHUSETTS INST OF TECH CAMBRIDGE DEPT OF OCEAN E--ETC F/G 13/5
STUDY OF RESIDUAL STRESSES AND DISTORTION IN STRUCTURAL WELDMEN--ETC(U)
NOV 79 V J PAPAZOGLOU, K MASUBUCHI N00014-75-C-0459

UNCLASSIFIED 82558 NL

1 OF 2
AD A
079920

LEVEL II

AD-A079920

AD-A062777

TECHNICAL PROGRESS REPORT
of

CONTRACT N00014-75-0469
(M.I.T. OSP #82558)

STUDY OF RESIDUAL STRESSES AND DISTORTION IN STRUCTURAL WELDMENTS IN HIGH-STRENGTH STEELS

BY

VASSILIOS J PAPAZOGLOU

KOICHI MASUBUCHI

TO

OFFICE OF NAVAL RESEARCH

NOVEMBER 30, 1979

MASSACHUSETTS INSTITUTE OF TECHNOLOGY
CAMBRIDGE, MASSACHUSETTS

MASSACHUSETTS INSTITUTE OF TECHNOLOGY
DEPARTMENT OF OCEAN ENGINEERING
CAMBRIDGE, MASS. 02139

TECHNICAL PROGRESS REPORT

of

Contract N00014-75-C-0469
(MIT OSP #82558)

STUDY OF RESIDUAL STRESSES AND DISTORTION IN STRUCTURAL WELDMENTS IN HIGH-STRENGTH STEELS

to

Office of Naval Research

November 30, 1979

by

Vassilios J. Papazoglou

Koichi Masubuchi

SECURITY CLASSIFICATION OF THIS PAGE (When Data Entered)

REPORT DOCUMENTATION PAGE		READ INSTRUCTIONS BEFORE COMPLETING FORM
1. REPORT NUMBER Technical Progress Report	2. GOVT ACCESSION NO.	3. RECIPIENT'S CATALOG NUMBER
4. ~~TITLE (and Subtitle)~~ 6 STUDY OF RESIDUAL STRESSES AND DISTORTION IN STRUCTURAL WELDMENTS IN HIGH STRENGTH STEELS.		5. TYPE OF REPORT & PERIOD COVERED Technical Report Dec. 1, 1977- Nov. 30, 1979
		6. PERFORMING ORG. REPORT NUMBER
7. ~~AUTHOR(s)~~ 10 Vassilios J. Papazoglou Koichi Masubuchi		8. ~~CONTRACT OR GRANT NUMBER(s)~~ 15 N00014-75-C-0459 NR 031-773
9. PERFORMING ORGANIZATION NAME AND ADDRESS Department of Ocean Engineering Massachusetts Institute of Technology Cambridge, ~~MA~~ 02139		10. PROGRAM ELEMENT, PROJECT, TASK AREA & WORK UNIT NUMBERS
11. CONTROLLING OFFICE NAME AND ADDRESS Department of the Navy Office of Naval Research Arlington, Virginia 22217	11 30	12. ~~REPORT DATE~~ Novem[redacted]79
		13. ~~NUMBER OF PAGES~~
14. MONITORING AGENCY NAME & ADDRESS (if different from Controlling Office) 12 99		15. SECURITY CLASS. (of this report) UNCLASSIFIED
		15a. DECLASSIFICATION/DOWNGRADING SCHEDULE

16. DISTRIBUTION STATEMENT (of this Report)

This document has been approved for public release and sale; its distribution is unlimited. Reproduction in whole or in part is permitted by the U.S. Government

17. DISTRIBUTION STATEMENT (of the abstract entered in Block 20, if different from Report)

9 Technical progress rept. 1 Dec 77-30 Nov 79,

18. SUPPLEMENTARY NOTES

14 82558

19. ~~KEY WORDS~~ (Continue on reverse side if necessary and identify by block number)

Welding
Residual Stresses
Distortion
High Strength Steels

20. ABSTRACT (Continue on reverse side if necessary and identify by block number)

Experimental results on temperature, strain and distortion during welding HY-130 steel are presented. The geometries include 1-inch thick plates and 0.75-inch cylindrical shells. Welding was performed using the gas metal arc, electron beam and laser processes. The experimental results are compared with predictions made by computer programs. Finally, through thickness distributions of residual stresses obtained using the Rosenthal-Norton sectioning technique are presented.

DD FORM 1 JAN 73 1473 EDITION OF 1 NOV 65 IS OBSOLETE
S/N 0102-014-6601

406 856

SECURITY CLASSIFICATION OF THIS PAGE (When Data Entered)

TABLE OF CONTENTS

PAGE

1. INTRODUCTION AND SUMMARY

The objective of this research program, which started on December 1, 1977, is to analytically and experimentally study residual stresses and distortion in structural weldments in high-strength steel.

The program includes (1) generation of experimental data and (2) development of analytical systems. HY-130 is the primary material to be investigated; a limited number of experiments are, however, to be conducted using low-carbon steel specimens. Experiments are to be made using the multipass gas metal arc welding and electron-beam welding (one pass) process.

More specifically,

Materials: HY-130 steel (with some control specimens in low-carbon steel)

Thickness: 1 inch (with some specimens 1/2" thick)

Welding processes: Electron beam (EB) and multipass gas metal arc (GMA) processes

Specimen geometries: The following types of specimens are considered

a. Butt welds in thick plates
   - (1) Unrestrained butt welds
   - (2) Simple restrained butt welds
   - (3) Restrained welds simulating practical weldments

b. Girth welds of cylindrical shells
   - (4) Girth welding along the groove of a cylindrical shell
   - (5) Girth welding between unstiffened cylindrical shells.

The work to be performed has been divided into two main tasks:

Task 1: Research on butt welds in thick plates

Task 2: Research on girth welds in cylindrical shells

The entire program is expected to be completed in three years. Table 1.1 illustrates the tasks and phases included in this study. The planned progress for each task appears in the original proposal, dated July 1977.

Table 1.2 summarizes test conditions and the number of specimens to be prepared. Since the major effort of the proposed research is to develop analytical systems, experiments will be made on a few specimens to verify the analysis. Table 1.3 illustrates how analyses will be improved during the

three-year program.

Two progress reports, dated October 10, 1978 and August 31, 1979, have already been issued describing the accomplishments made between December 1, 1979 and August 31, 1978, and between September 1, 1978 and August 31, 1979 respectively. This first technical report consolidates the information contained in the two aforementioned reports by covering all the efforts carried out during the first two years of the research program.

For the most part the program has been carried out as it was originally proposed. The few changes made will be dealt with in the appropriate places.

TABLE 1.1 Tasks and Phases of the Program

	Task 1: Thick Plate	Task 2: Cylindrical Shell
First Year	1.1 Develop details of research plan	2.1 Develop details of research plan
	1.2 Experiments on unrestrained butt welds	2.2 Experiment on girth welding along groove of a cylindrical shell
	1.3 Analysis of data obtained in 1.2	2.3 Analysis of data obtained in 2.2
Second Year	1.4 Develop details of research plan	2.4 Develop details of research plan
	1.5 Measurement of residual stresses in specimens made in 1.2	2.5 Measurement of residual stresses in specimens made in 2.2
	1.6 Experiment on simple restrained butt welds	2.6 Experiment on butt welds between unstiffened cylindrical shells
	1.7 Analyses of data obtained in 1.5 and 1.6	2.7 Analyses of data obtained in 2.5 and 2.6
Third Year	1.8 Develop details of research plan	2.8 Develop details of research plan
	1.9 Experiment on restrained cracking test specimens	2.9 - - -
	1.10 Measurement of strain energy release on specimens made in 1.6 and 1.9	2.10 Measurement of residual stresses in specimens made in 2.6
	1.11 Analysis of data obtained in 1.9 and 1.10	2.11 Analysis of data obtained in 2.10
	Preparation of the Final Report	

Information on residual stresses and strain energy release in specimens used for weld cracking and stress-corrosion cracking

Information on residual stresses and distortion of welded cylindrical shells

TABLE 1.2 Experimental Conditions and Number of Specimens

Specimen Geom. / Thickness / Material / Processes / Steps / Year			Thick Plate		Cylindrical Shell	Total
			1" thick		1/2" thick	
Year	Steps	Processes	Low-carbon steel	HY-130	HY-130	
First Year	1.2	EB	$1 + \alpha^{(1)}$	$1 + \alpha^{(1)}$	-	$5(1 + \alpha)$
	2.2	GMA	$1 + \alpha$	$1 + \alpha$	$1 + \alpha^{(1)}$	
Second Year	1.5	EB	Specimens made in 1.2 & 2.2 will be used			
	2.5	GMA				
	1.6	EB	-	2	-	$5 + \alpha$
	2.6	GMA	-	2	$1 + \alpha$	
Third Year	1.9	EB		$1 + \alpha^{(2)}$		$2(1 + \alpha)$
		GMA		$1 + \alpha^{(2)}$		
	1.10 2.10	EB	Specimens made in 1.6 & 2.6 will be used			
		GMA				

NOTE: (1) $(1 + \alpha)$ means that two specimens will be prepared, of which one will be the primarily specimen. If the first test is conducted successfully, only a limited experiment will be made on the second specimen.

(2) 2-inch thick plate may be used.

TABLE 1.3 Planned Improvements of Analyses

Current Status	I.0. Manuals #3, #4, #5	II.0. Muraki's analysis
First Year	<u>Unrestrained Butt Welds</u> I.1. Modify to improve compatibility I.2. Include effects of metallurgical transformation I.3. Include analysis of multipass welding	<u>Groove Weld</u> II.1. Modify to improve compatibility II.2. Develop simple analyses
Second Year	I.4. Analysis of residual stress I.5. Include effects of restraint I.6. Develop analysis of strain energy release	II.3. Analysis of residual stress II.4. Include effects of metallurgical transformation II.5. Include analysis of multipass welding
Third Year	I.7. Develop analysis of practical restrained specimens	(II.6. Possible analysis of effect of stiffeners)
	I.8. Develop final versions of computer programs	II.7. Develop final versions of computer programs

NOTE: This table lists those activities related to improvement of analyses. Efforts which will be spent for analyzing existing data, and possible modification of programs are not included here.

2. PROGRESS OF TASK 1 - THICK PLATES

December 1, 1977 to November 30, 1979

2.1 General Status

According to the original proposal, dated July, 1977, the research during the first two years would include the following, under Task 1:

1.1 Developmemt of details of research plan during the first year

1.2 Experiments on unrestrained butt welds

1.3 Analysis of data obtained in 1.2

1.4 Development of details of research plan for the second year

1.5 Measurement of residual stresses in specimens made in Step 1.2

1.6 Experiments on simple restrained butt welds

1.7 Analysis of data obtained in 1.5 and 1.6

The research program has been carried out as originally proposed with some modifications in Steps 1.3 and 1.5 .

2.2 Development of Details of the Research Plan for the First Year (Step 1.1)

It was decided that experiments would be made to determine changes of temperatures and transient thermal strains during butt welding unrestraint joints. After consulting representatives of the O.N.R. and the Electric Boat Division of General Dynamics Corporation, the experimental details were finalized as follows:

Two plates 24 inches long, 12 inches wide, and 1 inch thick would be joined resulting in a 24 in. x 24 in. configuration (Fig. 2.1). A total of 8 specimens would be prepared as follows:

Low-carbon steel, gas metal arc welding (multipass) 2
HY-130 steel, gas metal arc welding (multipass) 2
Low-carbon steel, electron beam welding (one pass) 2
HY-130 steel, electron beam welding (one-pass) 2

In each of the above four test conditions, one specimen would be used for the primary testing and the other specimen would be used as the back-up.

Measurements would be made of:

(1) Temperature changes using thermocouples

(2) Changes of thermal strains using electric resistance strain gages.

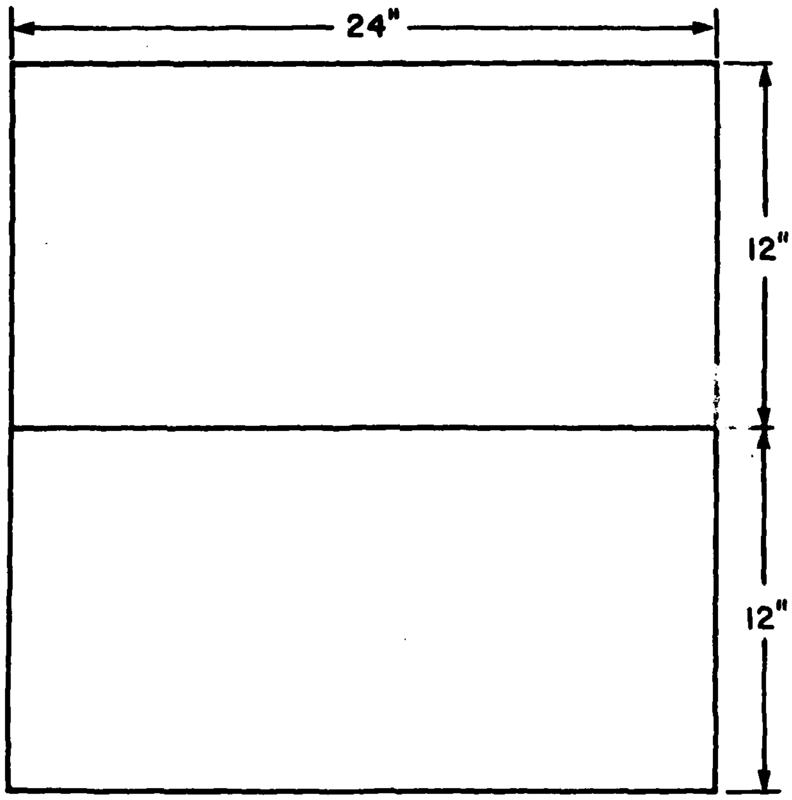

FIGURE 2.1 TEST PLATE ARRANGEMENT
FOR UNRESTRAINED BUTT JOINTS

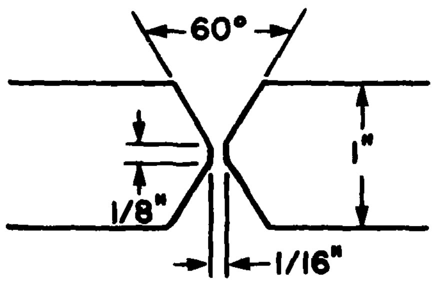

FIGURE 2.2 WELD JOINT CONFIGURATION
FOR THE GMAW EXPERIMENTS

The weld joint configuration would be that of a double vee for the gas metal arc welding (Fig. 2.2) and that of a square butt for the electron beam welding tests.

Low-carbon steel specimens were included as the control. Tests on electron-beam welding were included to generate information on temperature and strain changes during modern, high heat-intensity processes such as EB and laser welding. Tests of multipass welding using the GMA process were included to represent current shipyard practices.

Since M.I.T. has no facility with the ability to weld plates of the size mentioned above using EB welding, it was decided that these tests would be carried out at the facilities of the Applied Energy Co., Stoneham, Mass.

Regarding Step 1.3, it was decided to compare the experimental results obtained in Step 1.2 with predictions made using the M.I.T. one-dimensional computer program for the analysis of thermal stresses and metal movement during welding[1]. This decision was made in order to evaluate the program for the case of multipass and one-pass EB welding of a thick plate, although it was well understood that the one-dimensional assumptions were not valid in the case of the tests.

Finally, it was decided that no comparison should be made with predictions using the existing two-dimensional finite-element program before the proposed modifications were completed. One of the primary reasons for such a decision was the very high cost of a single run using this program and its questionable accuracy.

2.3 Experiments on Unrestrained Butt Welds (Step 1.2)

The following two theses, dealing with Step 1.2 and part of Step 1.3, have been completed:

1. Lipsey, M.D., "Investigation of Welding Thermal Strains in High Strength Quenched and Tempered Steel", Ocean Engineer Thesis, M.I.T., June 1978.

[1] Papazoglou, V.J., "Computer Programs for the One-Dimensional Analysis of Thermal Stresses and Metal Movement During Welding", M.I.T. OSP #82558.

2. Coneybear, G.W., "Analysis of Thermal Stresses and Metal Movement During Welding", S.M. Thesis, M.I.T., May 1978.

Major findings of the experiments conducted under this step are presented below.

2.3.1 GMA Welding Tests

The experimental investigation of the gas metal arc welding specimens was undertaken by Lipsey. Three specimens were used: one was a low-carbon steel with a designation 1020 and the other two were HY-130 steels. Welding on all tests was performed by the semi-automatic GMA method. Table 2.1 summarizes the welding conditions used. Note that six passes were required to fill the upper half of the double-V groove. Pre-heat was applied by oxy-acetylene torches and monitored by the installed thermocouples. Inter-pass temperature was also monitored by the installed thermocouples.

Three kinds of measurement were taken during the welding and cooling stages of the experiments:

(1) Transient thermal strains were measured using adhesive bonded, electric resistance strain gages.

(2) Temperature changes were measured on the surfaces of the specimen plates using adhesive bonded, Chromel/Alumel thermocouples.

(3) Metal movement, and in particular transverse shrinkage, was measured during one of the experiments.

Figures 2.3 and 2.4 show the thermocouple and strain gage locations on the specimens. Finally, it should be noted that the plates to be welded were positioned on knife edge supports, so that the unrestrained simply supported boundary condition could be approximated as close as possible.

Lipsey's thesis contains many figures showing results obtained during the experiments. Figures 2.5, 2.6 and 2.7 show typical results of transient thermal strains (in units of microstrain, which equals 10^{-6} in/in) during pass 4 for the two HY-130 and the 1020 specimens respectively. Each curve represents the longitudinal thermal strain history as measured by the strain gage located at the position shown. The time axis refers to the time elapsed from the start of one pass until the start of the next pass. The time scales for each pass have been adjusted and the data is presented so that the arc passes the point of observation at $t = 40$ sec. This point is marked

TABLE 2.1 Welding Conditions For The GMA Welded Specimens

TEST PLATE	1020	HY-130 SPECIMEN I	HY-130 SPECIMEN II
WELD TYPE	BUTT	BUTT	BUTT
PROCESS	GMA	GMA	GMA
ARC VOLTS	26	25	25
POLARITY	DCRP	DCRP	DCRP
TRAVEL SPEED (tpm)	12	12	12
HEAT INPUT (Kjoules/in)	39	37	37
FILLER WIRE	.0625" A-675	0.045" Linde-140	0.045" Linde-140
SHIELDING GAS	AR, 25% CO_2	AR, 2% O_2	AR, 2% O_2
NUMBER OF PASSES	6	6	6
PREHEAT & INTERPASS TEMP.	150–175°F	150–175°F	150–175°F

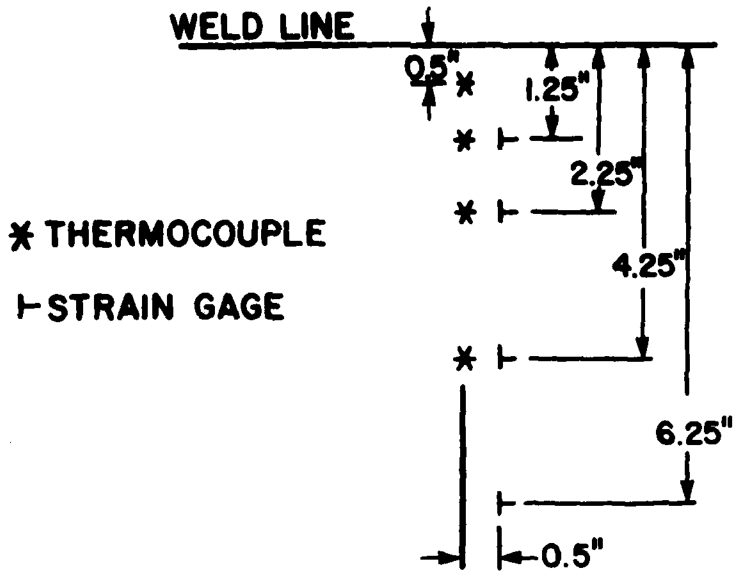

FIGURE 2.3 THERMOCOUPLE AND STRAIN GAGE LOCATION ON HY-130 SPECIMEN I AND 1020 STEEL (GMAW)

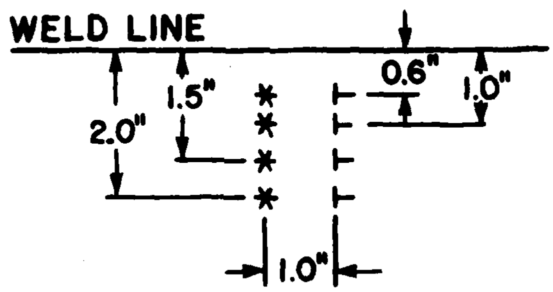

FIGURE 2.4 THERMOCOUPLE AND STRAIN GAGE LOCATION ON HY-130 SPECIMEN II (GMAW)

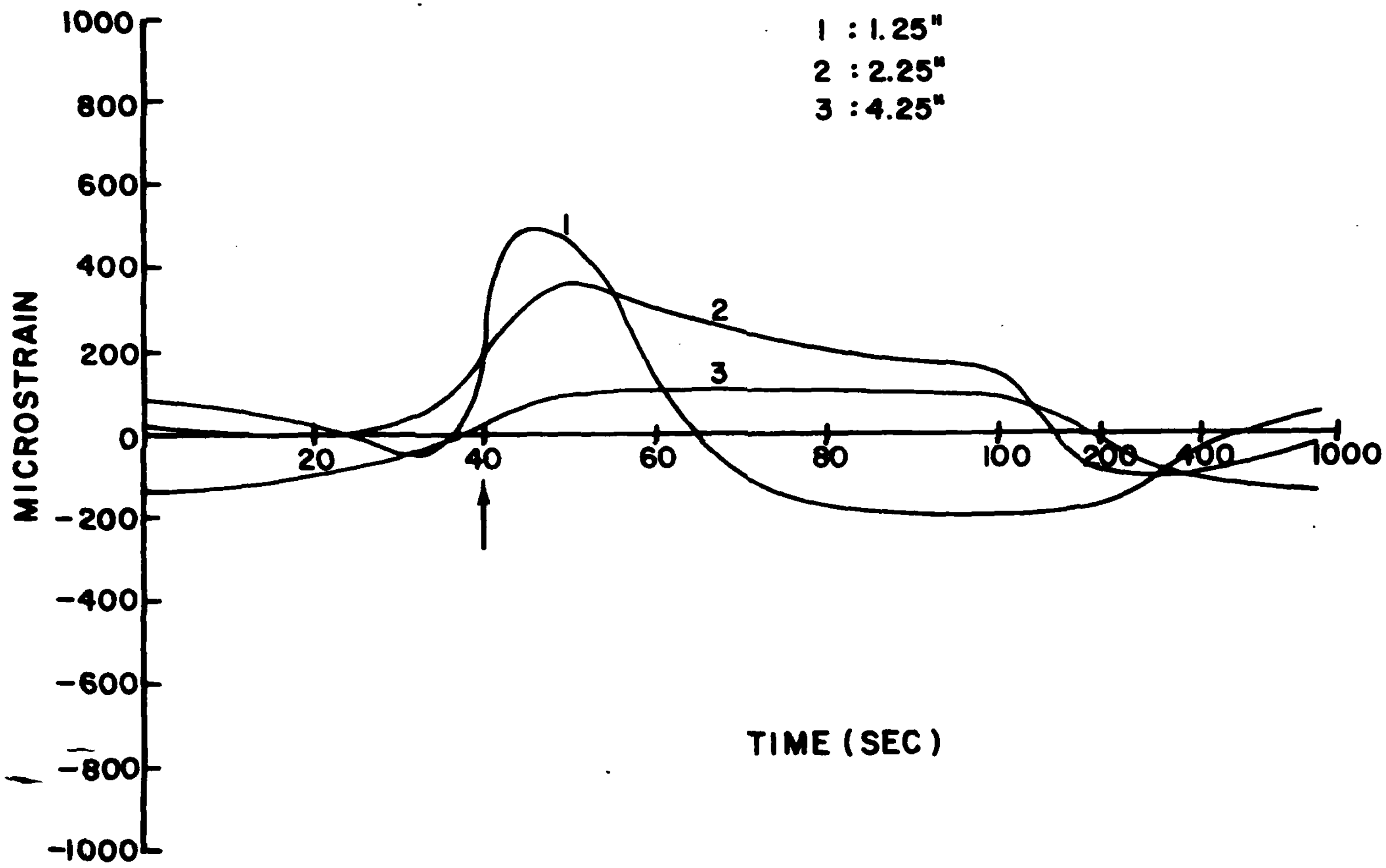

FIGURE 2.5 HY-130 SPECIMEN I, EXPERIMENTAL RESULTS, PASS 4

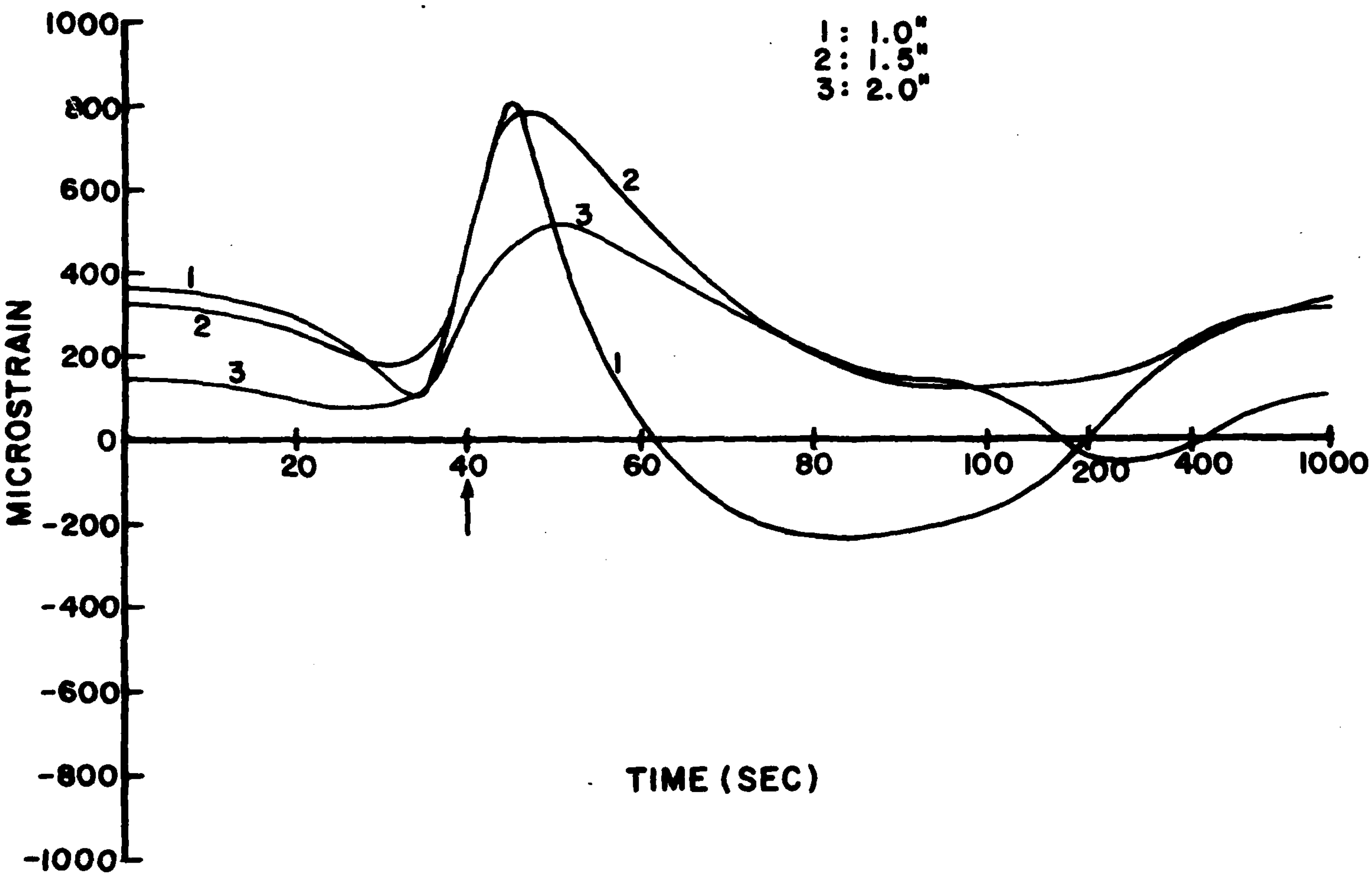

FIGURE 2.6 HY-130 SPECIMEN II, EXPERIMENTAL RESULTS, PASS 4

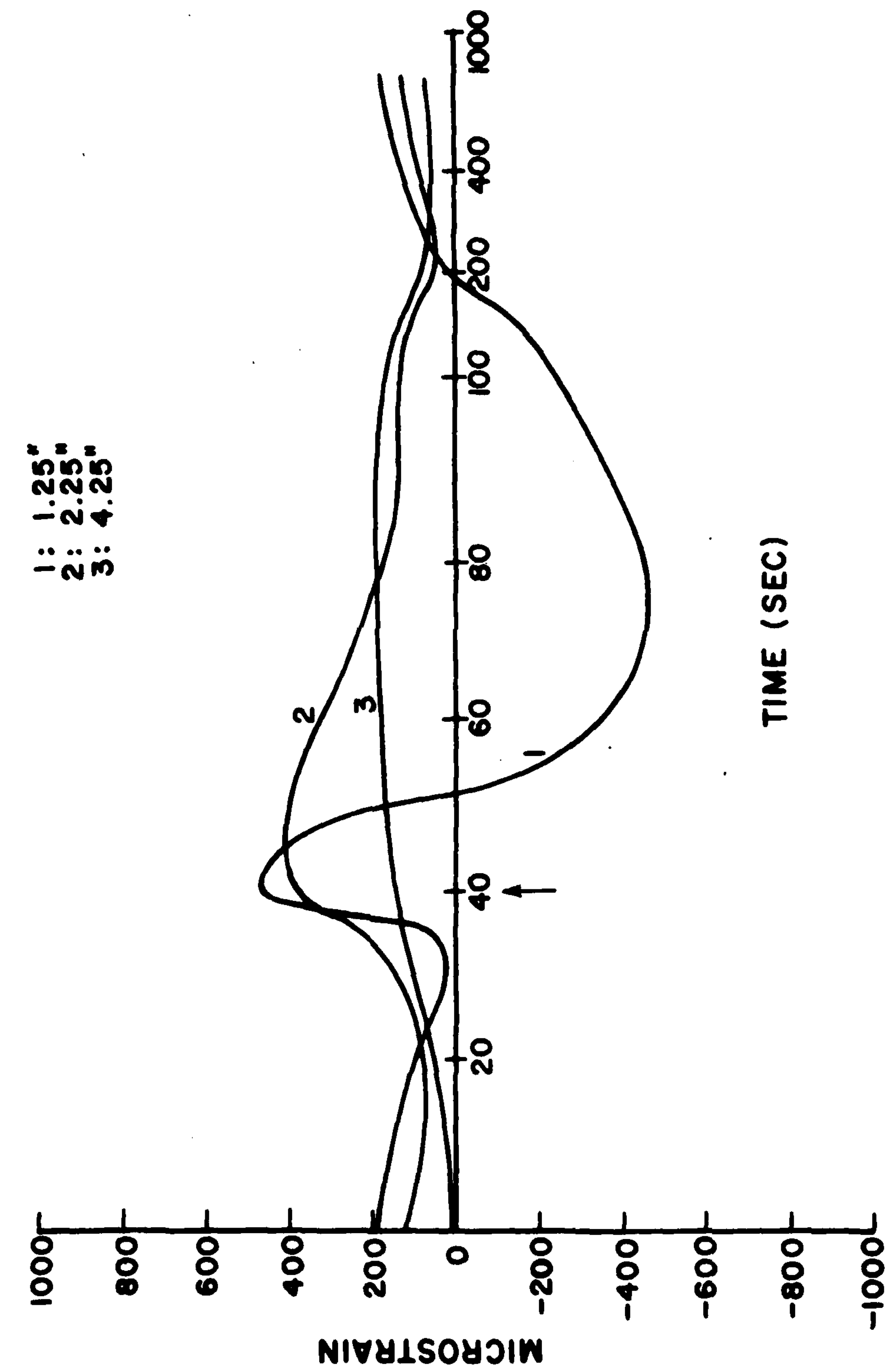

FIGURE 2.7 1020 STEEL, EXPERIMENTAL RESULTS, PASS 4

on each graph. Note also the change in scale at 100 sec to that of a semi-log plot from 100 to 1000 seconds. All three figures show, qualitatively, similar results, something which was expected. Most curves do not start from the origin, indicating that some strain has already been accumulated from the previous passes.

Figure 2.8 shows experimental results for the second HY-130 specimen as measured at a distance 0.6 inches from the weld line. This case is shown separately because of the interesting results recorded. The 0.6 in. location was the closest point of measurement and the first notable observation is that the strains which exist between passes reach very high levels in tension. These strain levels are appoximately four times the interpass strain levels measured at 1.0" from the weld line. The second notable aspect of the curves is the rapidity in which the strain changes from a smoothly decreasing tensile strain to a high tensile peak and its return to a smoothly decreasing tensile strain for passes 2, 3, and 4 (not shown). Following these strain movements, pass 5 shows no tensile peak at all. Strain starts at a high tensile level, reaches a minimum, and comes back to a high tensile strain level.

This behavior resembles that reported by Klein in his study on 3/4" thick HY-130 plate[2]. He reported two tensile peaks at points 1.0" or closer to the weld line. The differences between these results and those of Klein are most likely caused by the fact that his specimens were highly restrained whereas the specimens in this study were unrestrained. Klein attributed this behavior to the possibility that precipitates form in the fusion zone and weld metal upon solidification which will cause high tensile strains in the metal near the weld line. Stoop and Metzbower[3] recently reported that the microstructure in the HAZ of GMA weldments of HY-130 consisted of coarse grained Bainite close to the fusion zone and auto-tempered Martensite plus Ferrite further away from the fusion zone. Outside the HAZ, the base metal remained tempered Martensite.

The above hypotheses are presently tested at M.I.T. through an analytical study using the finite element method and taking into account effects of

2. Klein, K., "Investigation of Welding Thermal Strain in Marine Steels", O.E. Thesis, M.I.T., May 1971.

3. Stoop, J., and Metzbower, E.A., "A Metallurgical Characterization and Assessment of SMA, GMA, EB, and LB Welds of HY-130 Steel", NRL Report 8157, Sept. 1977.

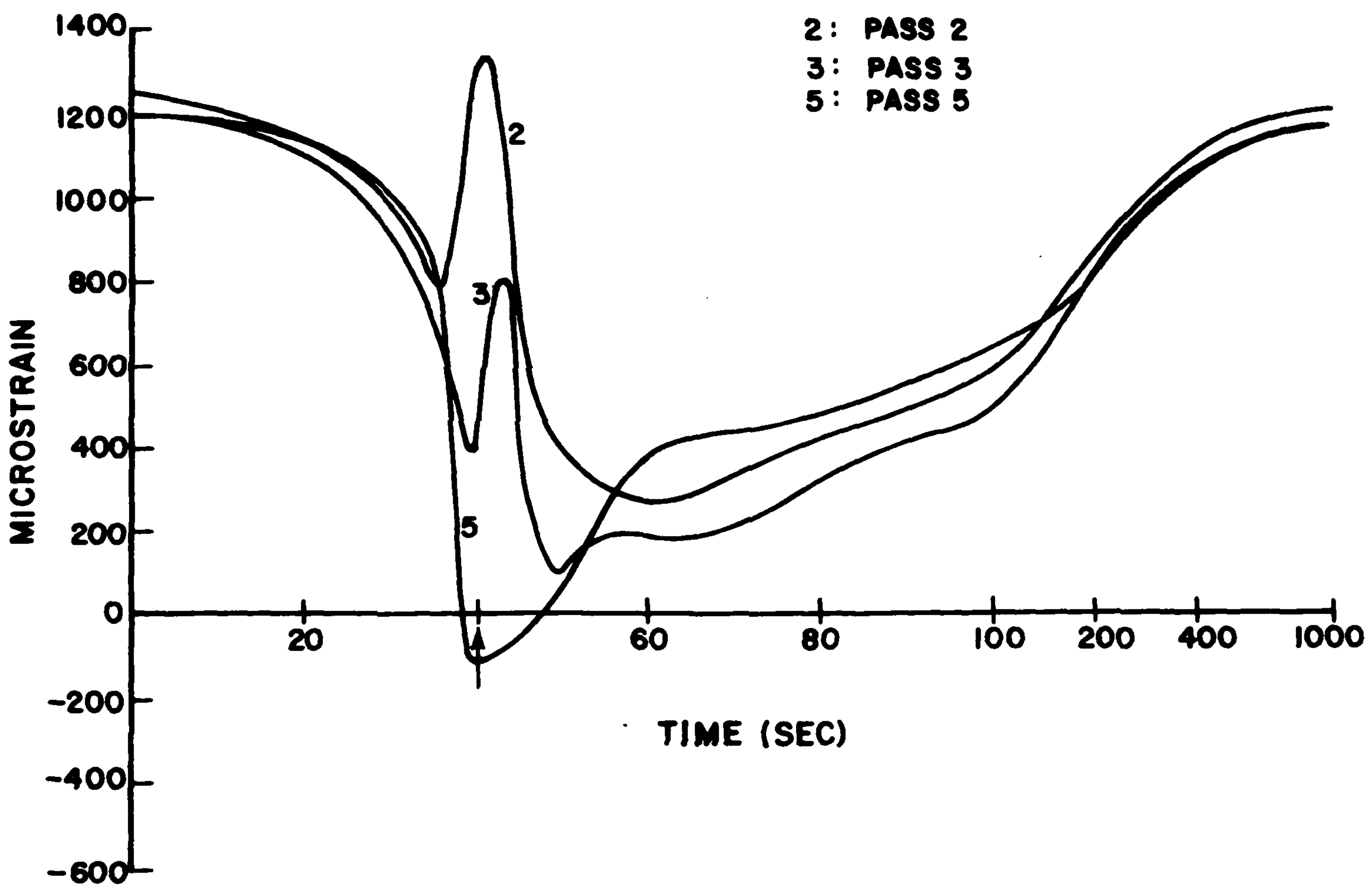

FIGURE 2.8 HY-130 SPECIMEN II, EXPERIMENTAL RESULTS AT 0.6" FROM WELD LINE

phase transformation on strain formation. More on this subject is reported at a later section of this report.

2.3.2 EB Welding Tests

The electron-beam welding tests were carried out by Coneybear, using the facilities of the Applied Energy Company, since no appropriate facilities were available at M.I.T. A Hamilton Zeiss Model SW5 machine capable of providing a maximum power of 7.5 kW at 150 kV and 50 mA was used. The welding was performed in a vacuum chamber 54 in. in diameter and 96 in. long. During the experiment the vacuum obtained measured 2×10^{-4} torr.

A total of four experiments, two with 1020 and two with HY-130 steel plates, were performed during this investigation. Only two of these welds yielded experimental results, however. The first experiment, using 1020 steel plates, was conducted in order to determine the appropriate welding parameters. No measurements were taken during this test, except for the use of heat sensitive paint to get a rough estimate of the temperature distribution. After this test was performed, the following welding conditions for the remaining cases were decided upon:

Voltage = 150 kV

Amperage = 0.045 A

Travel speed = 0.25 in/sec (15 ipm)

The second experiment, using HY-130 plates, was intended to be used for recording temperatures and strains during welding. The test was unsuccessful however, because it was found that the beam deflected away from the joint. Although the operator can aim the beam to some extend by the use of a magnetic field, it was not possible to keep the beam directed at the joint. Upon investigation, it was found that the plates were magnetized. This event prompted the use of wire coils to demagnetize the plates prior to the last two tests.

The last two tests, one using 1020 plates and one using HY-130 plates, were successful. Transient thermal strains and temperature changes were measured during the welding and cooling periods much in the same way as with GMA welded specimens. Figure 2.9 shows the specimen configurations and the locations of the strain gages and thermocouples for both specimens. It should be repeated here that the joint configuration was that of a square butt and that the welding was performed in one pass only.

1020 STEEL PLATE

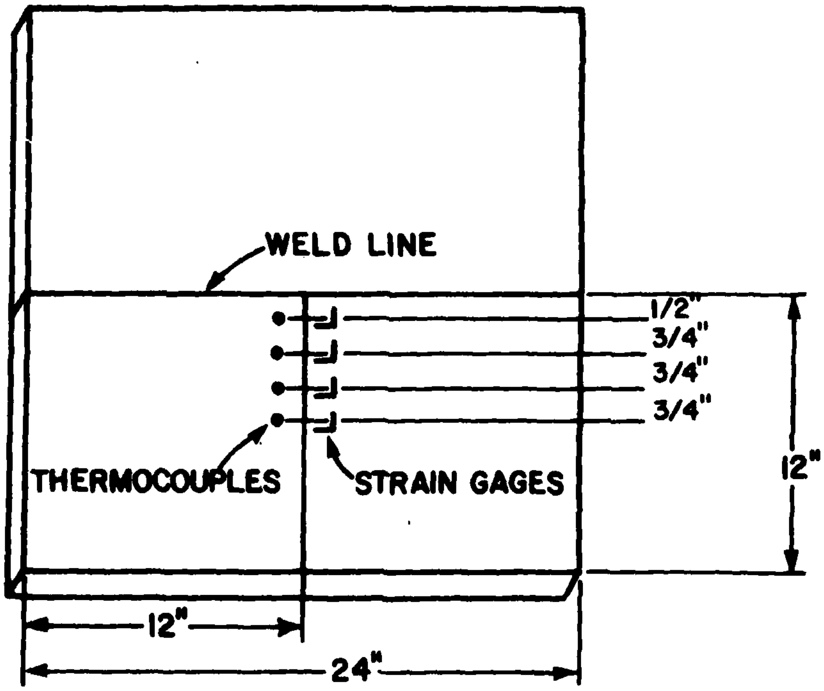

HY-130 STEEL PLATE

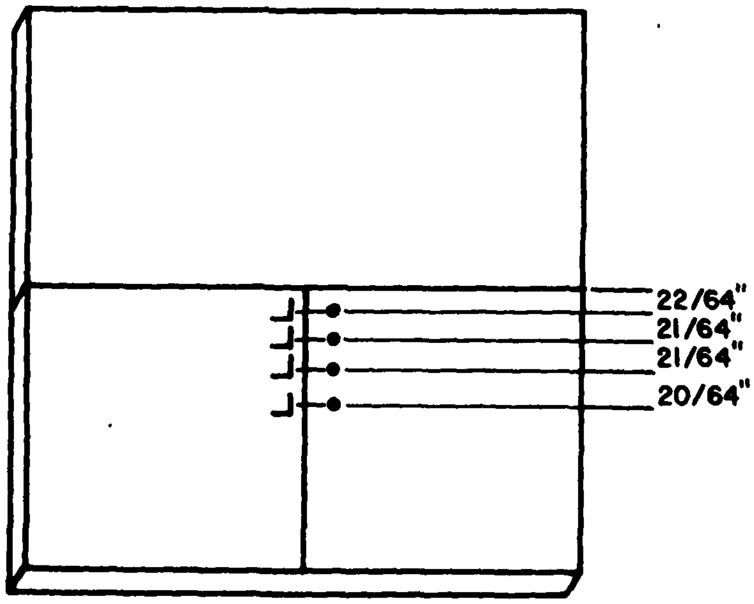

FIGURE 2.9 THERMOCOUPLE AND STRAIN GAGE LOCATIONS ON EB WELDED SPECIMENS

The experimental results obtained are reported in Coneybear's thesis. Some representative results are included here in Figures 2.10 through 2.20 . These figures show measurements of temperature, longitudinal strain, and transverse strain as a function of time for the 1020 steel (at 0.5" and 2.75" from the weld line) and the HY-130 steel (at 0.67" and 1.31" from the weld line) specimens. Shown on the same figures are results obtained using the M.I.T. one-dimensional computer program. Comparisons between the experimental and analytically generated results will be discussed in the next Section.

The following observations can be made. First of all, the results for both tests are qualitatively the same, something which was expected. Second, in some cases, especially close to the weld, the transverse strain can be as high as the longitudinal strains. Finally, the peculiar results found in the longitudinal strain history of the GMA welded HY-130 specimens (see Figure 2.8) were not repeated here (see, for example, Figure 2.17). It is believed that this can be explained by the lower heat input provided by the EB welding process. If the results recorded during the GMAW experiment are due to the cooling rates, then it is safe to assume that the lower heat input of the EB process results in slower cooling rates and hence different solid phase transformations. The latter transformations may be such as to not significantly alter the nature of the transient strain distributions. This hypothesis is currently tested using the finite element method.

2.4 Analysis of Data Obtained in Step 1.2 (Step 1.3)

2.4.1 One-Dimensional Computer Program

Both Lipsey and Coneybear compared the experimental results with predictions made using the M.I.T. one-dimensional computer program for the analysis of thermal strains and metal movement during welding. The program had, though, to be modified by Papazoglou to account for some numerical instabilities which occurred during the first trial runs.

Figures 2.10 through 2.20 show how the results obtained by the computer compare with the experimental ones for the case of the electron-beam welding. Figures 2.21 - 2.24 show typical results for the case of the multipass gas metal arc welding. The results for pass 3 were chosen to be shown as

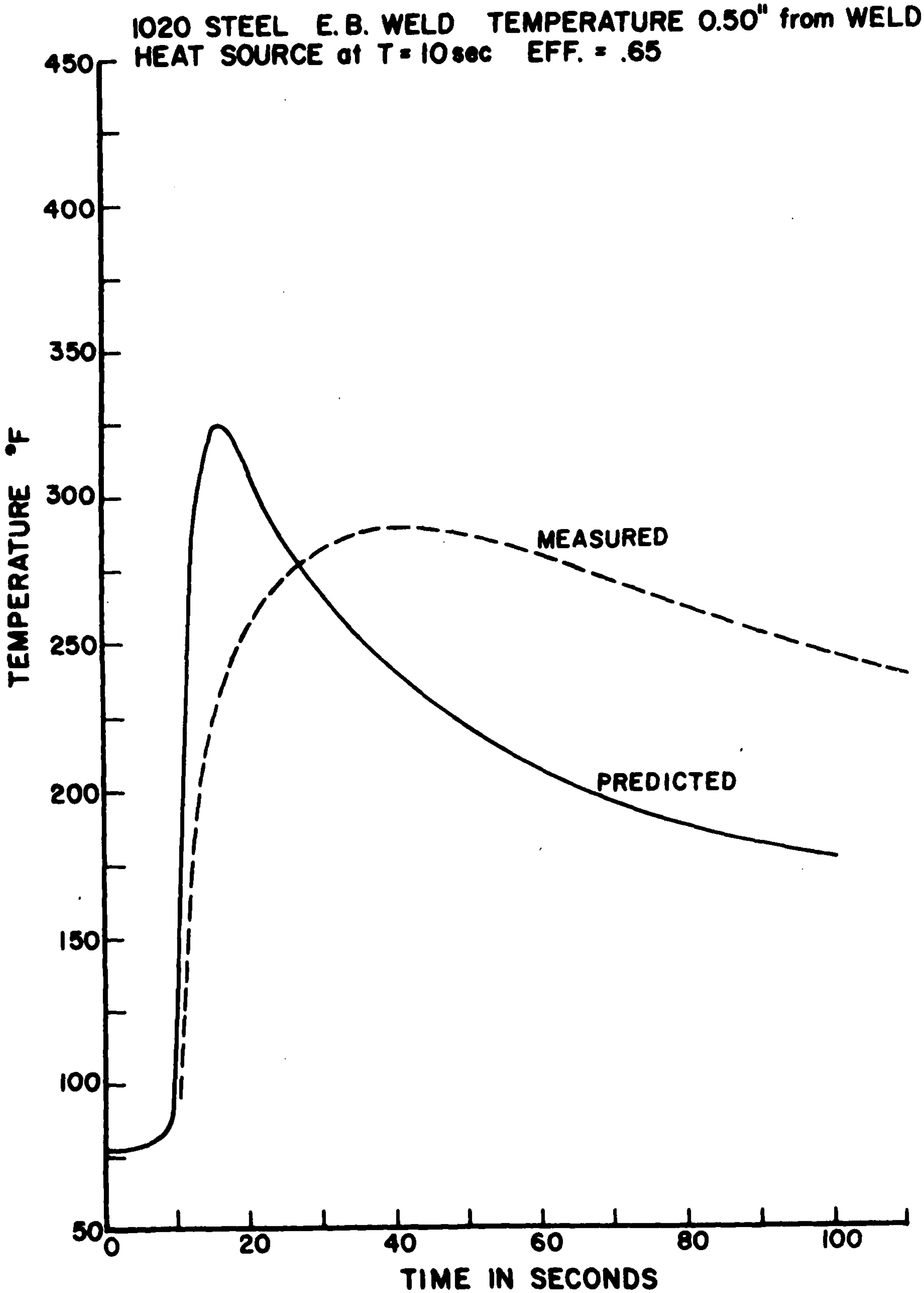

FIGURE 2.10 TEMPERATURE vs. TIME - 1020 SPECIMEN (EB)
0.5" FROM WELD LINE

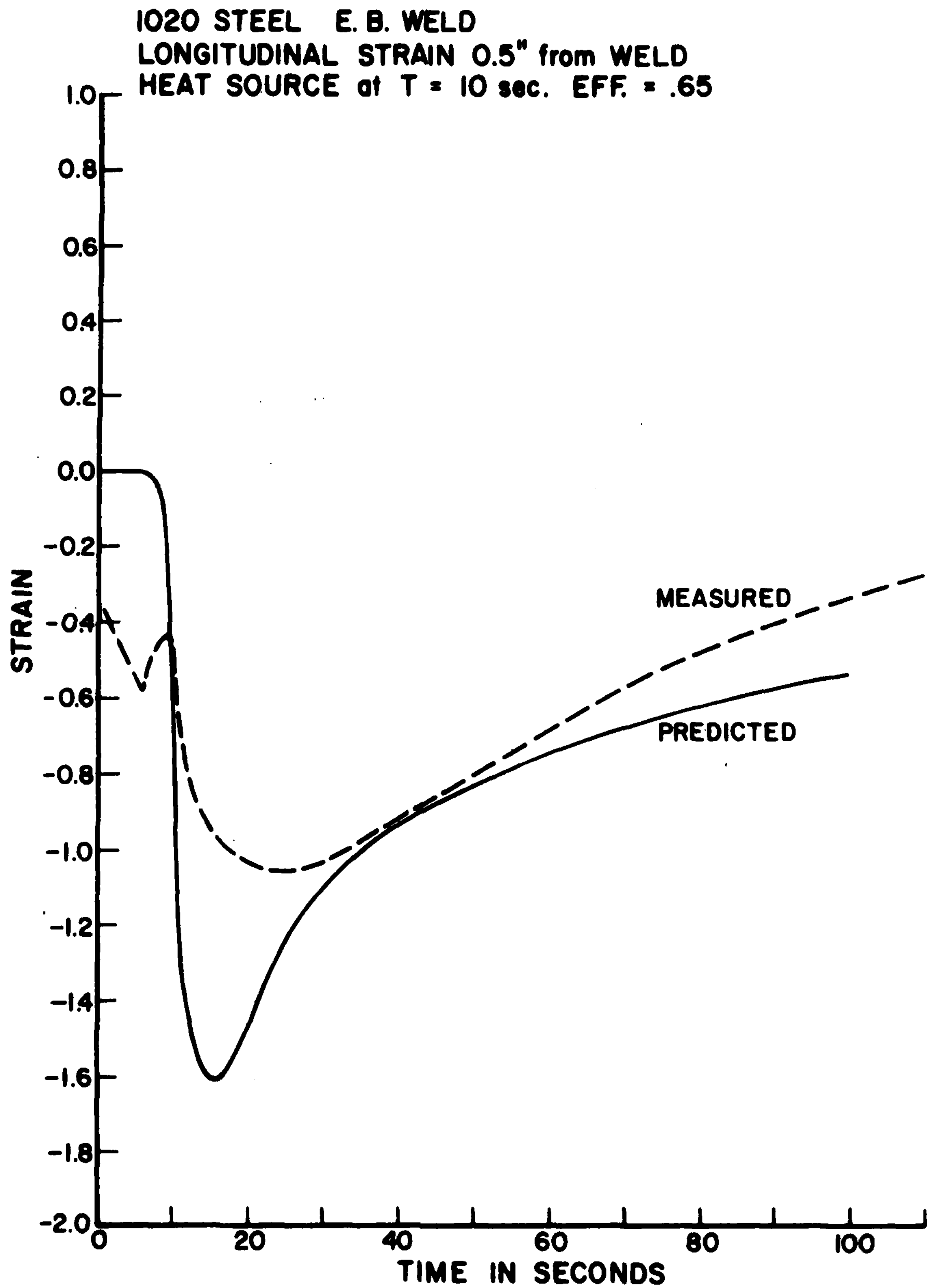

FIGURE 2.11 LONGITUDINAL STRAIN vs. TIME - 1020 SPECIMEN (EB) 0.5" FROM WELD LINE

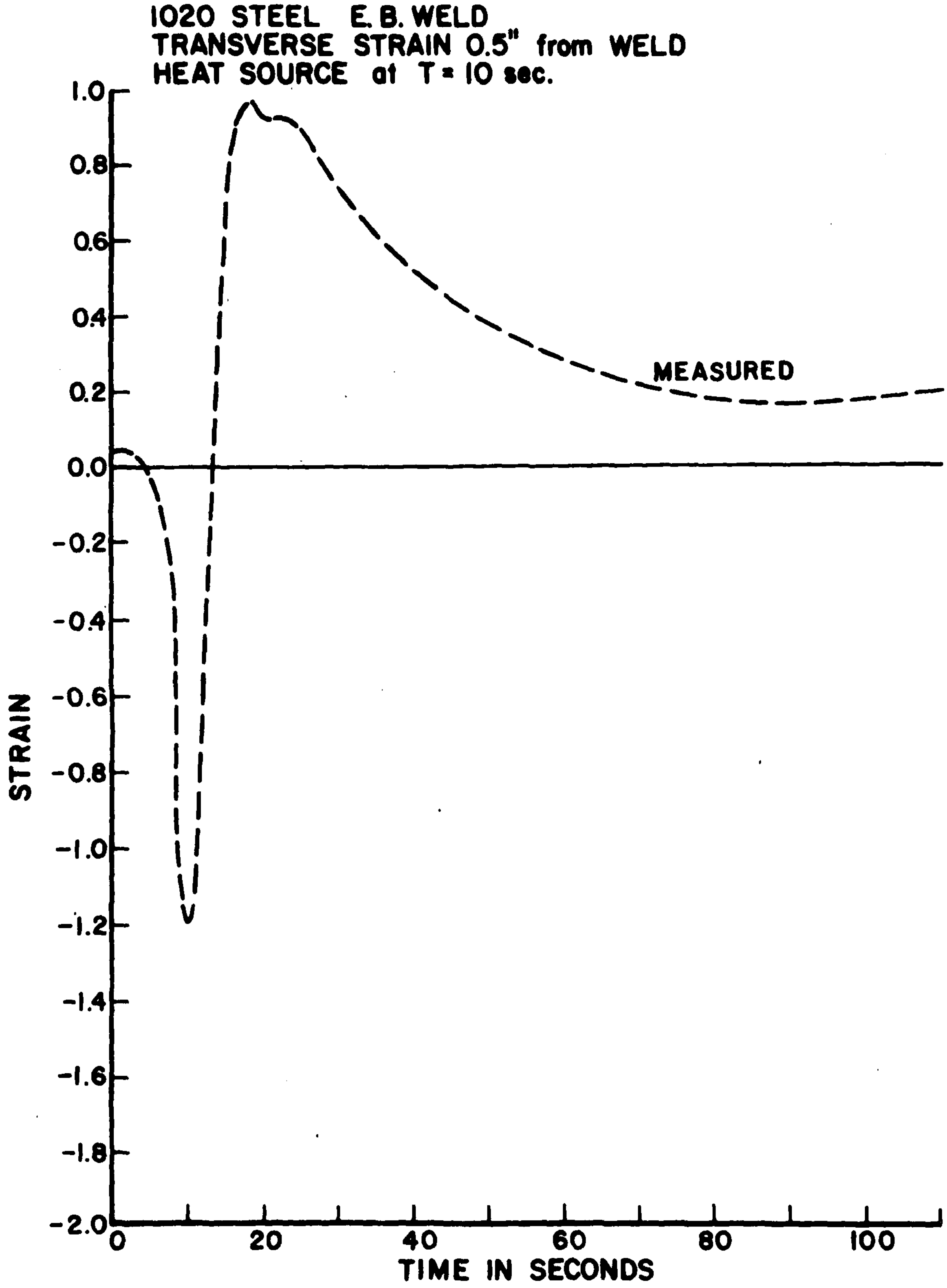

FIGURE 2.12 TRANSVERSE STRAIN vs. TIME - 1020 SPECIMEN (EB) 0.5" FROM WELD LINE

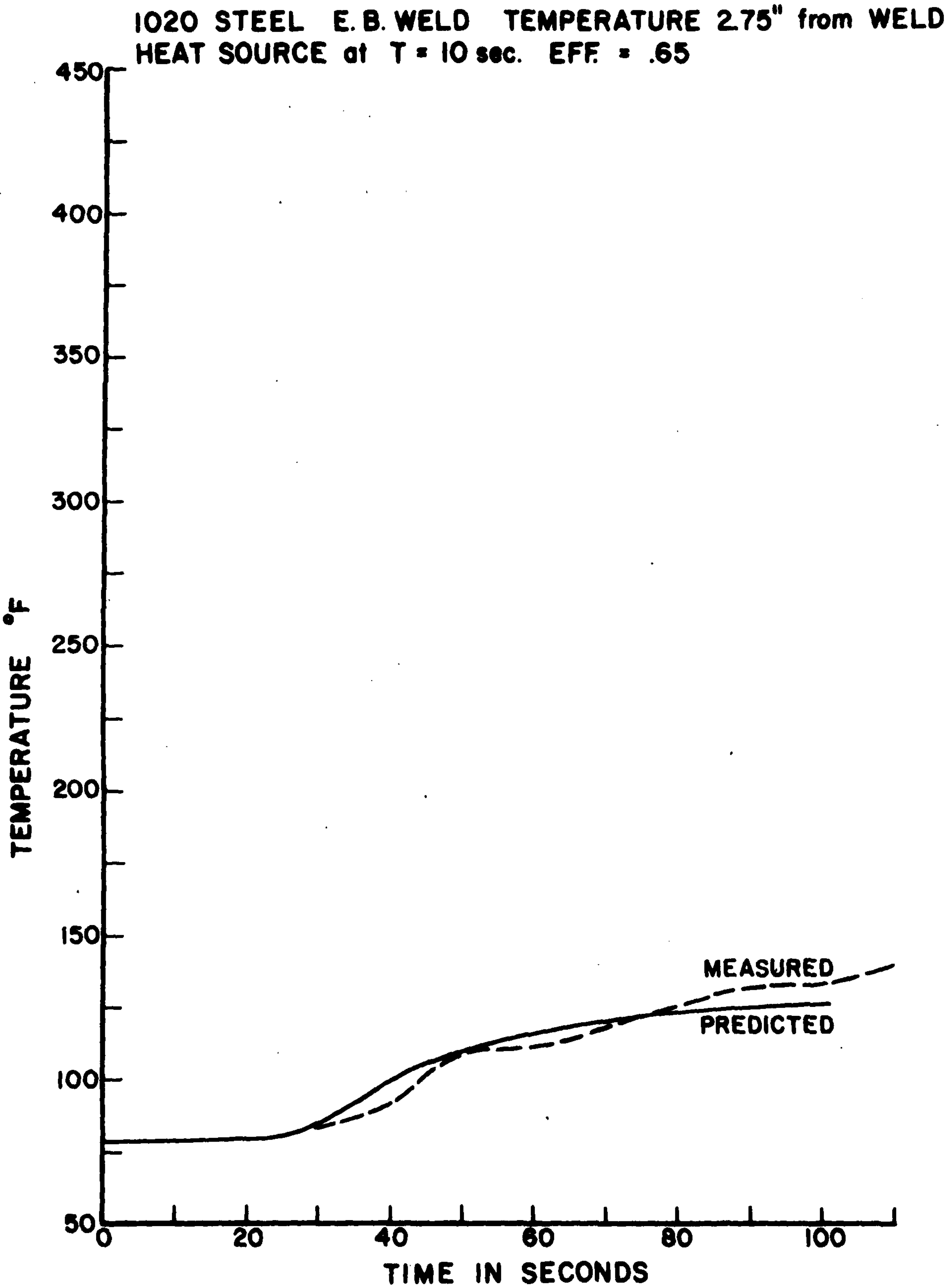

FIGURE 2.13 TEMPERATURE vs. TIME - 1020 SPECIMEN (EB)
2.75" FROM WELD LINE

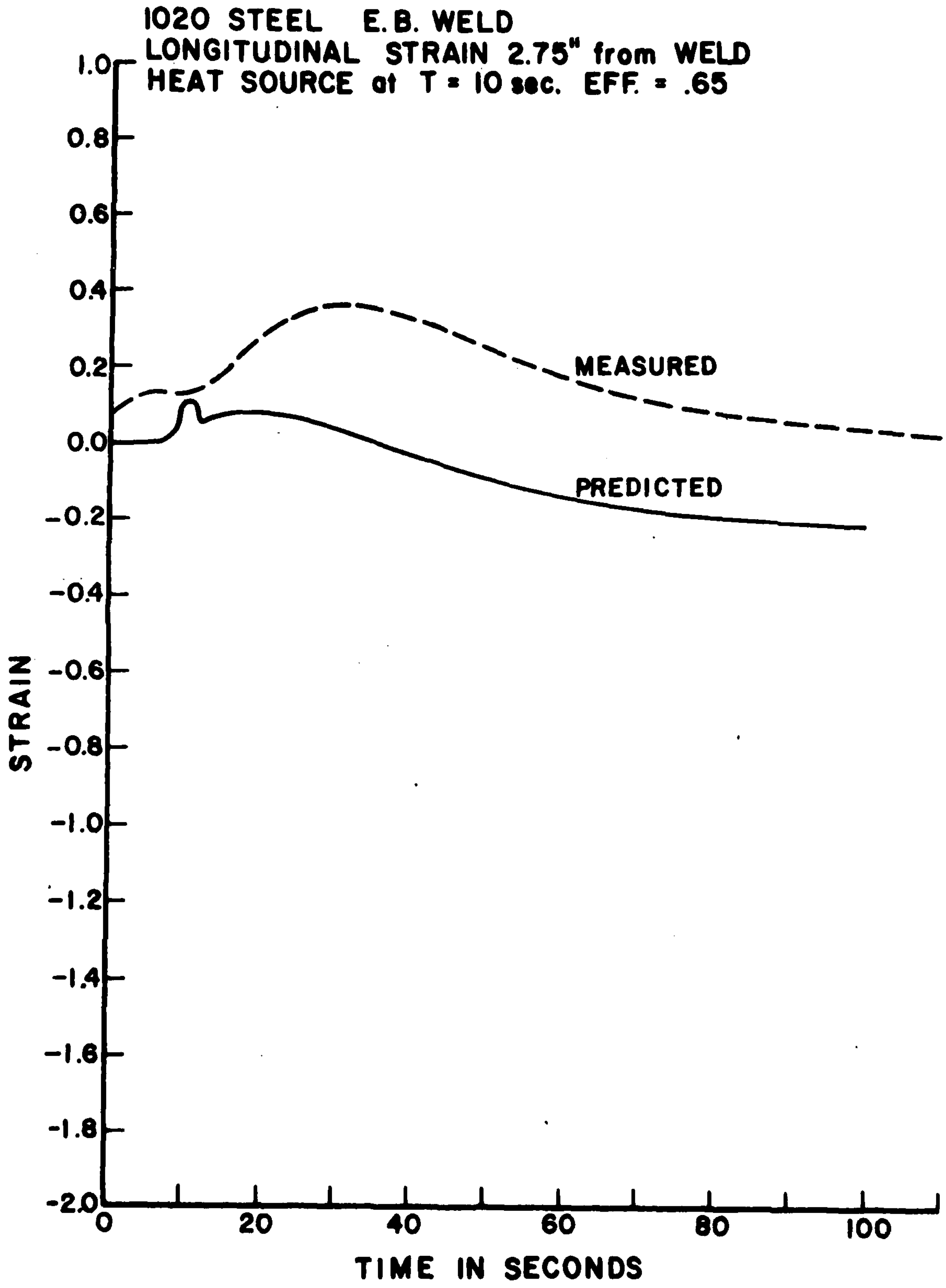

FIGURE 2.14 LONGITUDINAL STRAIN vs. TIME - 1020 SPECIMEN (EB) 2.75" FROM WELD LINE

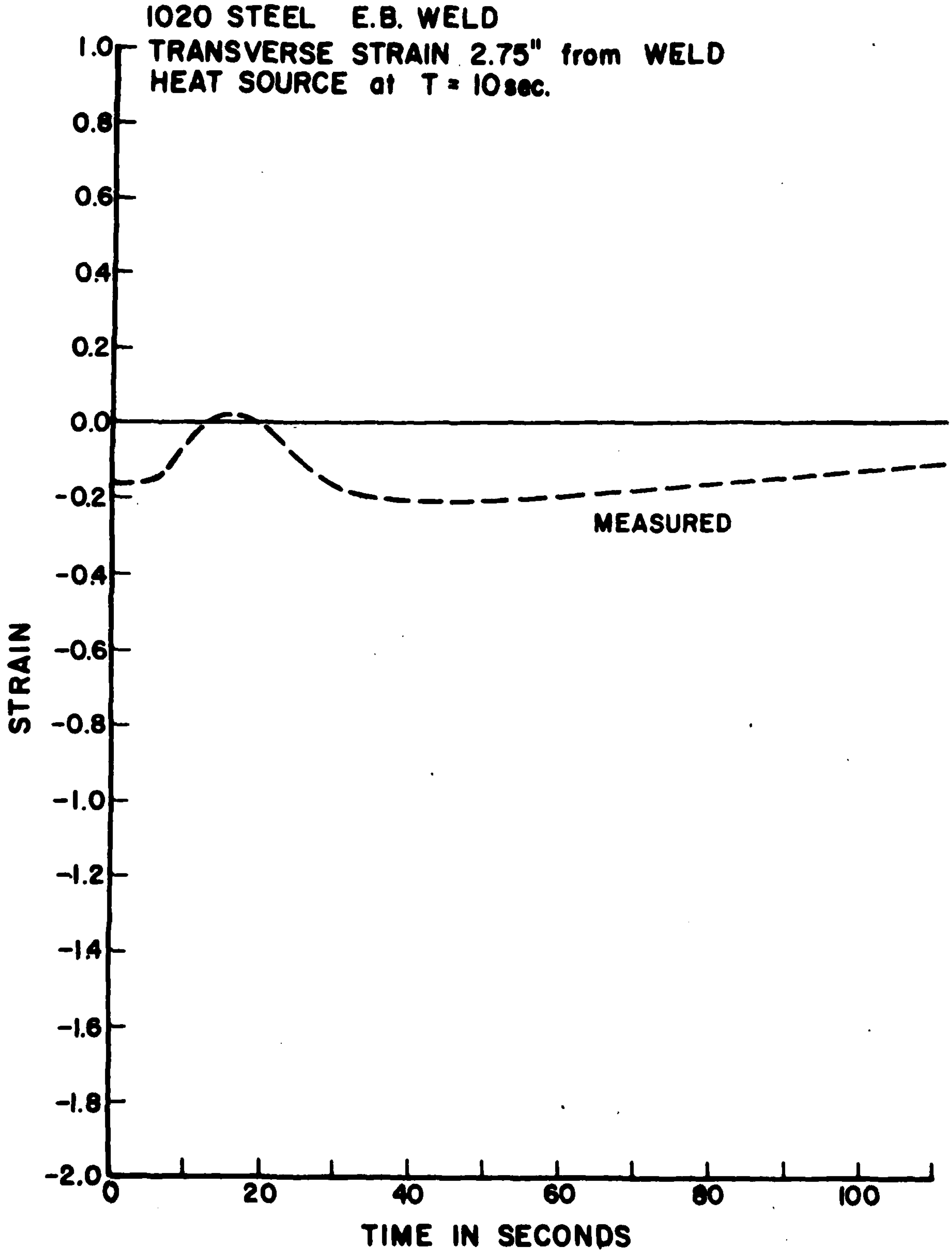

FIGURE 2.15 TRANSVERSE STRAIN vs. TIME - 1020 SPECIMEN (EB)
2.75" FROM WELD LINE

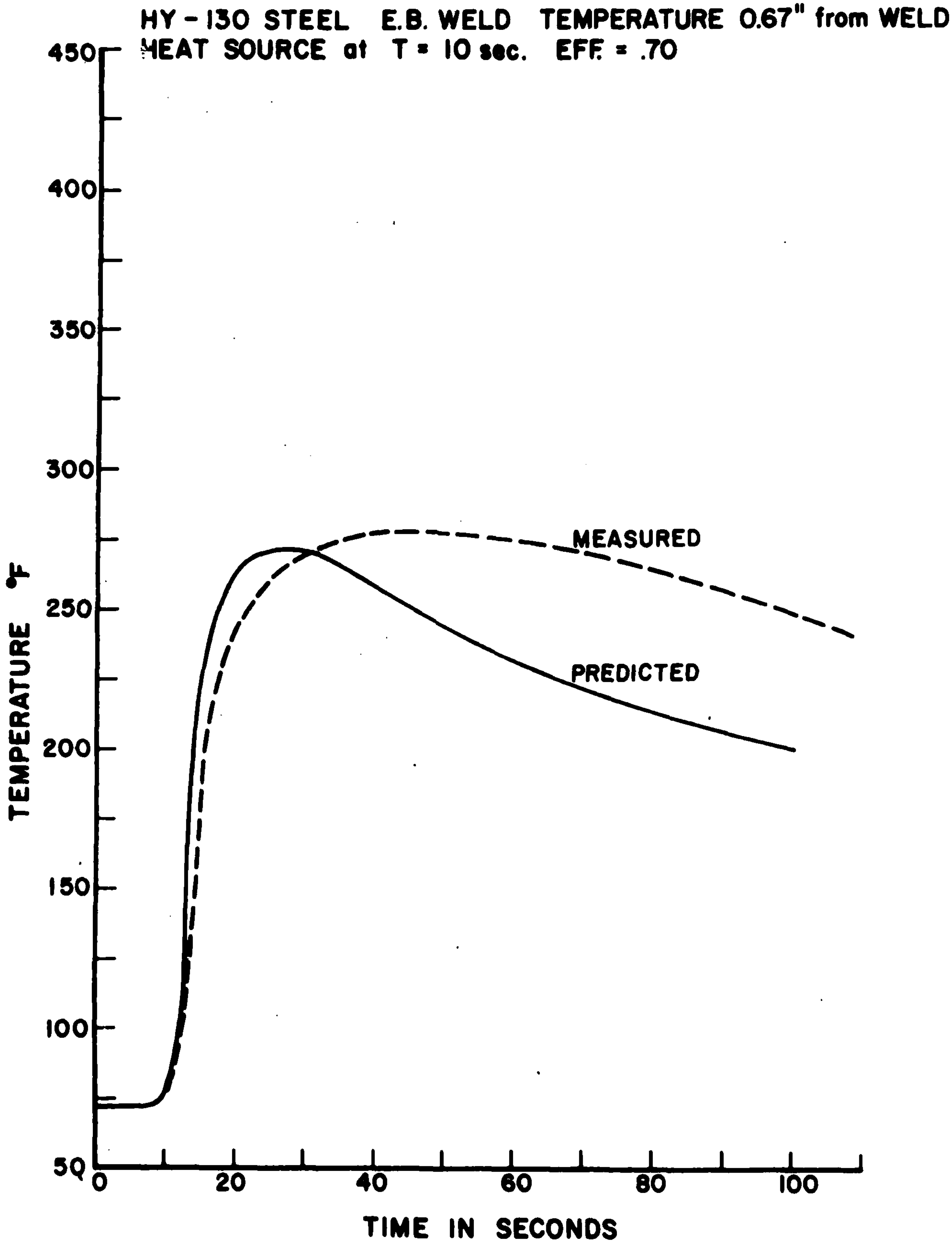

FIGURE 2.16 TEMPERATURE vs. TIME - HY-130 SPECIMEN (EB)
0.67" FROM WELD LINE

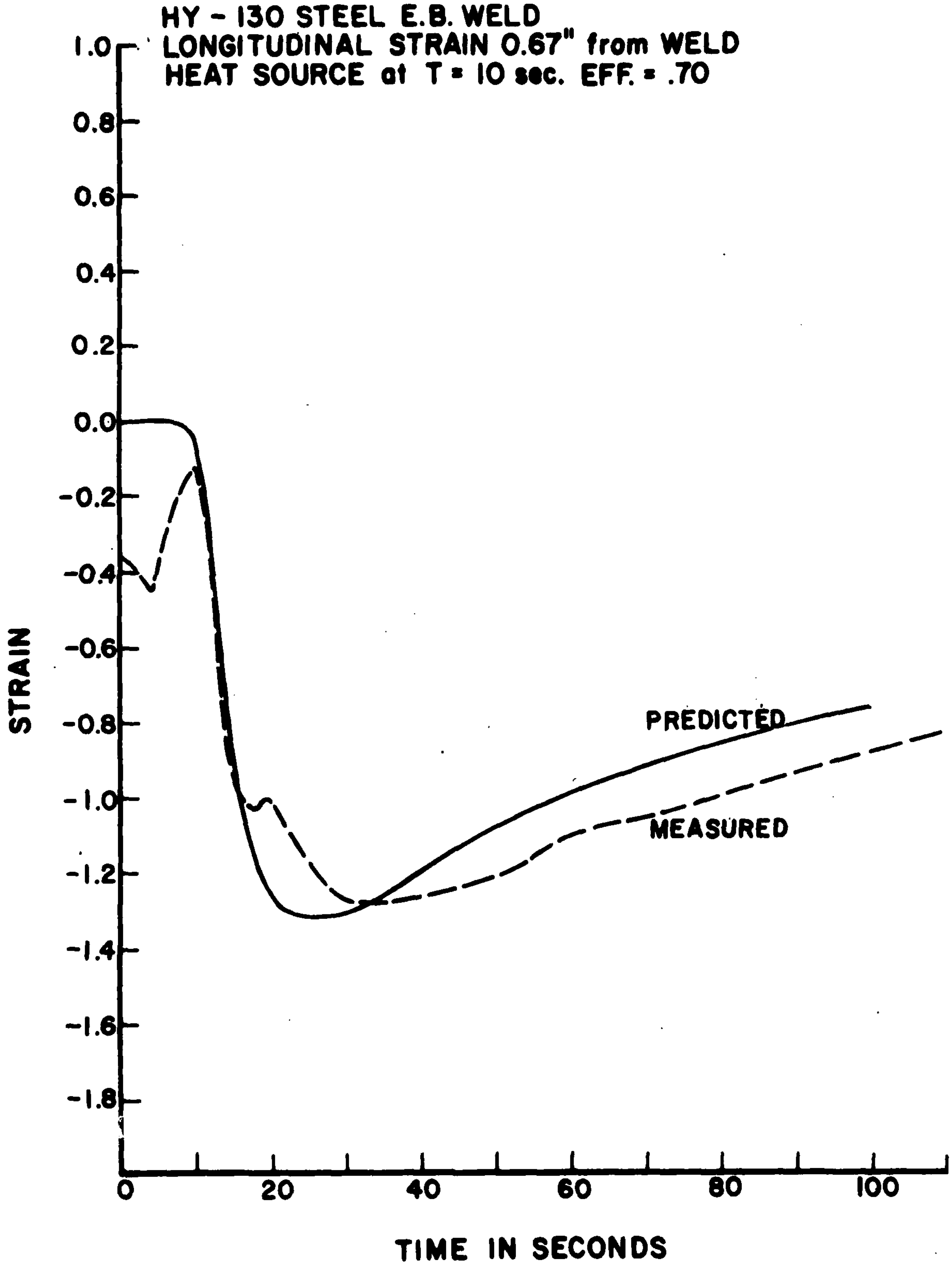

FIGURE 2.17 LONGITUDINAL STRAIN vs. TIME - HY-130 SPECIMEN (EB) 0.67" FROM WELD LINE

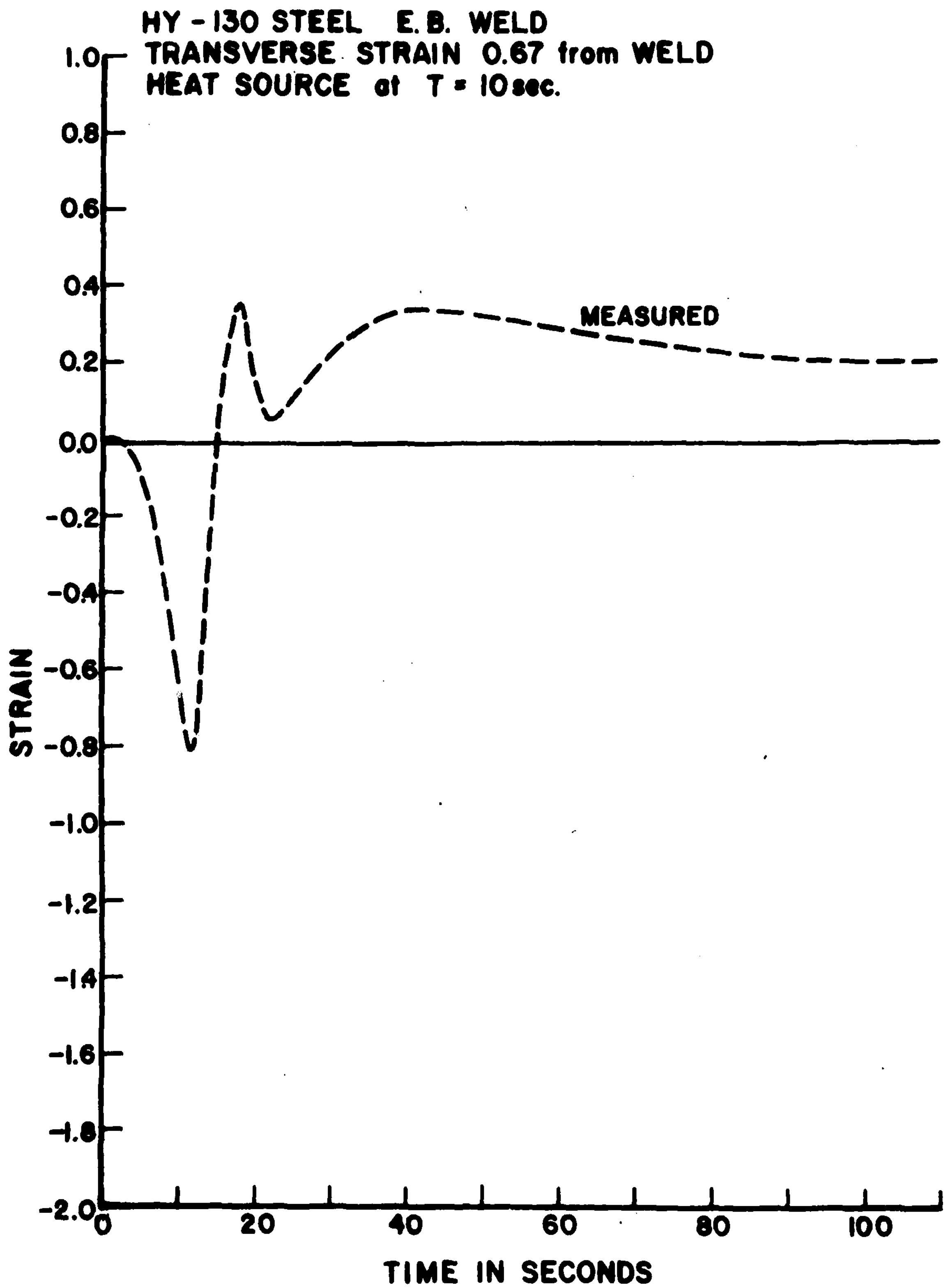

FIGURE 2.18 TRANSVERSE STRAIN vs. TIME - HY-130 SPECIMEN (EB) 0.67" FROM WELD LINE

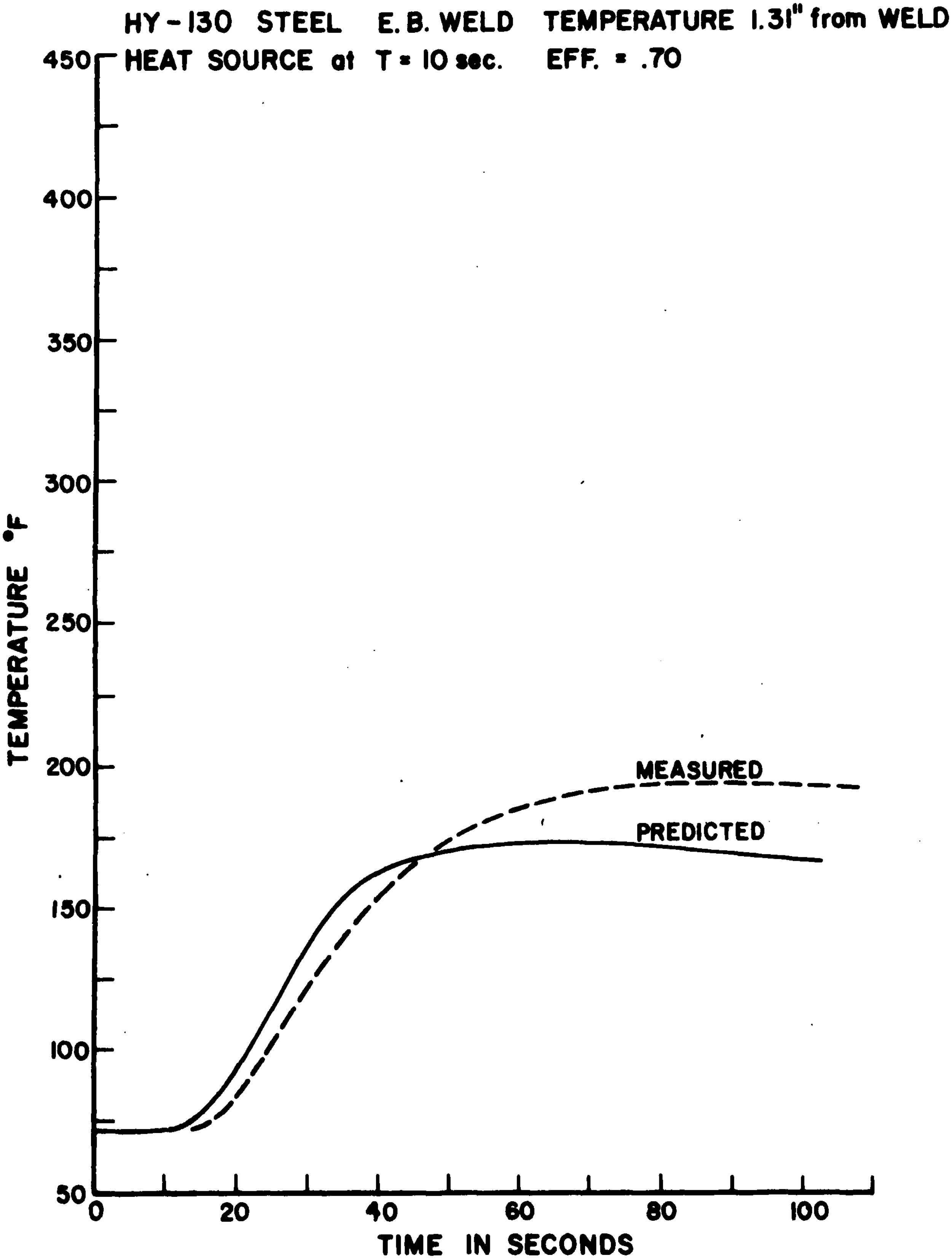

FIGURE 2.19 TEMPERATURE vs. TIME - HY-130 SPECIMEN 1.31" FROM WELD LINE

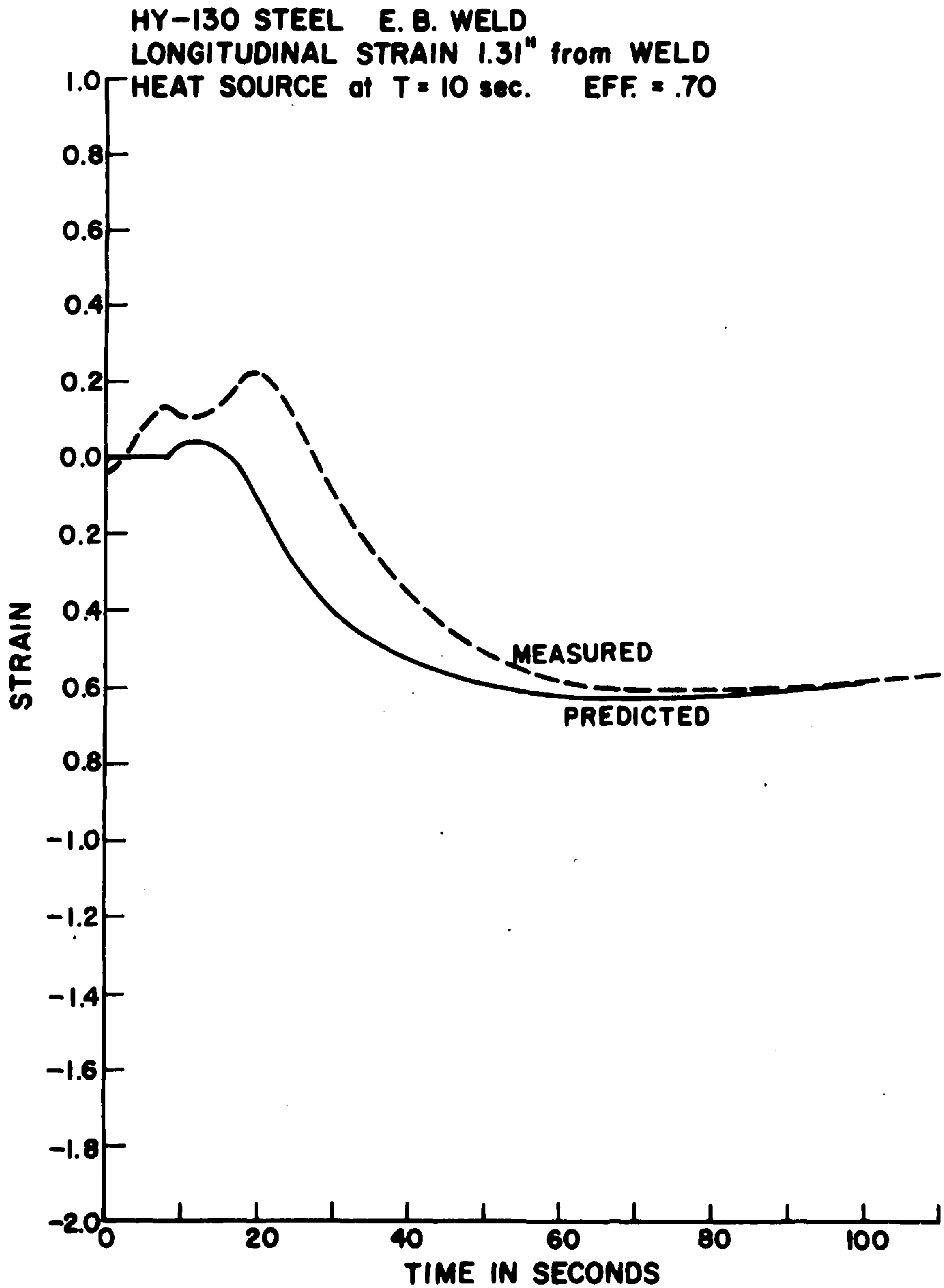

FIGURE 2.20 LONGITUDINAL STRAIN vs. TIME - HY-130 SPECIMEN 1.31" FROM WELD LINE

they are entirely typical of the comparisons for all passes.

Upon comparing the measured and predicted results for the temperature distributions, it becomes apparent that their correlation seems to be satisfactory in general terms. One should note, however, that the predicted cooling rates are always faster than the measured ones. This phenomenon becomes more obvious at points closer to the weld line (refer to Figures 2.10 and 2.16). The latter observation notwithstanding, one can thus reach the conclusion that the simple analytical solution for the moving point or line heat source can give a good first approximation of the temperature distribution during welding. Such a conclusion seems to be quite astonishing considering the complexity of the welding process and the fact that the iterative method used in the solution[4] does not satisfy the heat flow equilibrium conditions.

Of further interest is the fact that the arc efficiency used for calculating the heat input to the material to be welded was found to be independent of the material used. In the GMA welding process, for example, an arc efficiency equal to 0.70 was used for both the HY-130 and 1020 steels. Such a finding supports the contention that arc efficiency is mainly a function of the particular welding equipment used.

A point should be made here regarding the arc efficiency of the electron-beam welding process. In conventional arc welding processes, the arc efficiency is used as an approximation of the various energy losses that occur between the welding arc and the workpiece; so, the final heat input is given as the product of the arc efficiency, the arc voltage, and the arc current. In the EB process, however, there is no such thing as an arc and the voltage and current measured are the ones that are input to the machine itself. Consequently, the definition of the arc efficiency has to be modified in the case of the EB process to include the energy losses inside the machine. Having clarified this, however, one is astonished to discover that arc efficiencies in the vicinity of 0.70 are necessary, if one wants to match analytical with experimental results. Such low arc efficiencies

---

[4]This iterative method is employed to take into account the dependence of the material's thermal properties on temperature (for more details see the reference cited in note 1).

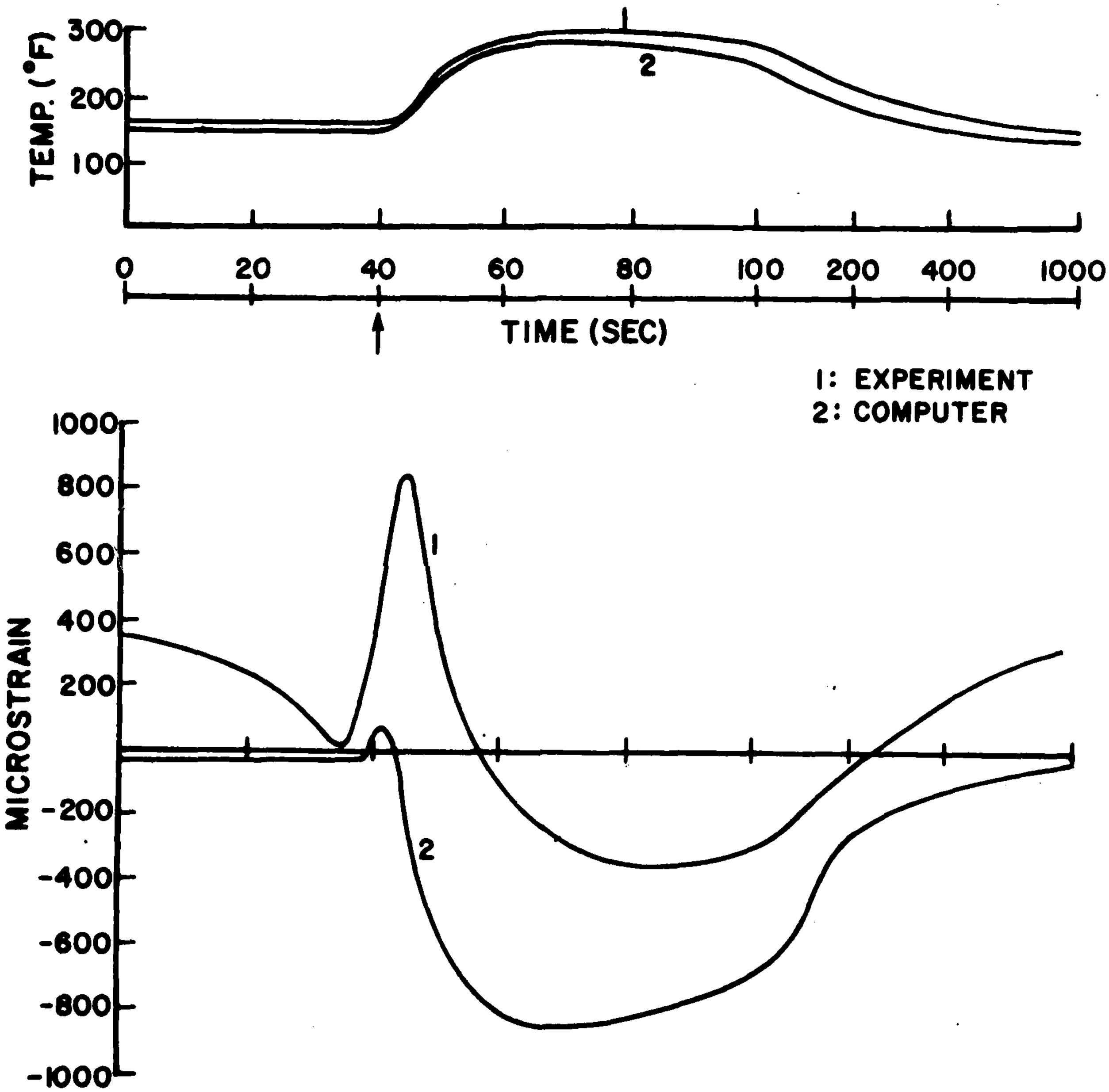

FIGURE 2.21 HY-130 SPECIMEN II, 1.0", TEMPERATURE AND STRAIN ANALYTICAL COMPARISON, PASS 3

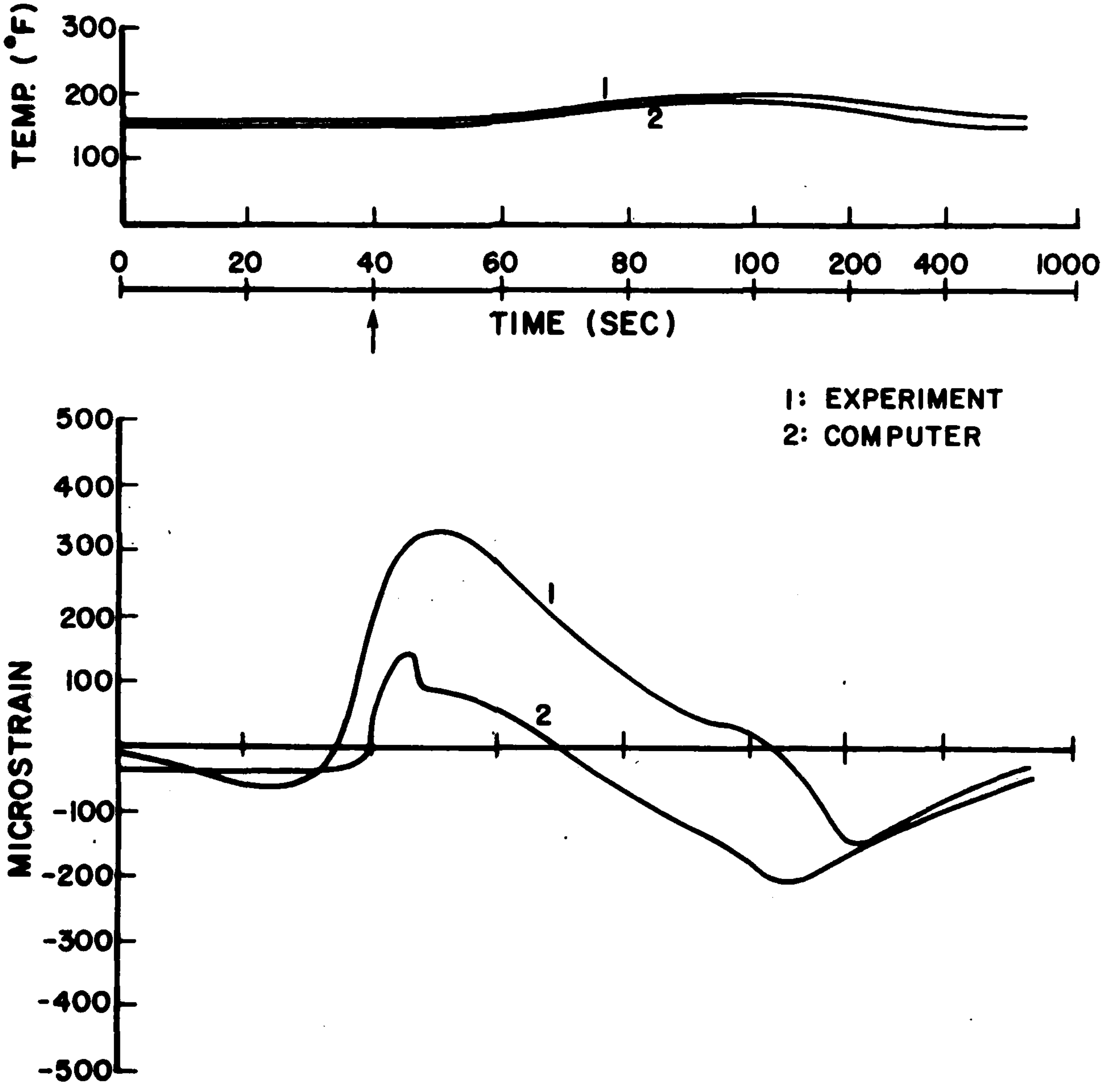

FIGURE 2.22 HY-130 SPECIMEN I, 2.25", TEMPERATURE AND STRAIN ANALYTICAL COMPARISON, PASS 3

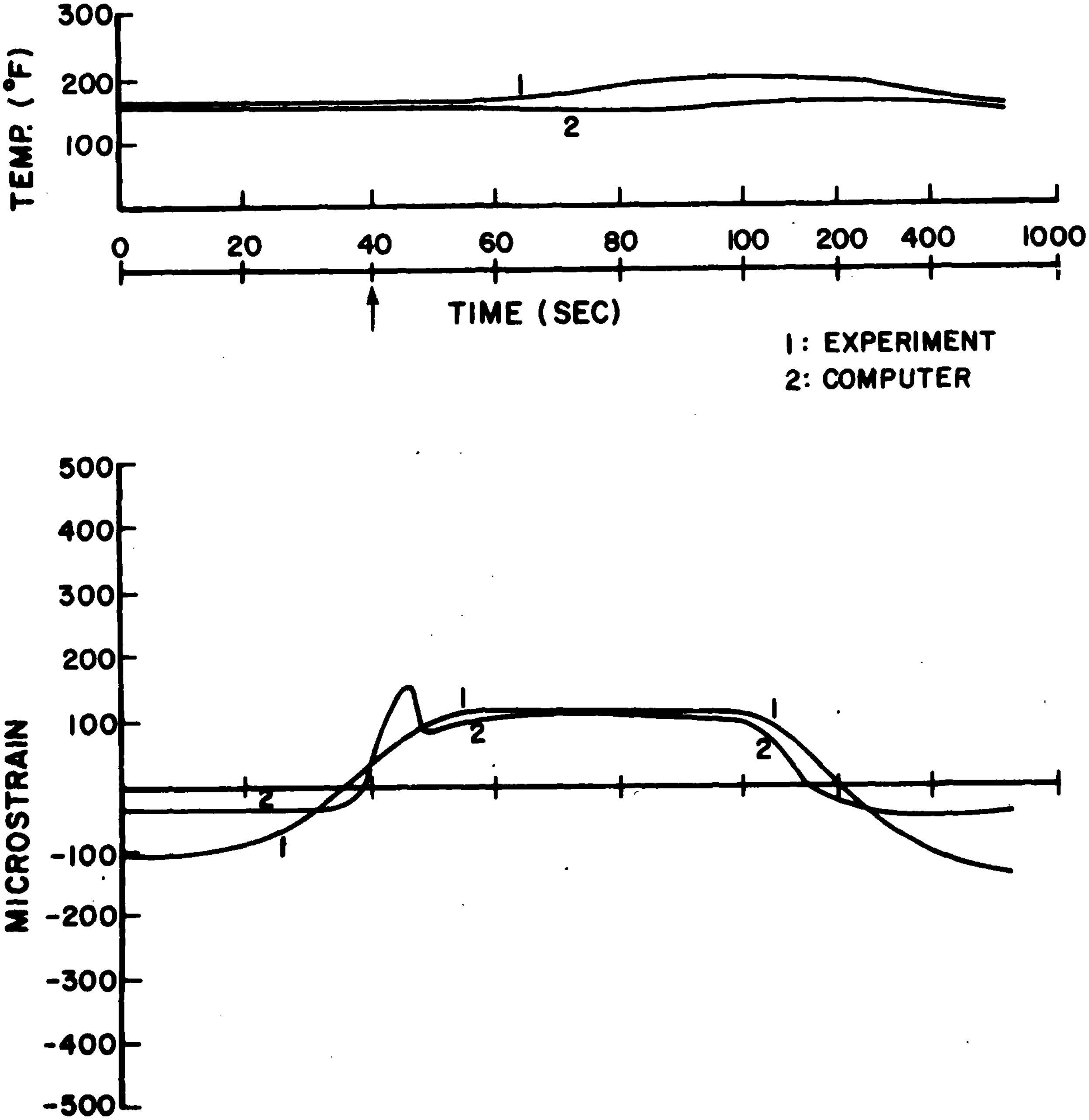

FIGURE 2.23 HY-130 SPECIMEN I, 4.25", TEMPERATURE AND STRAIN ANALYTICAL COMPARISON, PASS 3

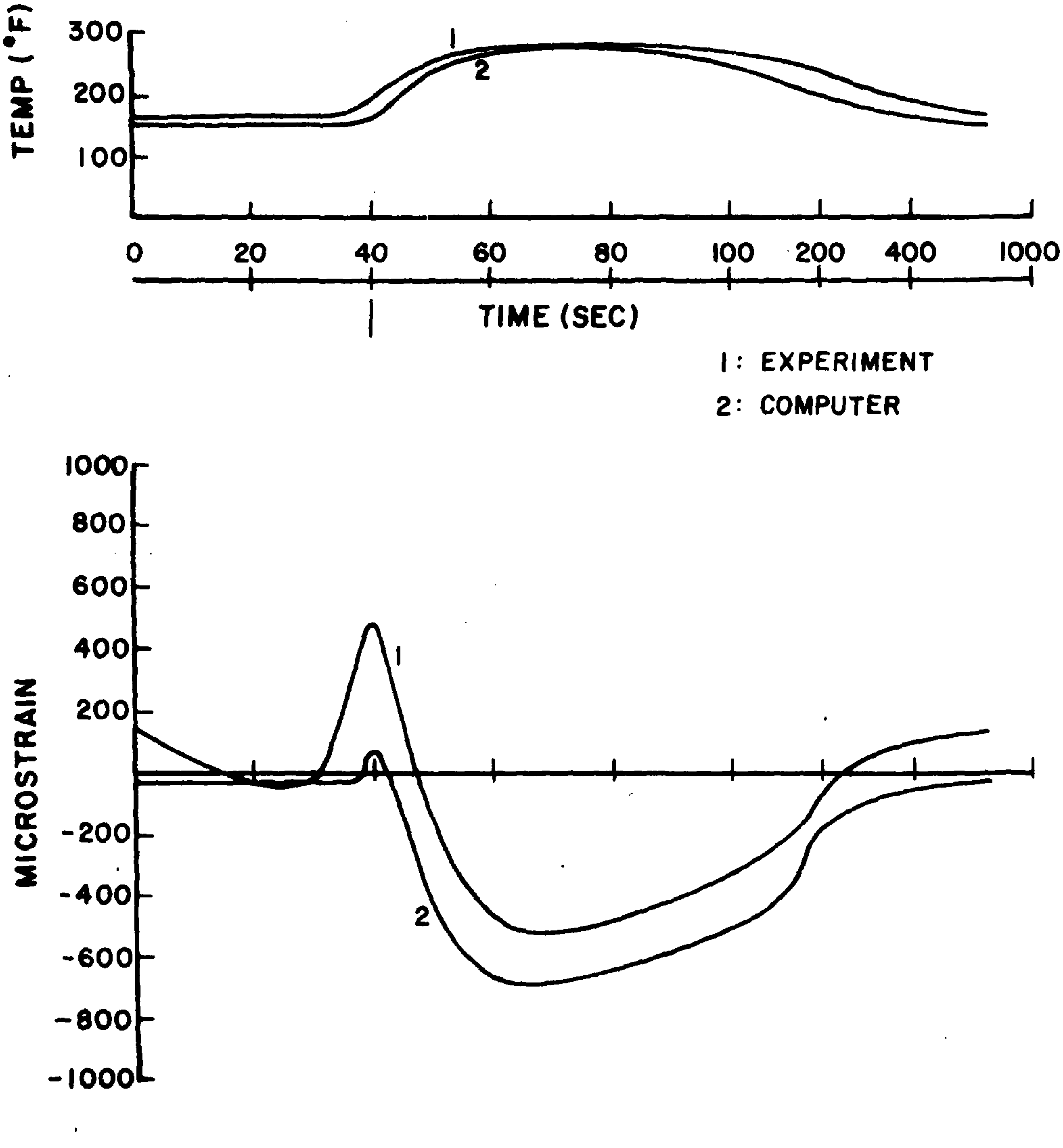

FIGURE 2.24 1020 STEEL, 1.25", TEMPERATURE AND STRAIN ANALYTICAL COMPARISON, PASS 3

cannot be explained easily, especially if one bears in mind the facts that the process takes place in a vacuum and that electric machines have usually very high efficiencies. It is thus concluded that more investigation is needed on the subject.

In analyzing strains, the one-dimensional program assumes that the longitudinal strain is only a function of the transverse distance from the weld and the transverse strain as well as the shear strain are assumed to be zero. In fact, the transverse strains measured were not zero and for distances from the weld line of up to approximately one inch, the transverse strains were of the same order of magnitude as the longitudinal strains. At transverse distances of approximately two inches, transverse strains are greatly reduced, but still significant. Only at greater transverse distances do they become relatively insignificant. It is thought that the presence of these transverse strains accounts for the poor comparisons between the experimental results and the one-dimensional program predictions because the assumptions used in calculating the longitudinal strains are not valid in these one inch thick plates. However, it can be seen that the results for the point 4.25" away from the weld line (Fig. 2.23) agree more closely than for points closer to the weld line. This appears to be due to the absence of any significant transverse strains this far from the weld line.

Another cause of the poor agreement between experimental and analytical results at points near the weld line is the finite size of the gages used. The strain gages measure about .3" across. When a high strain gradient exists, the side of the gage closest to the weld may be subject to a strain quite different than that seen by the side .3" away, resulting in experimental errors.

The above discussion leads to the conclusion that a two-dimensional program should be used for predicting thermal strains during welding.

2.4.2 Two-Dimensional Computer Program

No effort has been made to use the existing M.I.T. two-dimensional plane-strain finite element computer program to analyze thermal strains during welding. The decision for not using it has been discussed with representatives of the Office of Naval Research and the Electric Boat Division

of General Dynamic Corporation during a meeting held at M.I.T. on July, 1978. All parts agreed that such a step was justifiable on the grounds of previous experience with the program and its high running cost.

It was instead proposed that an effort should be undertaken to include capabilities for handling welding problems in the existing multi-purpose finite element programs ADINA and ADINAT developed by Prof. K. J. Bathe, Department of Mechanical Engineering, M.I.T. The first of these programs deals with stress analysis and the second with temperature analysis. The decision to use these two programs was based on a number of factors. First, these programs have been extensively tested in the past and were found to be both accurate and efficient. Second, the welding problem is an integral part of the more general structural analysis problem, so that compatibility between programs dealing with these problems is considered essential. For this reason a general purpose finite element program had to be selected and ADINA seemed to be the most appropriate since it was developed at M.I.T. Third, Papazoglou, who will be the person principally involved in the analytical part of this contract, has past experience in using both ADINA and ADINAT.

Details on the progress made on the two-dimensional analysis are included in Section 2.8.2 of this report.

2.5 Development of Details of the Research Plan for the Second Year (Step 1.4)

The measurement of the residual stresses present in the specimens welded during the first year of this project was one of the tasks that had to be carried out during the second year. Five such specimens were available, as follows (refer to Section 2.3):

a. One 1020 steel plate welded by the Gas Metal Arc Welding (GMAW) process.

b. Two HY-130 plates welded by the GMAW process.

c. One 1020 steel plate welded by the Electron Beam Welding (EBW) process.

d. One HY-130 plate welded by the EBW process.

All plates were 24" x 24" x 1" in dimensions. Due to the relative large thickness (1") of the specimens, it was decided that the through thickness distribution of residual stresses should also be measured.

A thorough literature search was carried out to determine the most appropriate method for measuring through thickness distributions of residual stresses. It turned out that the few papers that could be located tended to converge to two general methods: The sectioning technique and the boring method. Furthermore, most of the papers, especially the more recent ones, were describing methods suitable for much thicker specimens (100 mm and more in thickness).

In view of all the above, and given the fact that the boring technique could not be accurately applied to 1 in. thick specimens, the M.I.T. investigators decided to proceed and use the Rosenthal-Norton sectioning method, with possible modifications. As a test, and because the method is destructive, initial experiments were carried out using the low carbon 1020 steel specimens. First, the GMA welded specimens were to be used. After machining the weld reinforcement, an operation necessary for locating strain gages on the weld centerline, it was discovered that cracks were exposed to the surface. The presence of these cracks made the specimen unsuitable for measuring residual stresses.

The above fact led to the final use of the EB welded 1020 specimen. Details of the performed measurements are included in the next section. The same section includes comparisons of surface distributions of residual stresses measured by strain gages and the X-ray diffraction method.

Regarding step 1.6, it was decided to perform experiments on simple restrained butt welds using the laser welding process. These experimens were performed at AVCO Everett Metal Working Lasers located in Somerville, Massachusetts, and are described in Section 2.7.

Finally, progress has also been made towards improving available analytical tools for predicting temperature and strain changes during welding.

2.6 Measurement of Residual Stresses in Butt-Welded Thick Plates (Step 1.5)

The following thesis dealing with Step 1.5, has already been completed:

Mylonas, G. A., "Experimental Investigation of Residual Stress Distributions in Thick Welded Plates", S.M. Thesis, M.I.T., July 1979.

A summary of the results appearing in this thesis is presented below.

2.6.1 Brief Description of the Measurement Procedure

The Rosenthal-Norton sectioning technique for measuring triaxial distributions of residual stresses was developed by Rosenthal and Norton in 1945. A detailed description of the method can be found in the original paper.[5] In this section some highlights of the technique will be briefly discussed.

Let's assume that the through thickness distribution of the longitudinal residual stress σ_x at a certain location is desired (see Fig. 2.25). As a first step, a narrow block having the full thickness of the plate is removed with its long axis along the x-direction. Given that the block is narrow enough with respect to the plate thickness, it can be assumed that after its removal, all of the stress acting in the y-direction has been relieved, while only a part of the stress in the x-direction has done so. Moreover, if the block is long enough with respect to the thickness--say twice or more--then the further assumption can be made that the stress relieved in the central portion of the block is very nearly a linear function of its thickness. This last assumption, although questioned by various investigators, was felt to adequately serve the purposes of a first examination of the measuring technique. The linear stress distribution can be found by measuring the strains relieved at the top and bottom of the block.

[5] Rosenthal, D. and Norton, J.T., "A Method of Measuring Triaxial Residual Stress in Plates", The Welding Journal, Vol. 24, No. 5, May 1945, pp. 295-s to 307-s.

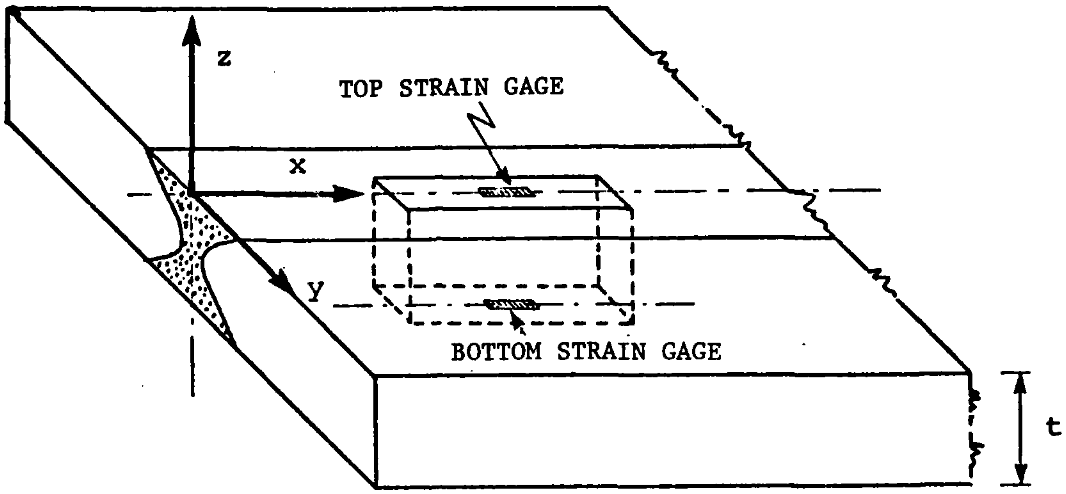

FIGURE 2.25 REMOVAL OF THE BLOCK FROM THE PLATE

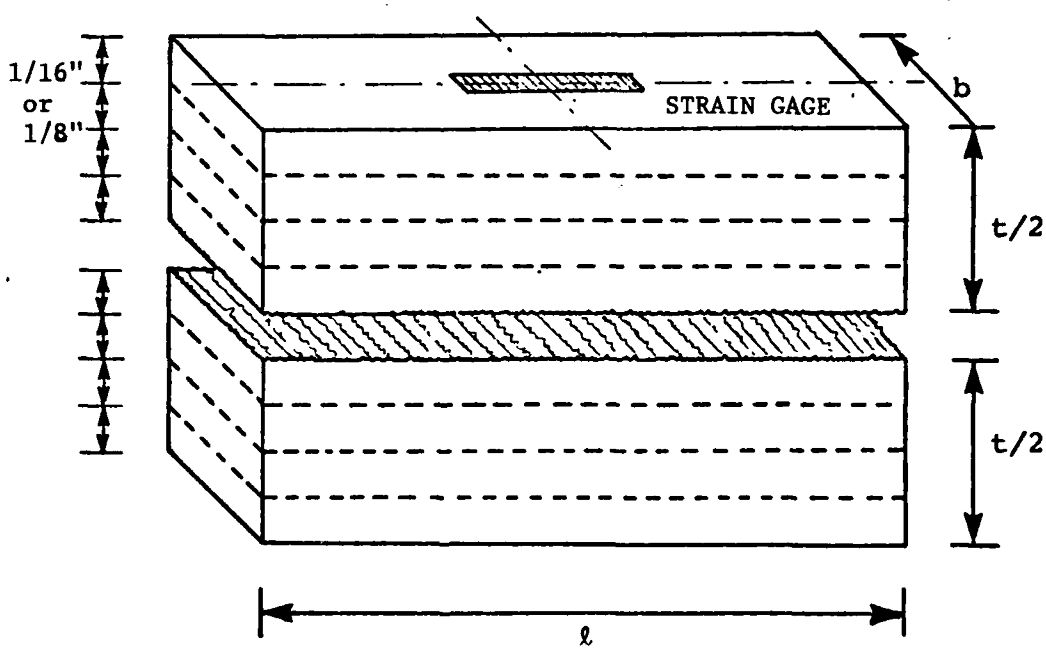

FIGURE 2.26 METHOD OF SLICING THE BLOCK

The second step of the measuring technique aims at relieving the remaining stresses acting in the x-direction that are still locked in the block. This is achieved by sectioning the block in two and then removing from each half slices of metal about 1/16" to 1/8" thick progressing from the mid-section outward to the top or bottom faces of the block (see Fig. 2.26). The strains relaxed by sectioning the block as well as during the slicing are measured by the strain gage located at the corresponding face. Using a simple mathematical model one can then compute the full distribution of residual stresses.

To summarize, the total amount of stress at different levels throughout the plate thickness is simply the sum of the values obtained from two operations:

(i) the removal of the block from the plate, and

(ii) the cutting of the block in half and the subsequent slicing of each half.

It should be noted at this point that the computation of the through thickness distribution of σ_x, as well as σ_y, at any location requires measuring the relaxation of strains in both the x- and y-direction. This means that two blocks, one in each direction, must be cut at each location, something impossible. Fortunately, however, the symmetry of the residual stress distribution about the x-axis and the fact that residual stresses do not vary much at the midportion of a long welded plate allow the measurement to take place. Figure 2.27 shows two possible block layouts that utilize the above properties (for point A blocks 1 and 2 or 1, 2, and 3 can be used, whereas for point B blocks 4 and 5 or 4 and 6 depending on the plate's length).

The procedure described above holds for the measurement of longitudinal and transverse stresses as well as for the shearing stress. The through thickness distribution of the stress acting in the thickness direction, σ_z, cannot be measured directly. It can be computed, however, from the equilibrium equations and using the values of the other measured stresses.

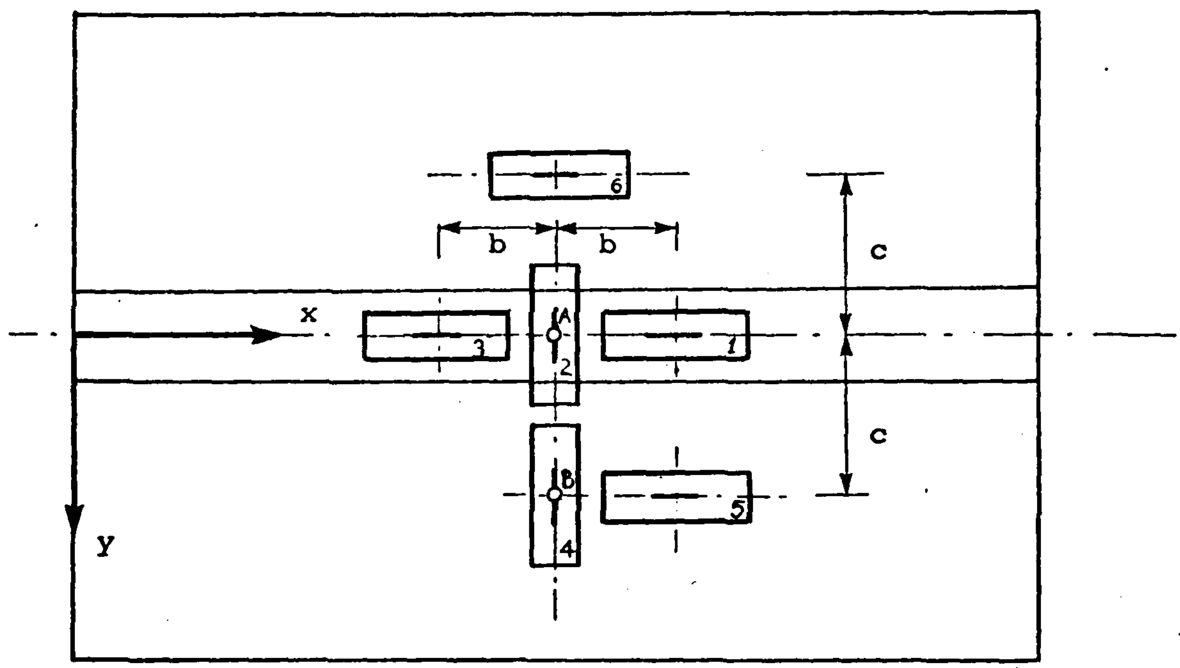

FIGURE 2.27 STRAIN GAGE ARRANGEMENT

2.6.2 Experimental Application

The Rosenthal-Norton method for measuring triaxial residual stresses was applied in an experiment conducted at the M.I.T. Welding Laboratory. An electron-beam welded mild steel 1020 plate was used for this purpose. The plate was 24" x 24" x 1" and was welded during the first year of this project (see Section 2.3.2).

Both surfaces of the plate were properly cleaned and twelve grain gages (six on each side) were installed, as shown in Figure 2.28. As can be seen from the figure, strain gages A and B were used in order to measure stresses σ_x and σ_y at the midpoint of the plate and on the weld line; strain gages E and F in order to measure σ_x and σ_y at a distance 2.5" from the weld line and at the midpoint; and strain gages C and D in order to measure the shearing stress τ_{xy}. It is apparent that this arrangement was chosen because the plate is long enough causing no significant changes in the residual stress distribution at its midportion.

The removal of the blocks from the plate was done by a band saw and utilizing slow cutting and feeding speeds to avoid excessive heating of the plate, something that would relieve the locked-in stresses. The blocks were cut in half by the same saw, while slicing was performed by machining at a very slow speed and by removing a metal layer of 0.003" to 0.005" in each pass.

Figures 2.29 through 2.32 show the through thickness distributions of stresses σ_x and σ_y as computed from the measured strain relaxations. In each figure the left graph shows the component of the final residual stress distribution which is due to the strain relaxations that occurred during the cutting in half and slicing operations. The right graph shows, in solid lines, the final computed through thickness residual stress distribution and, in intermittent lines, the linear stress distribution that resulted from the partial strain relieving during the removal of the block from the plate. It should be apparent that the final distribution is a superposition of the other two.

Figure 2.33 shows the through thickness distribution of the shearing stress τ_{xy} at a midpoint and on the weld line. Note that although this

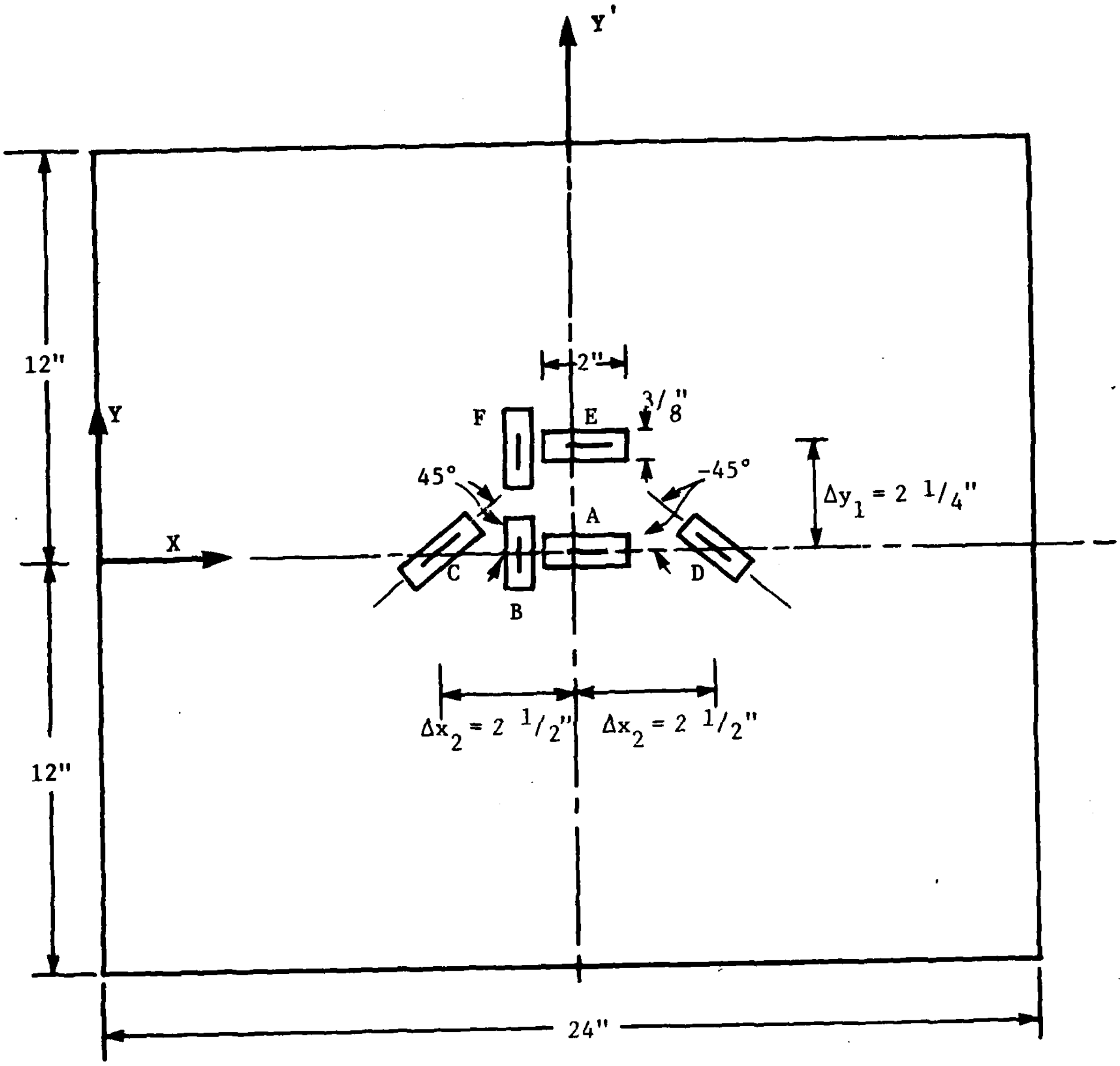

FIGURE 2.28 LAYOUT OF BLOCKS AND STRAIN GAGES

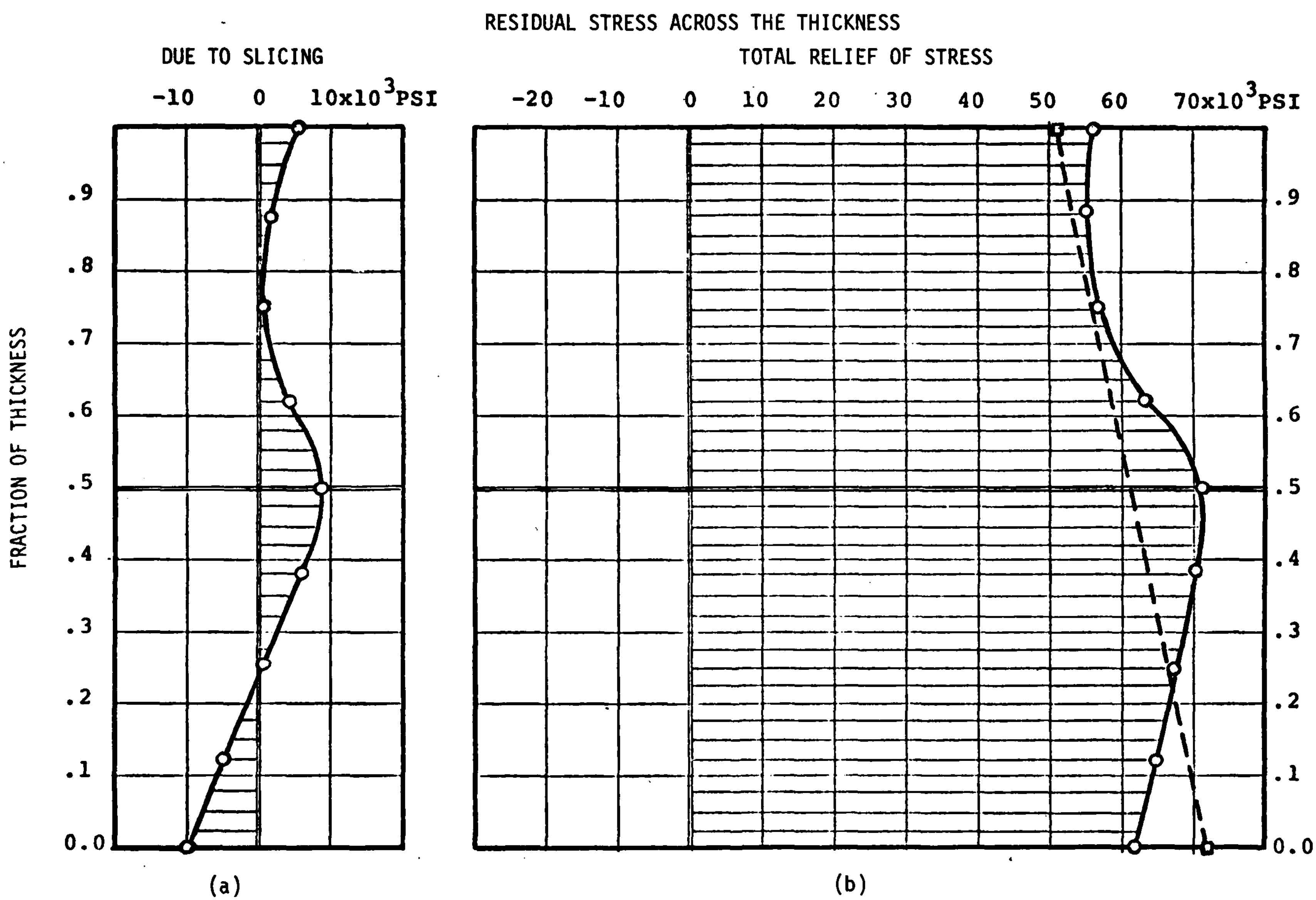

FIGURE 2.29 RESIDUAL STRESSES σ_x IN BLOCK A

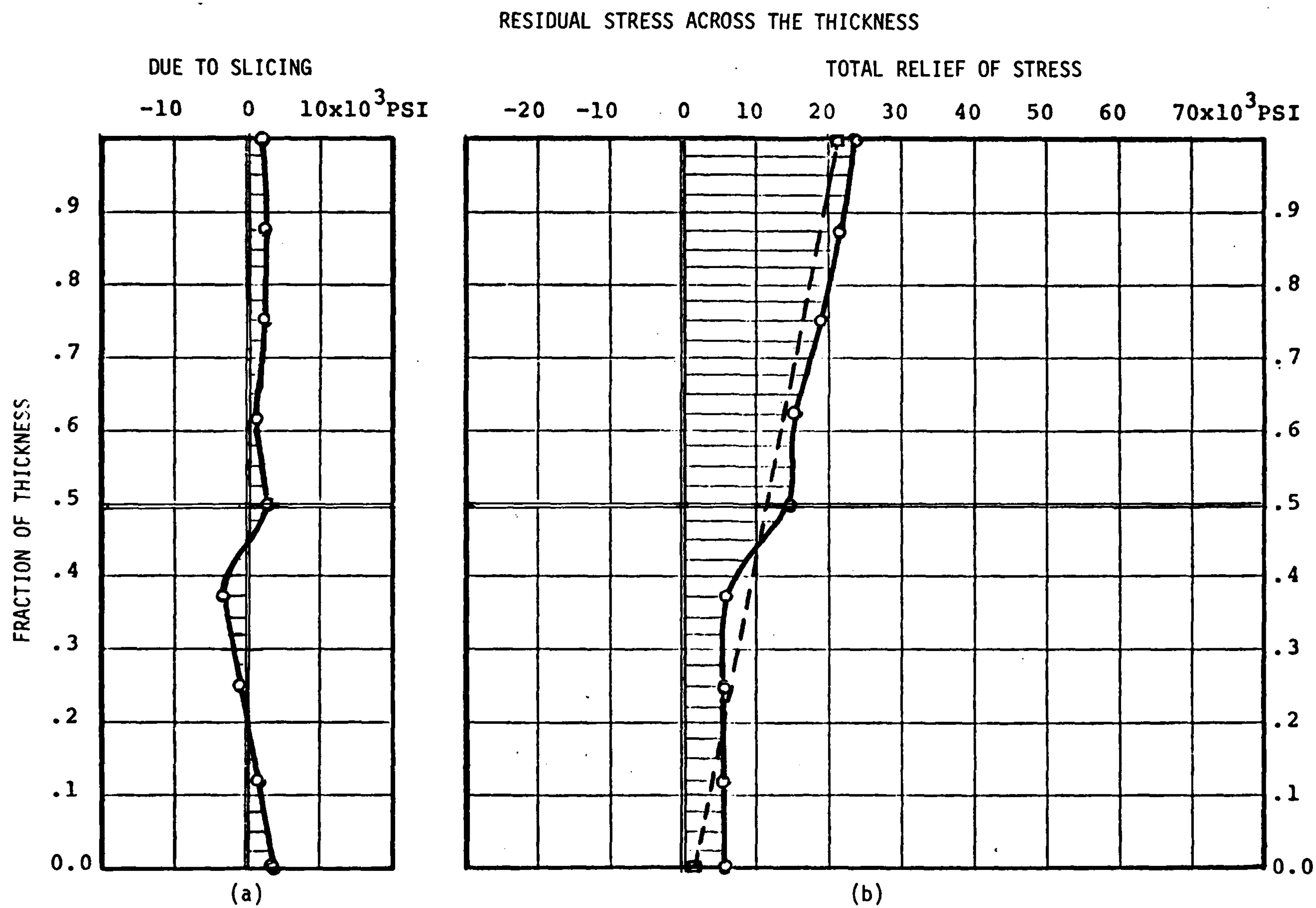

FIGURE 2.30 RESIDUAL STRESSES σ_y IN BLOCK B (at midpoint and on the weld line)

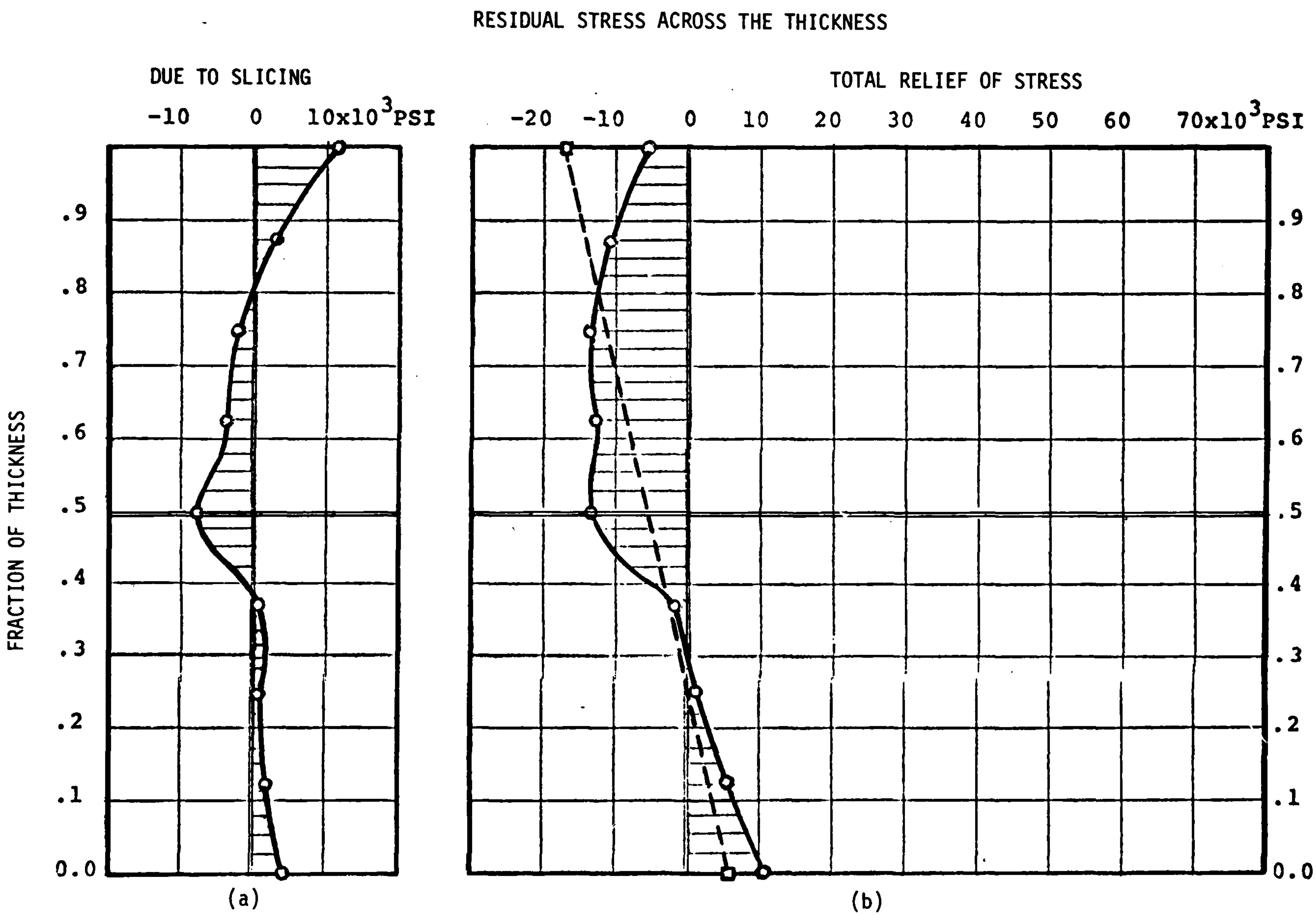

FIGURE 2.31 RESIDUAL STRESS σ_x IN BLOCK E (at midpoint and 2.5" from the weld line)

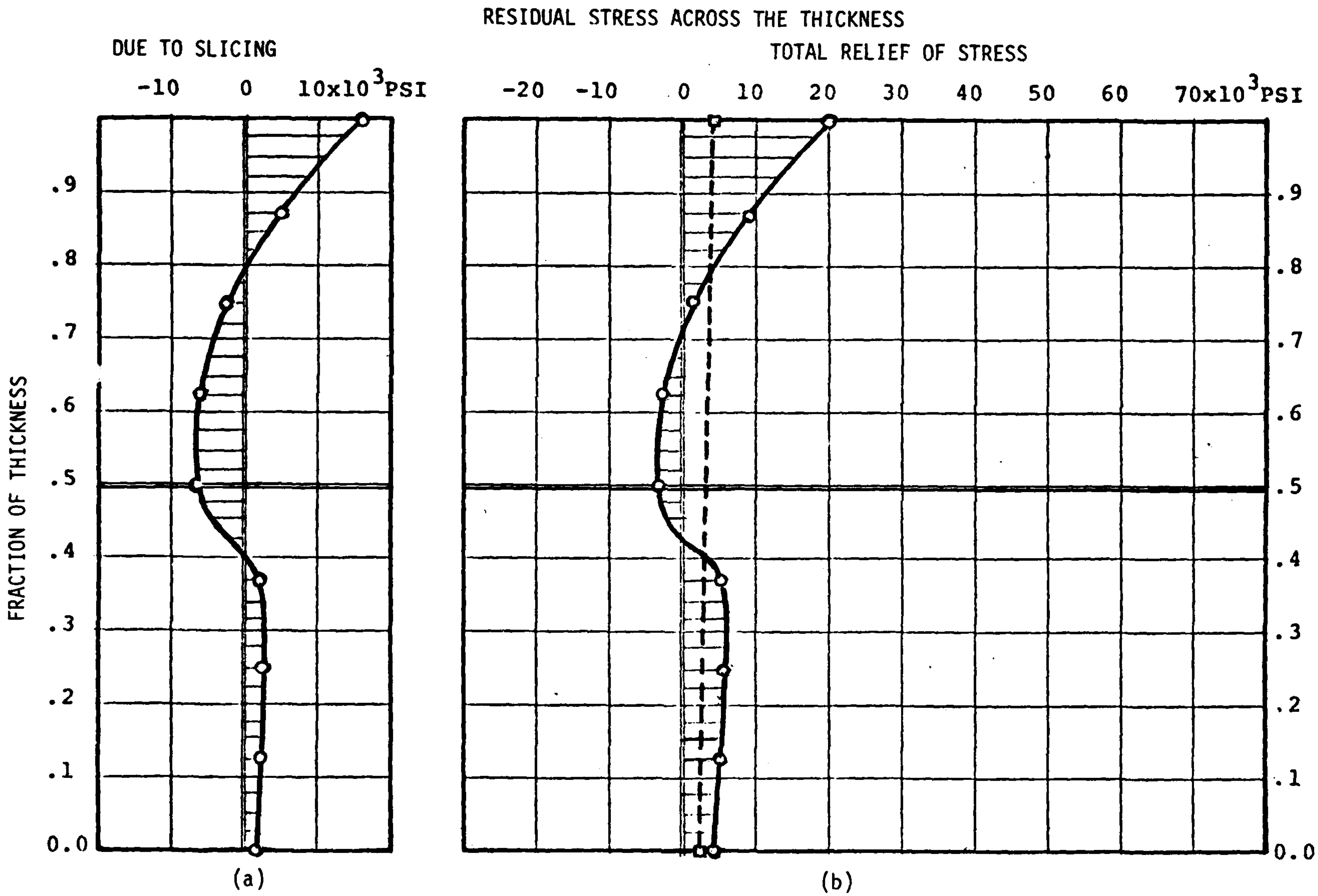

FIGURE 2.32 RESIDUAL STRESS σ_y IN BLOCK F (at midpoint and 2.5" from the weld line)

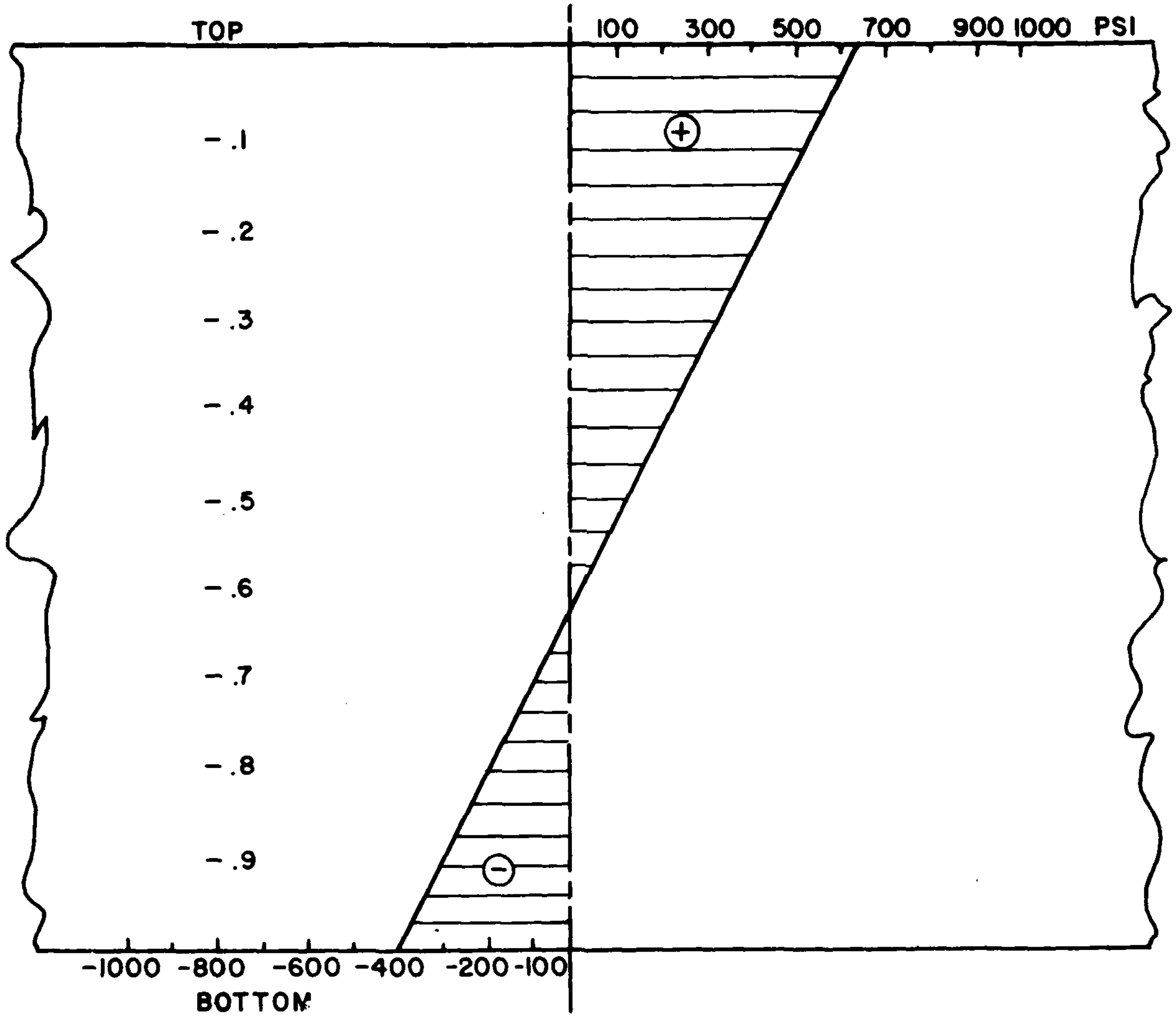

FIGURE 2.33 SHEARING STRESS DISTRIBUTION τ_{xy} IN THE THICKNESS DIRECTION

stress should theoretically be zero, due to the symmetry of stress σ_x about the x-axis, it has nonzero values. Nevertheless these values are negligibly small, giving an indication that the measuring technique is relatively accurate.

Finally, Figure 2.34 shows the through thickness distribution of σ_z as it was computed using the equilibrium equations and the values of the other stresses.

Concluding, it should be noted that the method seems to give reasonable results, qualitatively speaking. Although the general trends seem to make sense, however, nothing can be said about the quantitative accuracy of the technique. When the experimental results will be compared with the analysis, something that is intended to be done during the third year of the project, more positive conclusions will be drawn.

2.6.3 Surface Distribution of Residual Stresses

To make a comparison of surface distributions of residual stresses as measured by electric resistance strain gages and the X-ray diffraction method, the following test was conducted.[6]

Two pieces A and B, each 9" x 5" x 1", were cut from the original electron beam welded specimen described in Section 2.6.2 (see Fig. 2.35). Piece A was then sent to Lambda Research, Inc., Cincinnati, Ohio where the locked-in stresses in the x- and y-directions, on both surfaces were measured at the locations shown in Fig. 2.36. The results are shown in Fig. 2.37. It is apparent that the observed results are not consistent with the type of residual stress distribution one would anticipate from a welded specimen. One possible explanation is that the observed stress distribution is a superposition of residual stresses due to welding and of stresses which may have already been present in the plate material prior to welding.

The second piece cut from the original plate, piece B, was used to measure surface residual stress distributions by applying electric

[6]Note that this test was not included in the original proposal to the O.N.R.

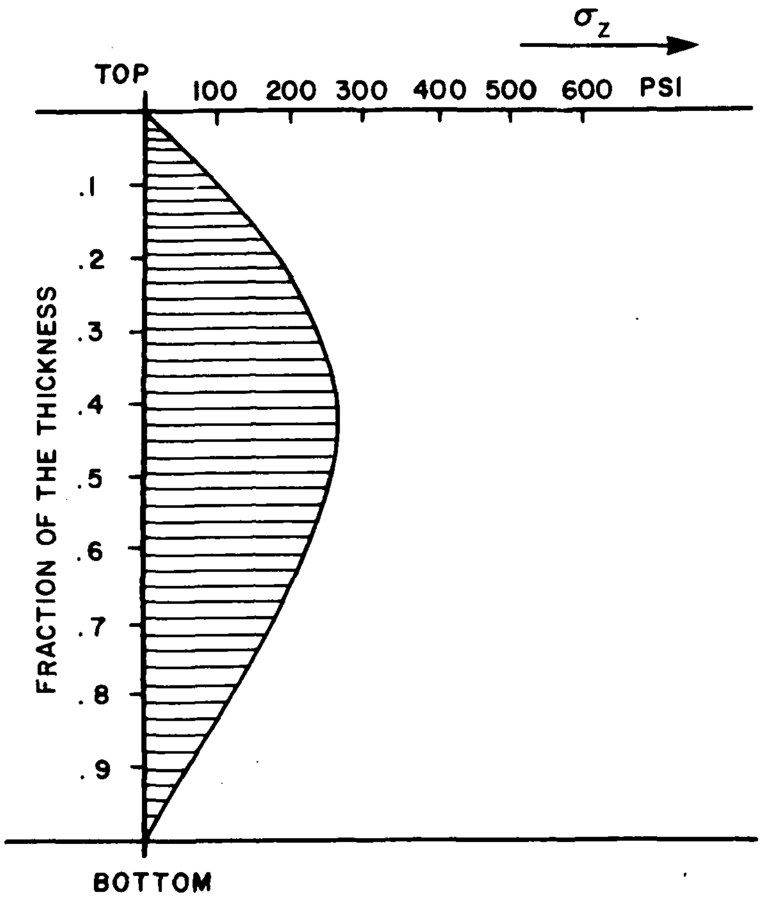

FIGURE 2.34 RESIDUAL STRESS IN THE THICKNESS DIRECTION σ_z

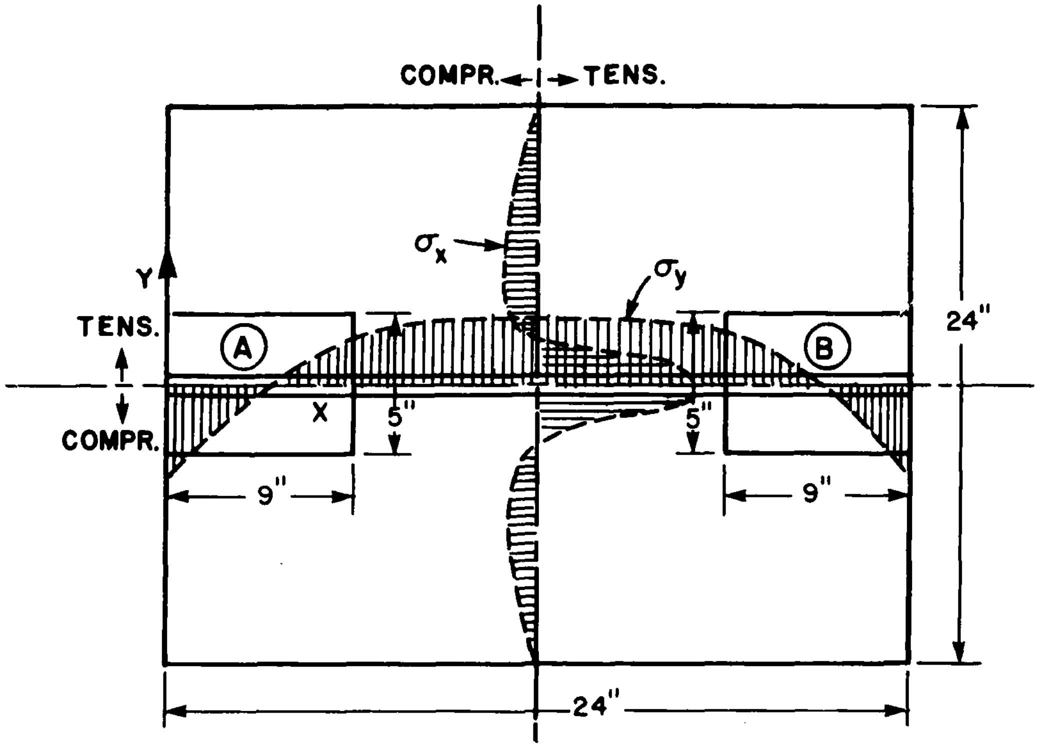

FIGURE 2.35 LOCATION OF PIECES CUT FOR SURFACE RESIDUAL STRESS MEASUREMENTS

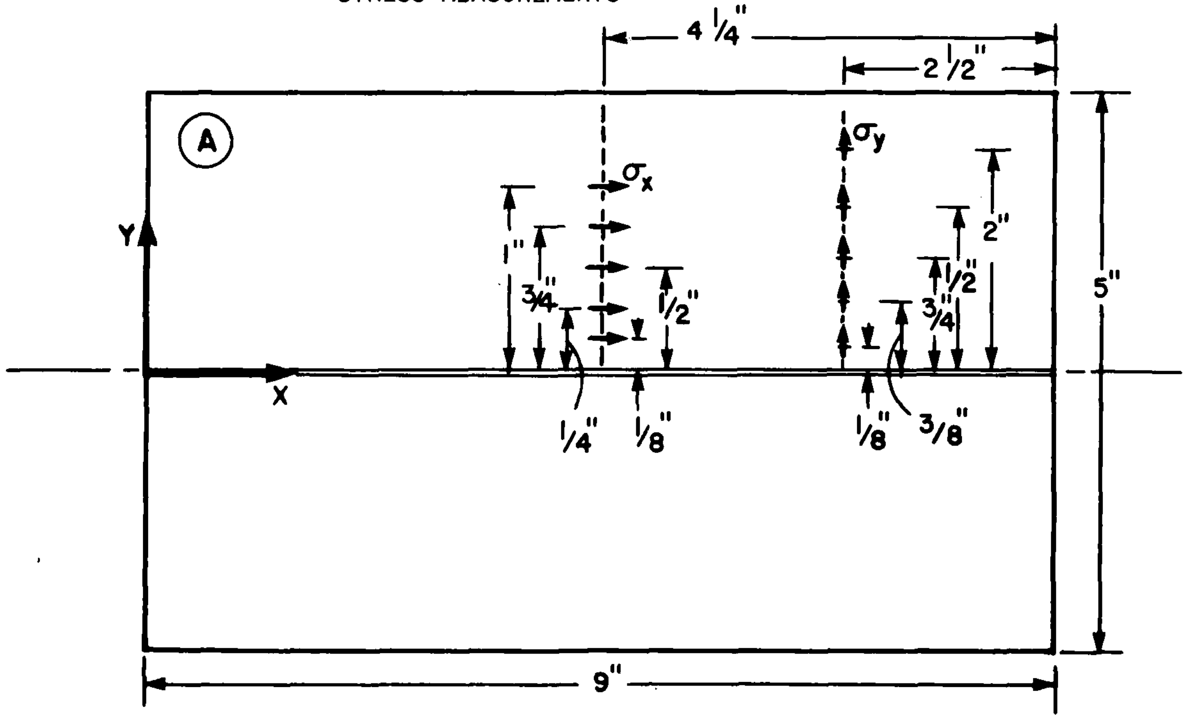

FIGURE 2.36 LOCATIONS OF X-RAY MEASUREMENTS

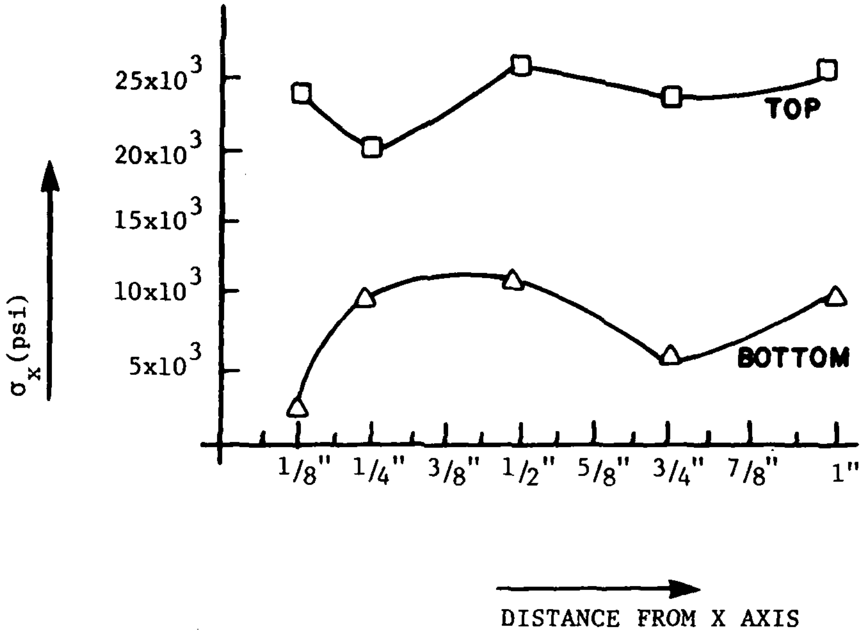

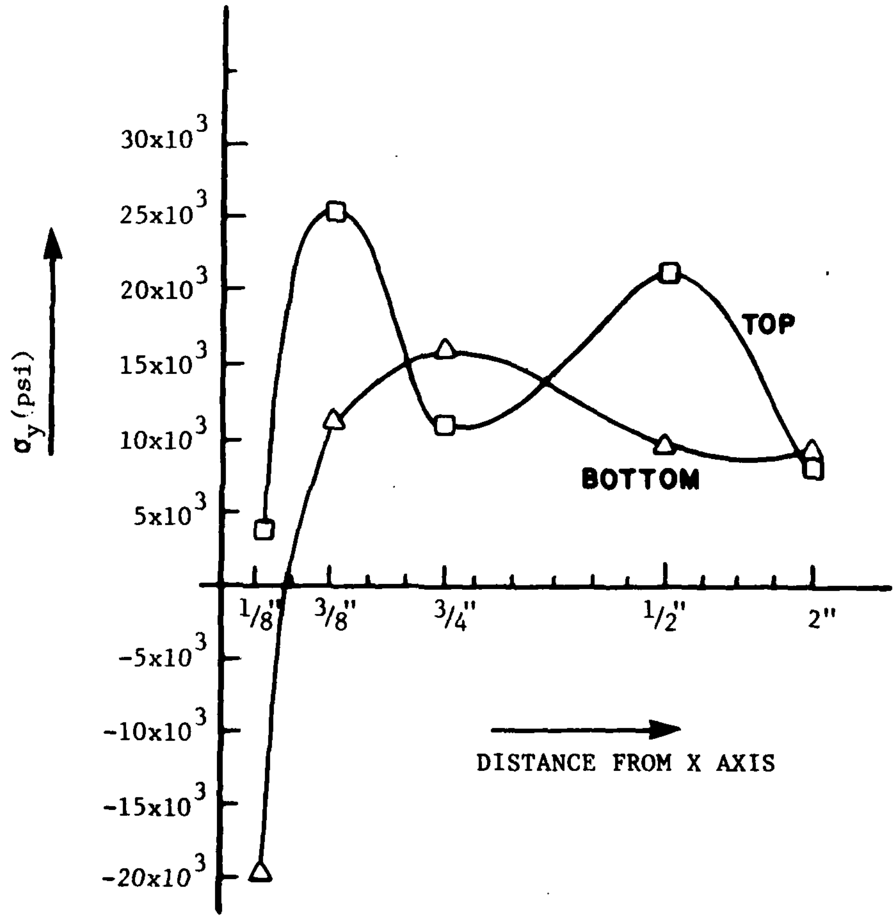

FIGURE 2.37 SURFACE RESIDUAL STRESS DISTRIBUTION (X-Ray)

resistance strain gages on the top and bottom faces as shown in Fig. 2.38. The results of this measurements are shown in Fig. 2.39. One can observe reasonable predictions for the transverse distribution of the longitudinal residual stress, σ_x. The same cannot be said, however, for the case of the σ_y stresses. First of all the fact that the stress alternates between tension and compression was not expected. Possible explanations of this behavior range from experimental error, supported by the very small magnitude of the stresses, to the fact that the stresses might not have been fully relieved by the cutting operation. Second, the appearance of relatively large negative stresses near the weld line comes in contrast to results obtained from previous investigations both at M.I.T. and elsewhere. This occurrence cannot be adequately explained at the present time.

2.7 Experiments on Simple Restrained Butt Welds (Step 1.6)

The results presented below form part of the following thesis, already completed:

Rogalski, W. J., "An Economic and Technical Study on the Feasibility of Using Advanced Joining Techniques in Constructing Critical Naval Marine Structures", Ocean Engineer Thesis, M.I.T., May 1979.

2.7.1 Experimental Procedure

Five specimens were used in a series of experiments aimed at investigating temperature and strain changes during laser welding one-inch thick HY-130 plates.[7] For the three specimens no instrumentation was used; instead, several combinations of welding parameters were tested to determine which one would give the best overall welding and penetration properties. The other two specimens were used for measuring temperature

[7] This series of experiments was not included in the original proposal to the O.N.R. They were performed so as to enhance the understanding of the effects of various welding processes when applied to the HY-130 steel.

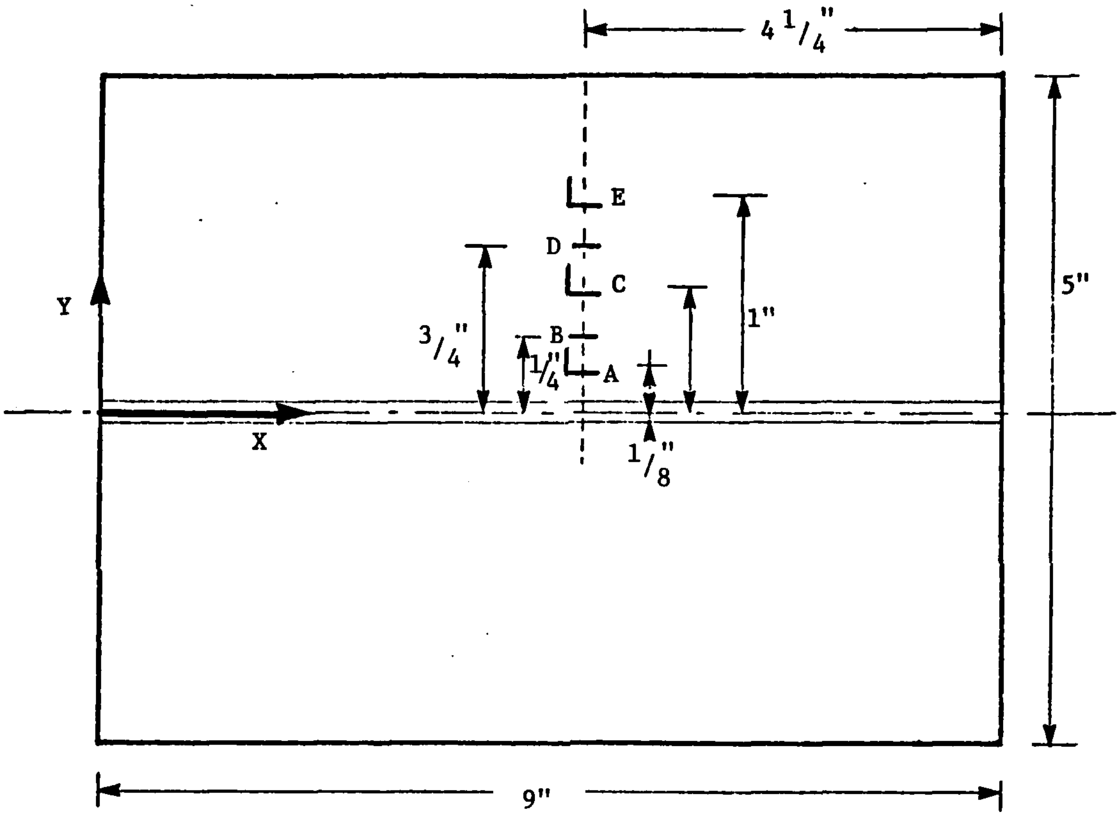

FIGURE 2.38 STRAIN GAGES LAYOUT

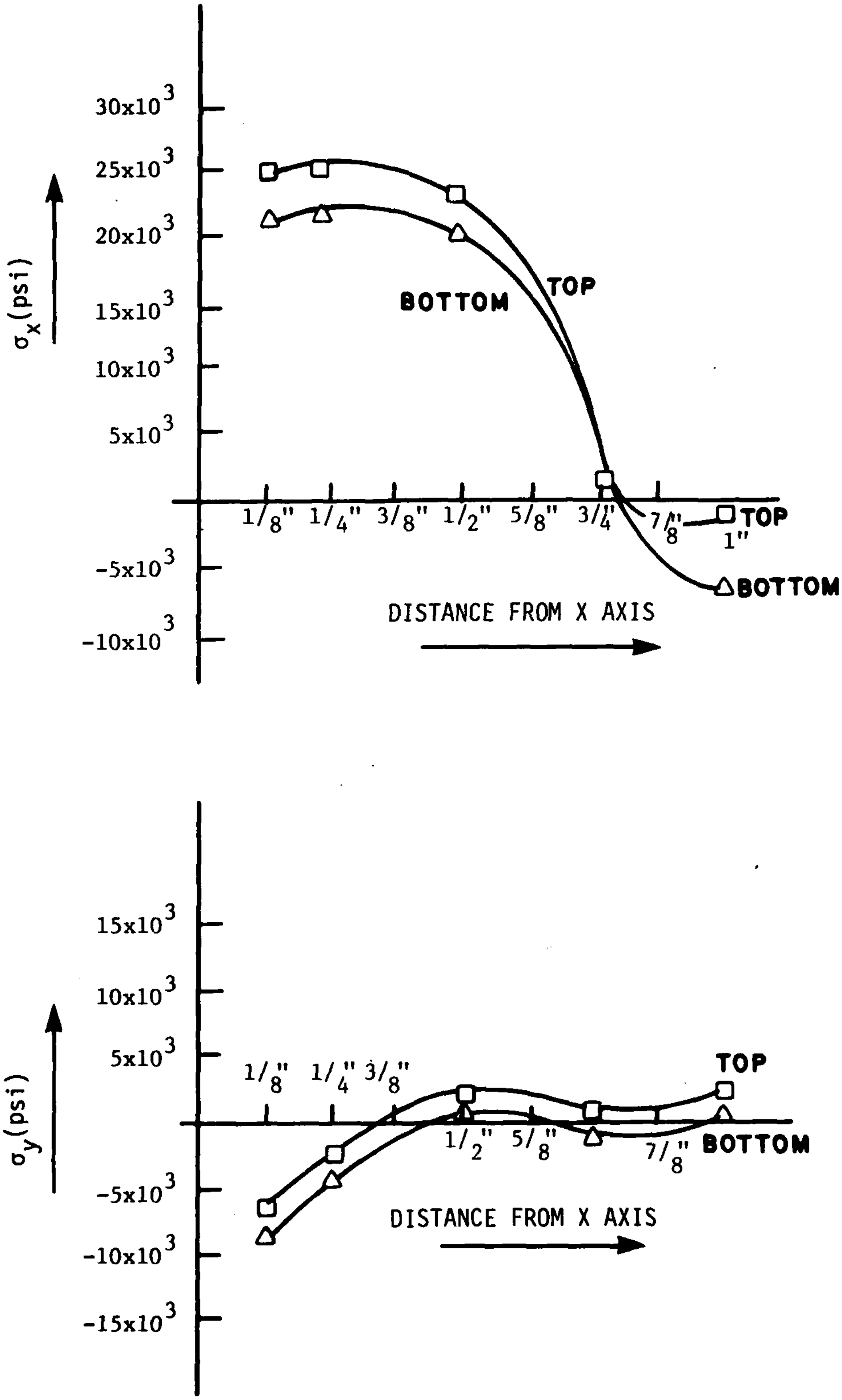

FIGURE 2.39 SURFACE RESIDUAL STRESS DISTRIBUTION
(Strain Gages)

distributions and strain changes during welding. Figure 2.40 shows the locations of Chromel/Alumel thermocouples and electric resistance strain gages installed on the two specimens. Note that all instrumentation was located on one surface of the specimens only.

Welding was performed using a continuous-wave electric industrial CO_2 laser. The multikilowatt capable laser and F-21 optics were made available for experimental welding by AVCO Everett Metal Working Lasers of Somerville, Massachusetts. Electric power supplied to the laser was approximately 140 kW, whereas power as measured on the work surface was 12 kW. Helium, provided by an off-axis nozzle, was used in all cases as the shielding gas.

The weld joint configuration was that of a flat butt joint. The welding speed chosen for the two instrumented specimens was 30 inches per minute and the focal length $33^{1/4}$ inches. These parameters gave a penetration of 23/32 inches, something that necessitated the use of two passes, one from each side, for the successful butt welding of the plates.

Both instrumented specimens were clamped to the work table prior to welding. Tack welds at each end, and on both sides, were made on one of the two specimens (hereafter called specimen I), whereas no prior tack welding was made on the other (hereafter called specimen II). The first welding pass for both specimens was made on the surface containing the thermocouples and strain gages.

2.7.2 Experimental Results

Similar results were obtained from both specimens. Figures 2.41 and 2.42 show the experimentally determined temperature histories at the four measuring points of specimen II for the first and second pass respectively. The time axis refers to the time elapsed from the commencement of welding until the specimen cooled down.

Figures 2.43 through 2.46 present experimentally obtained data on the longitudinal and transverse strain disrributions.

If one compares the above experimentally determined temperature and strain changes with the ones obtained from the electron beam welded

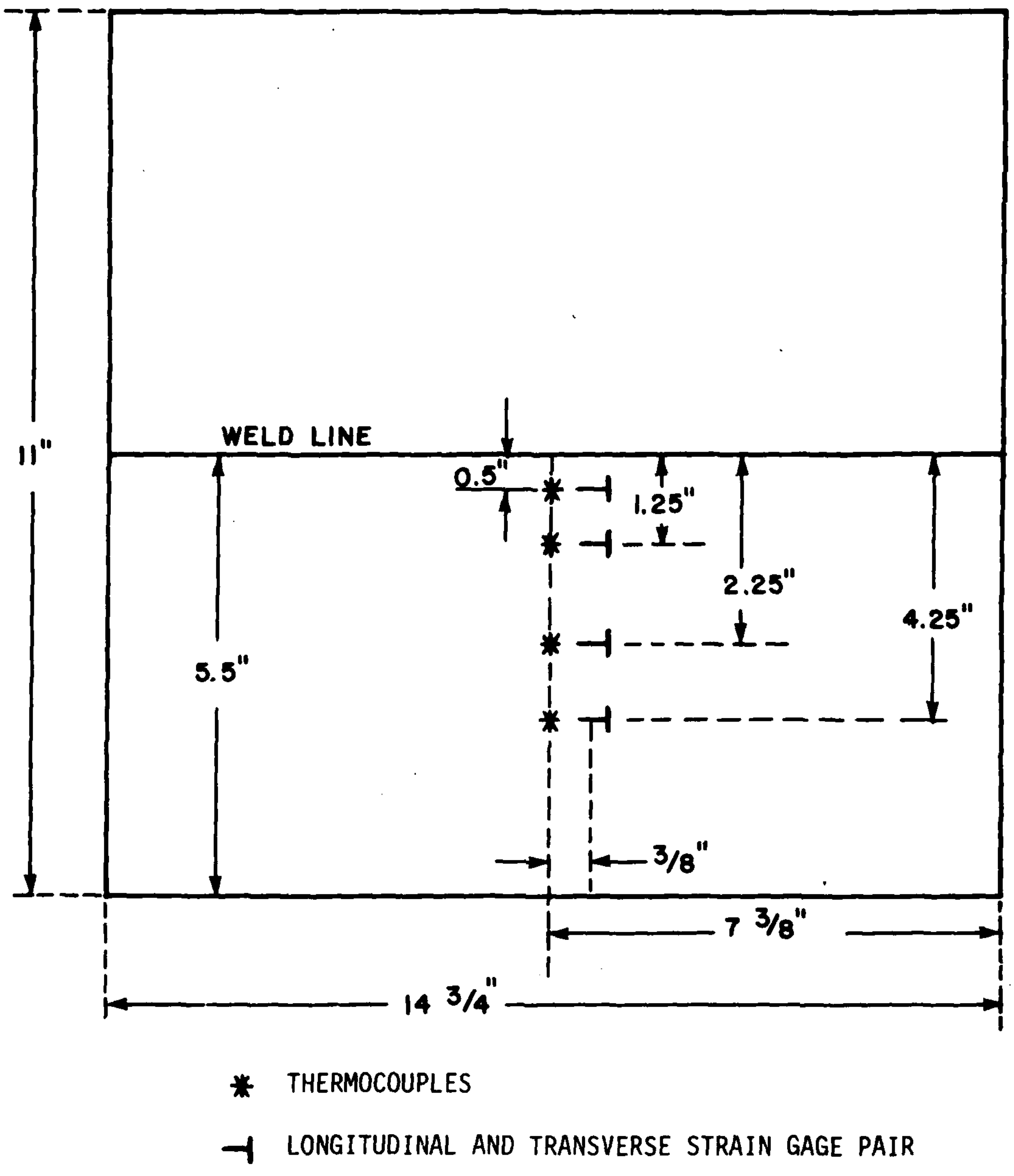

FIGURE 2.40 THERMOCOUPLE AND STRAIN GAGE LOCATION ON HY-130 SPECIMENS (LASER WELDING)

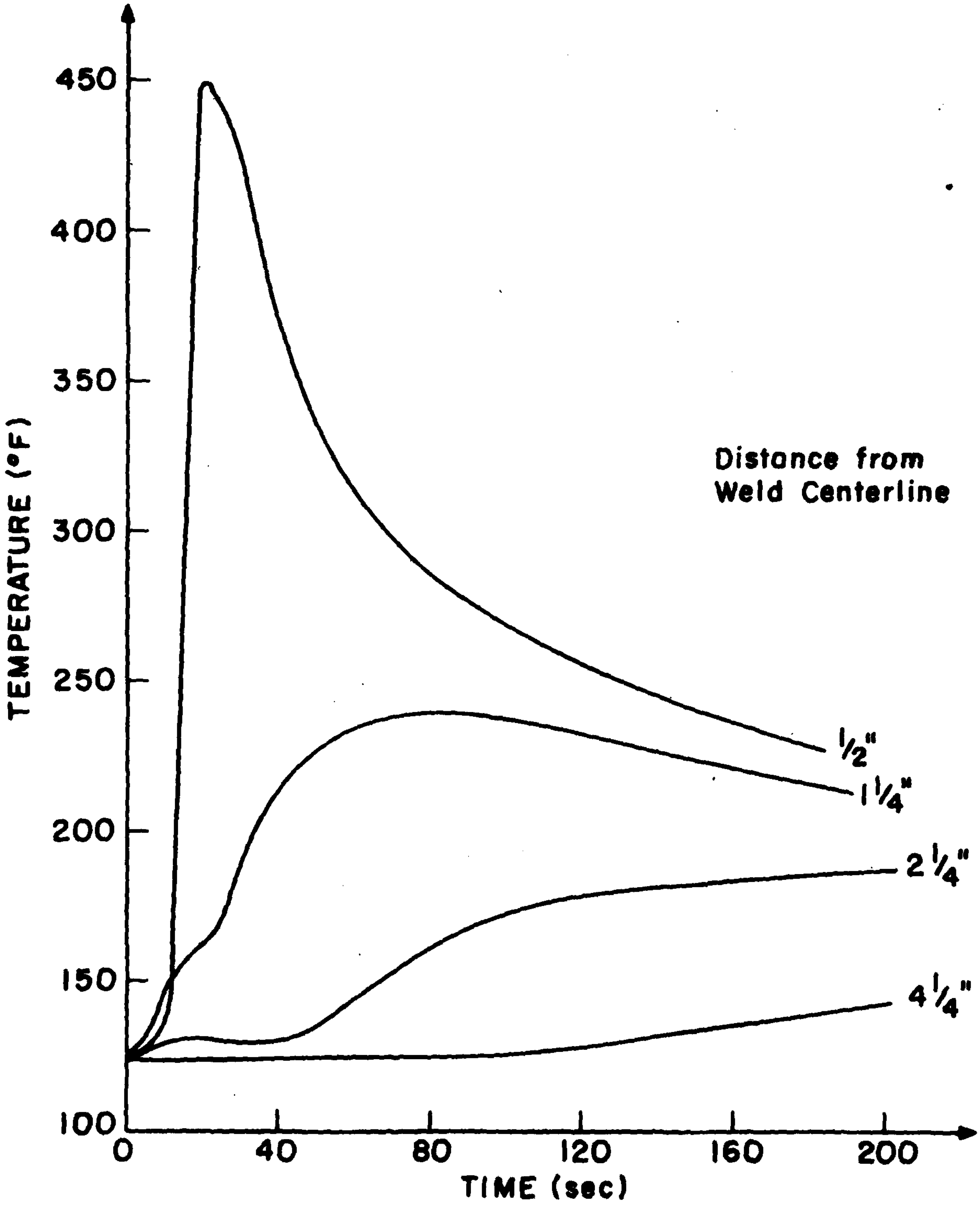

FIGURE 2.41 EXPERIMENTAL TEMPERATURE DISTRIBUTION FOR SPECIMEN II (Pass # 1)

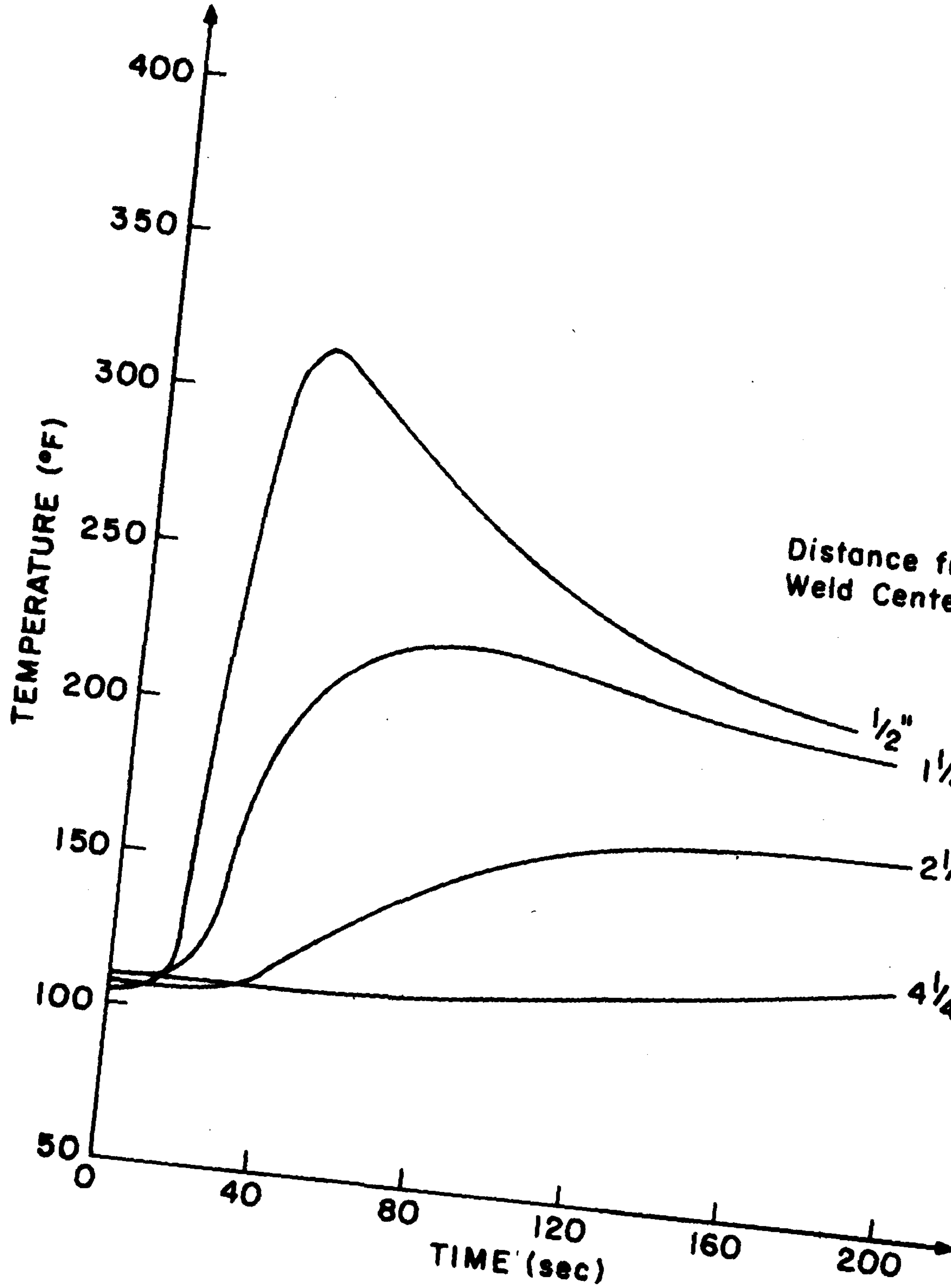

FIGURE 2.42. EXPERIMENTAL TEMPERATURE DISTRIBUTION FOR SPECIMEN II (Pass #2)

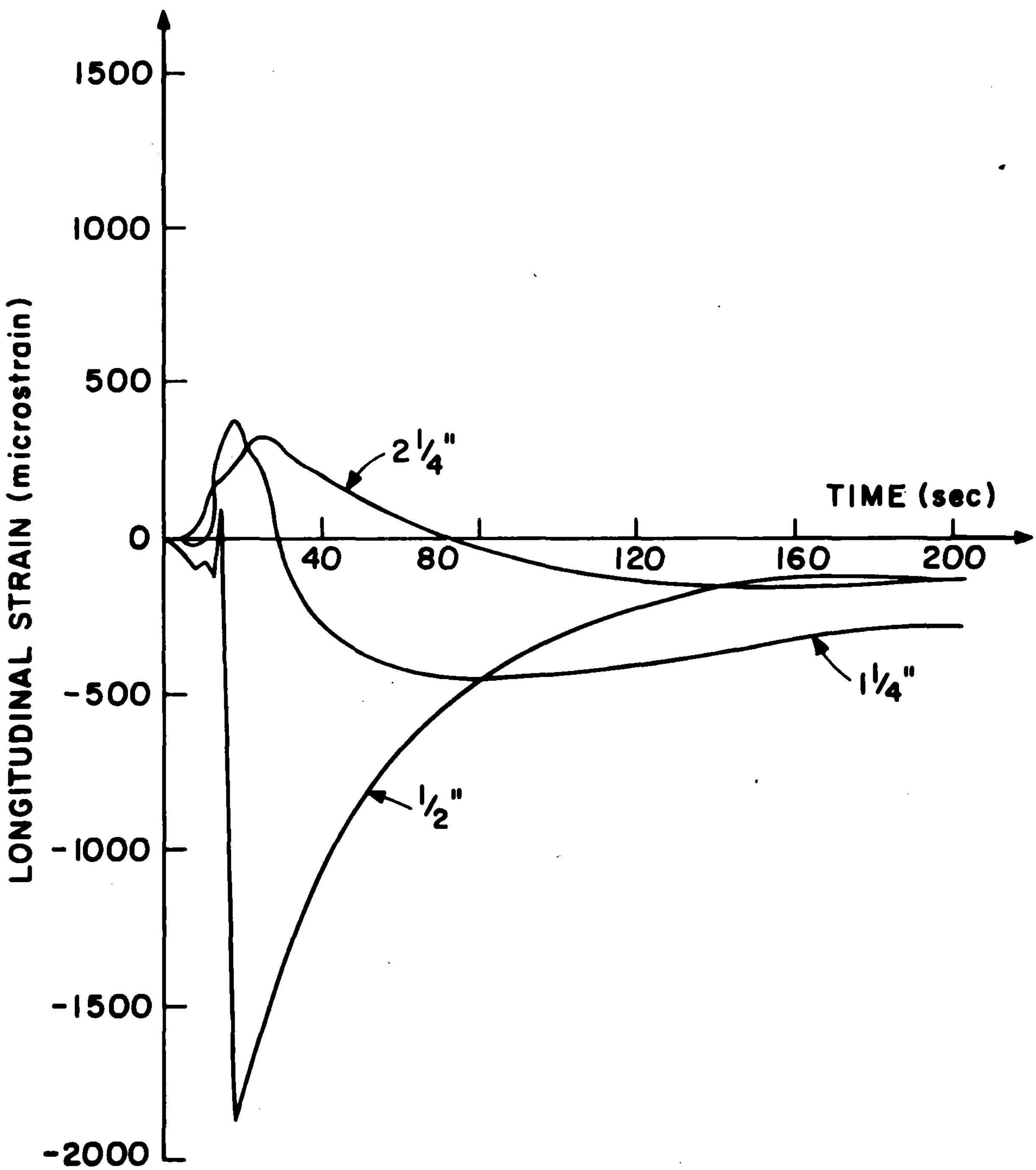

FIGURE 2.43 EXPERIMENTAL LONGITUDINAL STRAIN DISTRIBUTION FOR SPECIMEN II (Pass #1)

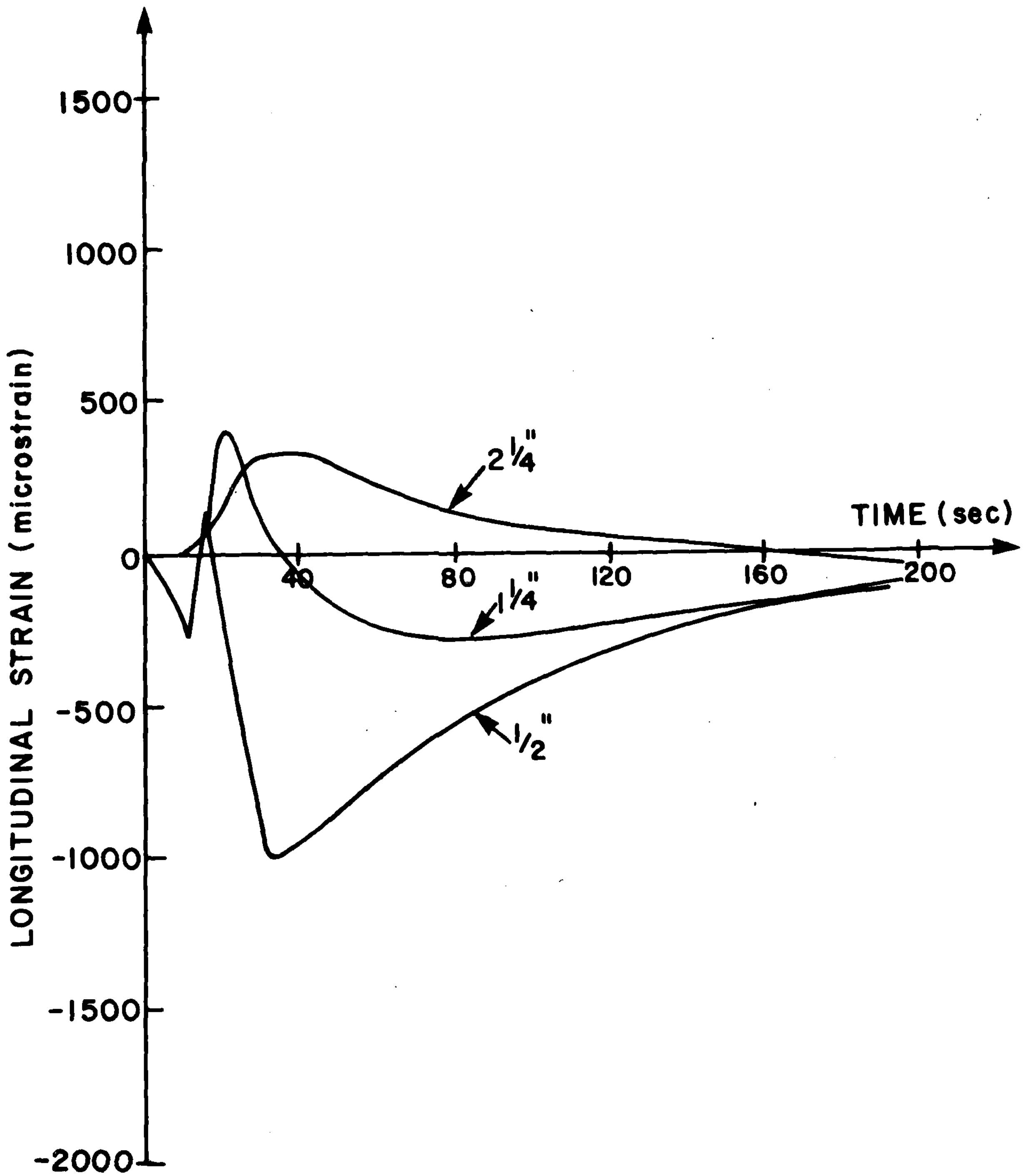

FIGURE 2.44 EXPERIMENTAL LONGITUDINAL STRAIN DISTRIBUTION FOR SPECIMEN II (Pass #2)

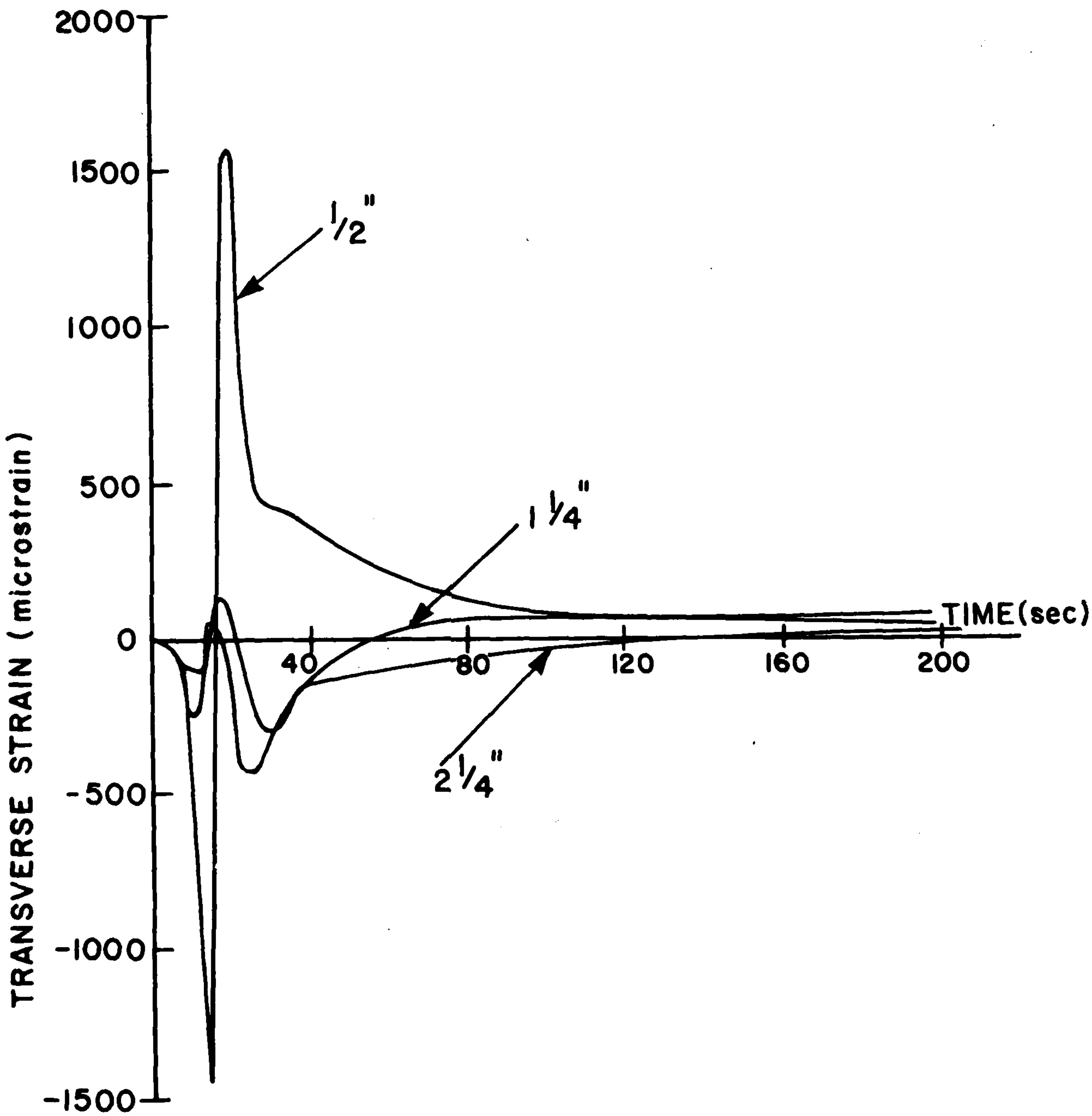

FIGURE 2.45 EXPERIMENTAL TRANSVERSE STRAIN DISTRIBUTION FOR SPECIMEN II (Pass #1)

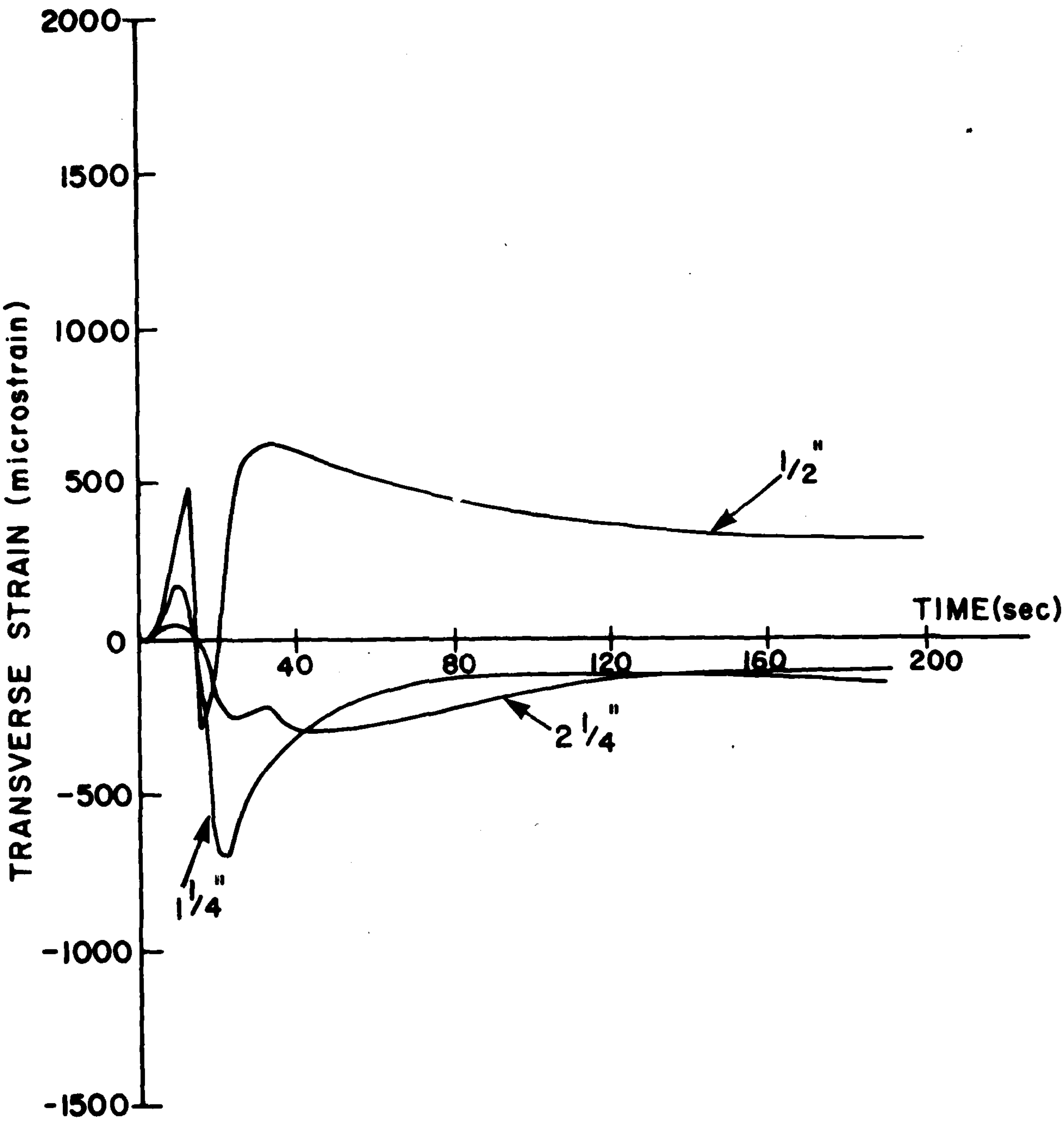

FIGURE 2.46 EXPERIMENTAL TRANSVERSE STRAIN DISTRIBUTION FOR SPECIMEN II (Pass #2)

specimens (as presented in Section 2.3.2 of this report), one finds many qualitative similarities. Nevertheless, more conclusive observations will be made after all data are analyzed using the finite element programs now under development.

2.8 Analysis of Data Obtained in Steps 1.5 and 1.6 (Step 1.7)

The efforts towards improving the prediction of temperatures and strains during welding were focused in two directions:

(a) The improvement of closed-form analytical solutions.

(b) The improvement of numerical solutions, with special emphasis on the finite element method.

Following is a summary of the progress made during the first two years of this project.

2.8.1 Closed-Form Solutions

An effort was carried out to find more accurate closed-form solutions than the ones provided by moving point or line sources for the problem of heat flow during welding. A mathematical model was developed for solving the governing partial differential equation for heat transfer under the following assumptions:

a. Quasi-stationary state.
b. Heat input is provided by a three-dimensional skewed normally distributed heat source.
c. The thermal conductivity of the material is a linear function of temperature.
d. The thermal diffusivity of the material is constant.
e. Convective boundary heat losses are taken into account through a constant convective heat transfer coefficient.
f. Radiation boundary heat losses are taken into account through a constant effective heat transfer coefficient.
g. Phase transformation effects are neglected.

Based on the above assumptions, a closed-form solution in series form was obtained.[8] A computer program was then developed that implemented this solution.

Figure 2.47 shows a sample result of the analysis and compares it with experimental observations. The case under consideration involves the GMA welded HY-130 steel plates referred to earlier (pass number 3 at a point 1" away from the weld line). It can be observed that the analysis predicts faster cooling rates than the experiment shows. This observations holds for all different constant convective heat transfer coefficients, $\bar{h}$, used. Similar results were obtained for all other locations, as well as for other tests.

Furthermore, one might note that the results shown in Fig. 2.47 are "worse" than the ones appearing in Section 2.4.1 (refer to Fig. 2.21), although a better representation of the arc heat source is claimed here. Such a phenomenon occurs because in the present solution care is taken not to violate the heat flow equilibrium conditions, at the expense of assuming a constant thermal diffusivity for the material and a linear temperature dependence of thermal conductivity. On the other hand, the results shown in Fig. 2.21 were obtained using an iterative procedure in order to take into account the temperature dependence of the thermal properties, something that violated the equilibrium conditions and that could lead in certain cases to unstable solution schemes.

The aforementioned discussion leads to the conclusion that the complexity of the welding problem does not easily allow for the effective application of purely analytical techniques. Numerical methods should therefore be employed if good predictive capabilities are required.

2.8.2 Numerical Solutions

As originally proposed, efforts were made to develop a finite element computer program capable of predicting temperatures, strains, and

[8] More details on the solution technique used, as well as on the finally derived expression and the computer program developed, will be included in Papazoglou's Sc.D. Thesis, to be completed in May, 1980.

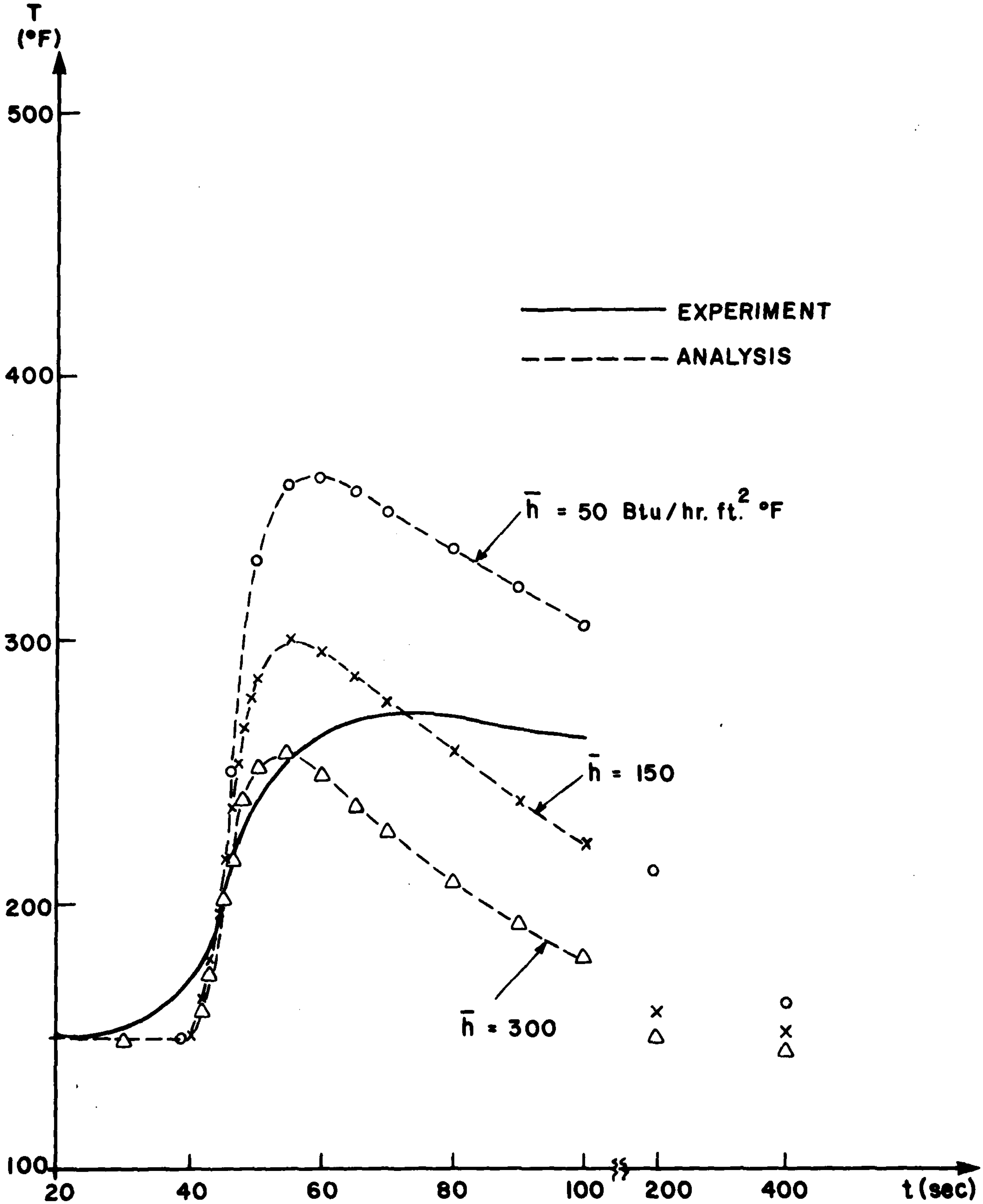

FIGURE 2.47 TEMPERATURE DISTRIBUTION DURING WELDING
(closed form solution)

distortion during welding. The efforts so far have been mainly concentrated on the heat transfer part of the welding problem.

The multi-purpose finite element computer program ADINAT (Automatic Dynamic Incremental Nonlinear Analysis of Temperature) was used as a basis on which modifications were made for the handling of the heat flow during welding problem. These modifications included among others the incorporation of a variable time step during the transient analysis and the addition of phase transformation capabilities.[9] It should also be mentioned at this point that the present version of ADINAT is capable of performing non-linear transient heat transfer analyses. The possible nonlinearities include dependence of material thermal properties on temperature, element birth-and-death options, temperature dependence of convective heat transfer coefficient, and incorporation of radiation heat losses.

The above program was used for modeling the multi pass GMA butt welding of 1 in. thick HY-130 plates. A transverse cross section, 1" thick, located at the mid-portion of the plate was analyzed. The analysis performed was thus a two-dimensional transient non-linear one. Figure 2.48 shows the mesh used. This mesh is rather crude and was used to establish the various parameters that are input to the program. Furthermore, only the first three passes were analyzed for the same reasons.

Figure 2.49 is a sample of the results obtained and their comparison with experiments. The correlation is generally good with the exception of the later stages of the cooling at which the analysis predicts slower cooling rates than the ones observed. It is, however, believed that when a finer mesh is used an even better correlation will result. Computer runs using a finer finite element mesh are going to be performed in the near future.

Regarding the strain analysis, initial efforts were made using the multi-purpose finite element program ADINA (Automatic Dynamic Incremental

---

[9] These changes are indicated by the M.I.T. welding group but were actually carried out by Professor Bathe's assistants for propriatory reasons.

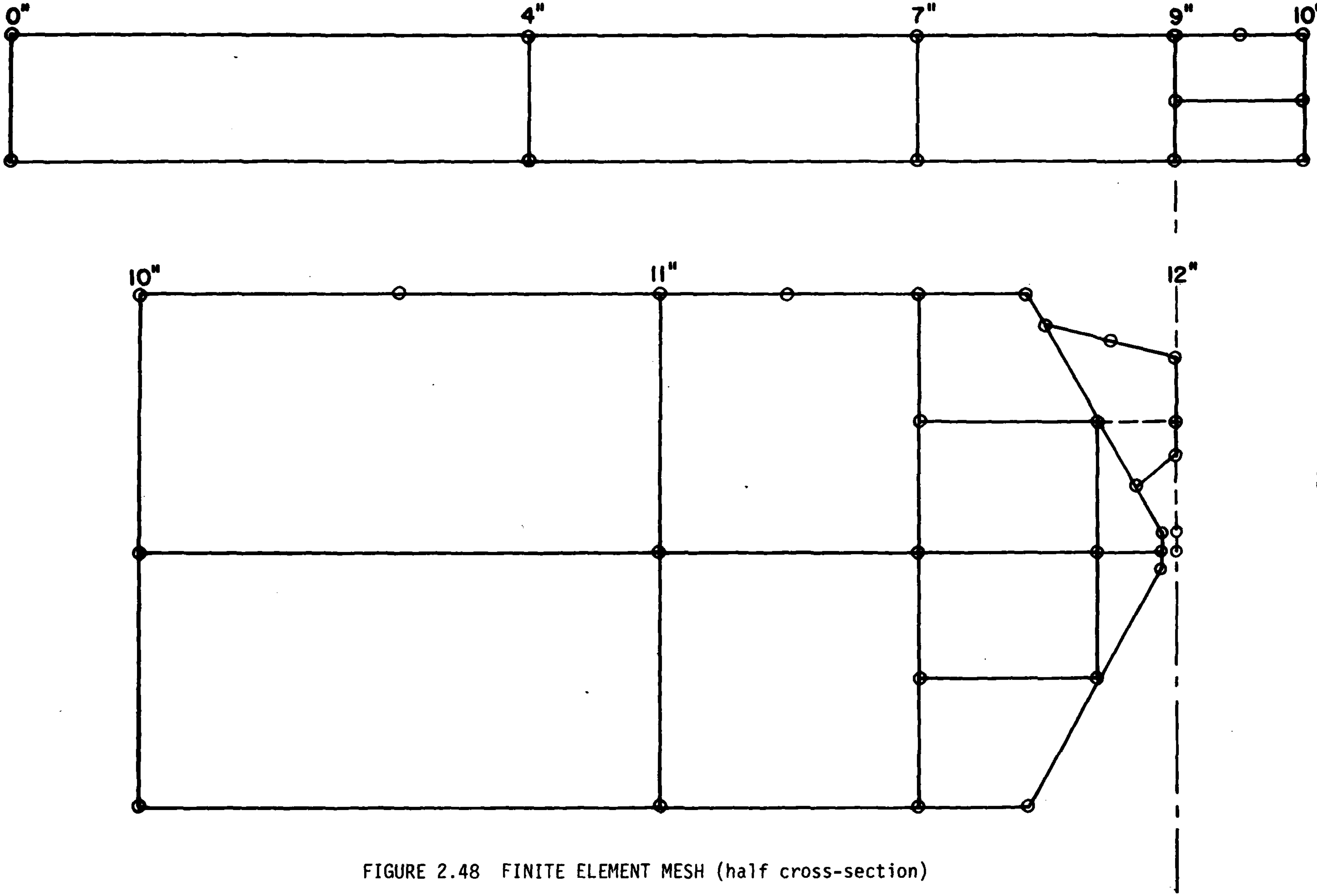

FIGURE 2.48 FINITE ELEMENT MESH (half cross-section)

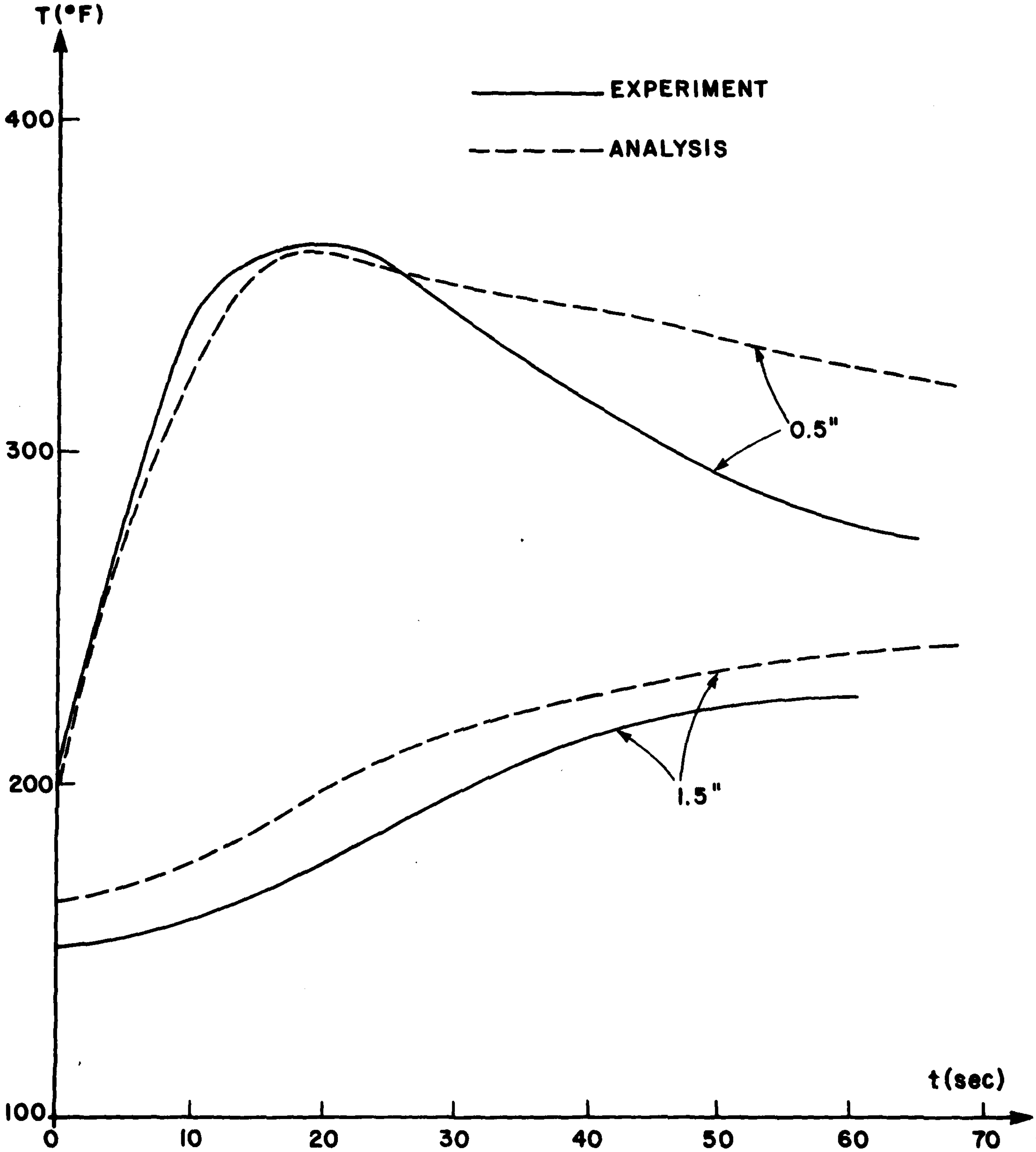

FIGURE 2.49 TEMPERATURE DISTRIBUTION DURING GMA WELDING OF 1" THICK HY-130 PLATE (pass #2)

Non-linear Analysis). The current version of the program was used without any modifications. It should be noted that ADINA is capable of performing thermo-elastic-plastic and creep calculations by using constitutive equations modified for high temperatures. Furthermore, both plane strain and plane stress two-dimensional analyses can be performed.

Despite of all these, however, some modifications have to be made on the program to suit the welding problem. These are the following:

1. In its current version, ADINA prints out as final results stress-histories, whereas during the experiments strain histories are measured. A modification should, therefore, be made in the program's logic to calculate and print-out strain histories.

2. A single time step is currently used in ADINA for transient analyses. This means that when analyzing the welding problem, which for efficiency requires different time steps during the early and late stages of cooling, the program should be stopped and restarted, a very time consuming operation. Efforts will thus be made to incorporate a variable time step into the program.

3. Finally, ADINA does not take into account phase transformation effects. At the present time Papazoglou is at the last stages of developing subroutines that will be incorporated into ADINA and which will be capable of predicting the metallurgical microstructures resulting from the welding operation and of subsequently modifying the strain tensor to take into account transformation effects.

Given the fact that the above modifications are in the process of being implemented, no results of the initial computer runs are presented, basically because no meaningful comparison can be made between the predicted stresses and the experimental strains.

3. PROGRESS OF TASK 2 - CYLINDRICAL SHELLS
December 1, 1977 to November 30, 1979

3.1 General Status

According to the original proposal the research during the first two years of this project would include the following under Task 2:

2.1 Development of details of research plan for the first year.

2.2 Experiment of girth welding along a groove of a cylindrical shell.

2.3 Analysis of data obtained in 2.2.

2.4 Development of details of research plan for the second year.

2.5 Measurement of residual stresses in specimens made in Step 2.2.

2.6 Experiment on butt welds between unstiffened cylindrical shells.

2.7 Analysis of data obtained in 2.5 and 2.6.

This research program has been slightly modified. The modifications will be dealt with in the appropriate places.

3.2 Development of Details of the Research Plan

It was originally proposed that an experiment would be carried out during the first year of this research project on measuring temperature and strain changes during girth welding along the machined groove of a cylindrical shell. Discussions among the M.I.T. investigators involved in this research project, however, led to the conclusion that such a test did not represent a realistic simulation of practical applications. It was therefore tentatively decided to skip Steps 2.2, 2.3, and 2.5 (refer to Section 3.1) and proceed with Step 2.6. These thoughts were communicated to representatives of the Office of Naval Research from where a positive response was received. The decision was thus finalized.

A first experiment was performed outside M.I.T. on butt welding two unstiffened low-carbon steel cylindrical shells. This exploratory experiment was of great value, providing the M.I.T. investigators with experience that could be applied to similar experiments conducted at M.I.T. and using HY-130 steel cylinders.

The following two sections describe such experiments and the analysis done on the collected data.

3.3 Experiment on Butt Welds Between Unstiffened Cylindrical Shells (Step 2.6)

The following thesis, dealing with Step 2.6 and part of Step 2.7, has already been completed:

Mabry, J. P., "Prediction and Control of Residual Stresses and Distortion in HY-130 Thick Pipe Weldments", Ocean Engineer Thesis, M.I.T. May 1979.

A summary of the results appearing in this thesis is presented below.

3.3.1 Description of Experimental Procedure

The objective of the experiment was to measure temperature, strains, and distortion during the butt welding of two unstiffened cylindrical shells made of HY-130 steel. The cylindrical shells were to be formed from flat plates since no cylinders of the material and dimensions required were readily available.

The initial material was obtained from the NSRDC, Annapolis Laboratory in the form of HY-130 plates 60" x 63" x 3/4". A request was then made to Portsmouth Naval Shipyard to roll the plates into cylindrical shapes. Due to the thickness (3/4") of the plate to be formed into a small outside diameter (18"), however, the shipyard engineers suggested that it would be necessary to form a cylinder by bending two plates to semi-circular cylindrical shapes and then welding the two halves together. This suggestion was followed as seen in Fig. 3.1.

The two semi-cylinders were seam welded at the M.I.T. Laboratory by the gas metal arc welding (GMAW) process, using Argon/1%O_2 as shielding gas and a 1/16" diameter Linde 140S filler wire. Seven passes were required to fill the 60° Single V Groove joint geometry. A common preheat and interpass temperature of 200°F was applied. Table 3.1 provides the welding conditions during each pass (note that it also provides the welding conditions for the subsequent butt welds). Prior to

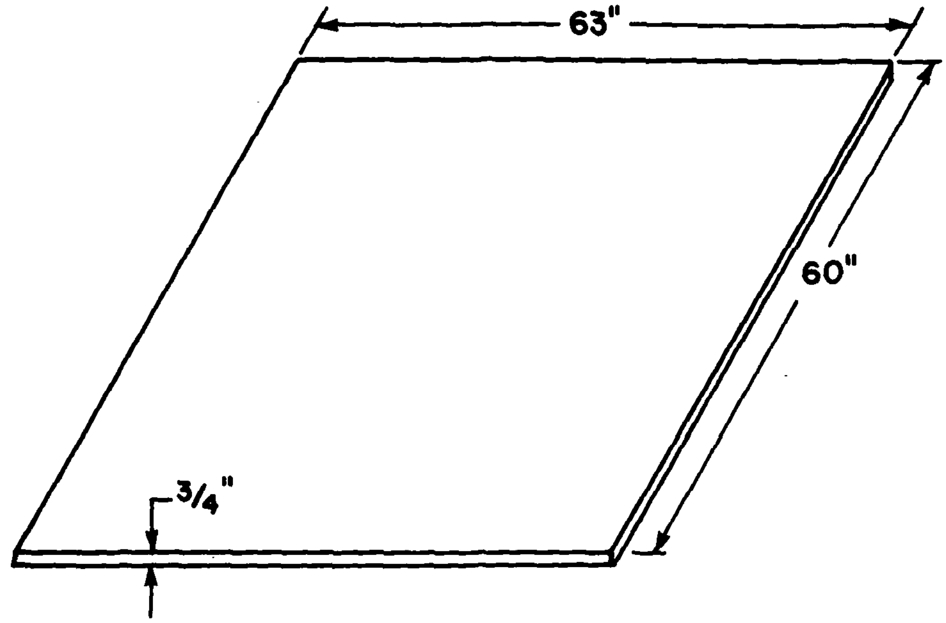

STAGE 1 - HY-130 PLATE WITH DIMENSIONS SHOWN

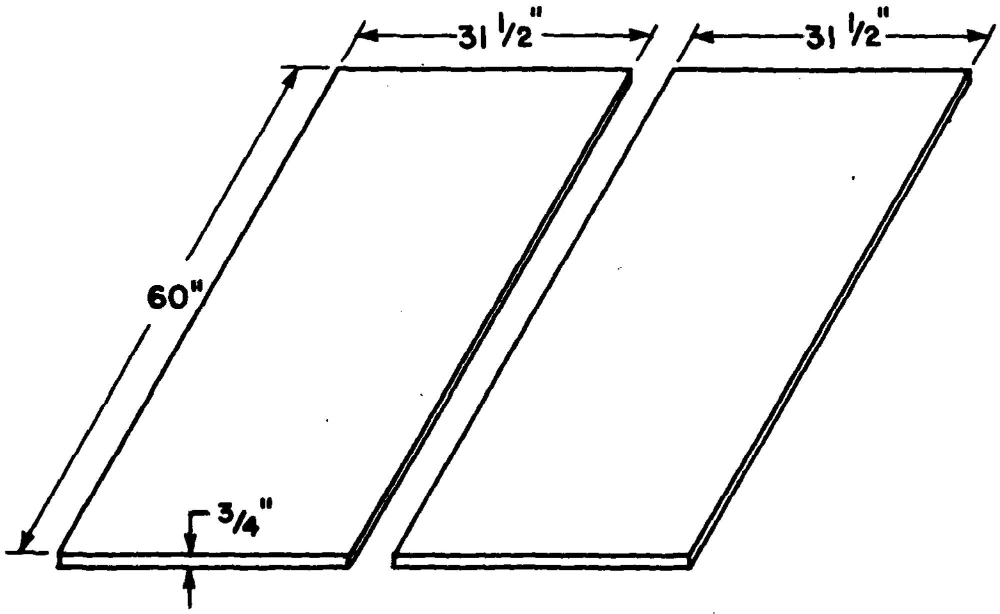

STAGE 2 - PLATE FLAME CUT TO DIMENSIONS SHOWN

FIGURE 3.1 STAGES OF CYLINDER FABRICATION

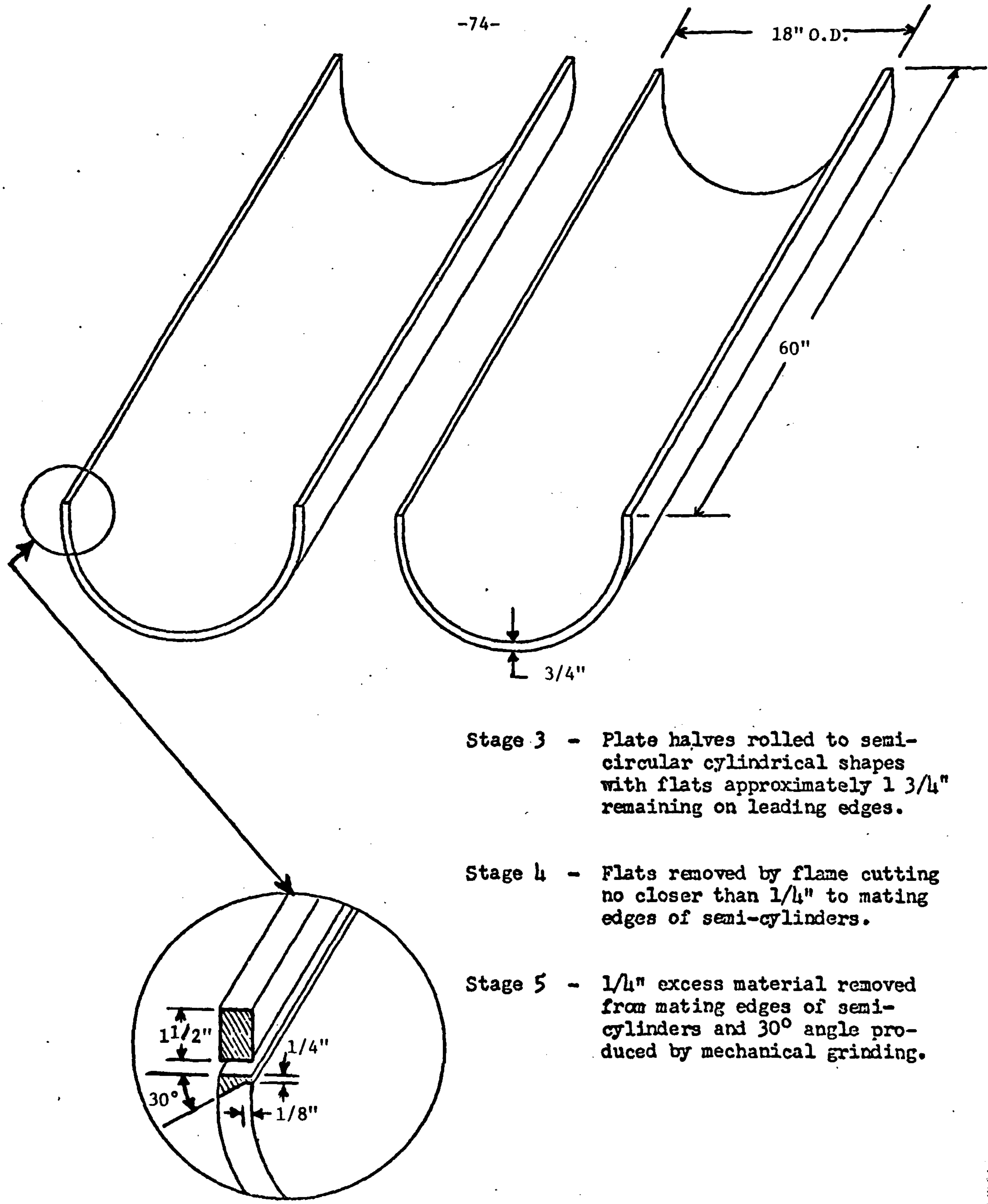

Stage 3 - Plate halves rolled to semi-circular cylindrical shapes with flats approximately 1 3/4" remaining on leading edges.

Stage 4 - Flats removed by flame cutting no closer than 1/4" to mating edges of semi-cylinders.

Stage 5 - 1/4" excess material removed from mating edges of semi-cylinders and 30° angle produced by mechanical grinding.

FIGURE 3.1 STAGES OF CYLINDER FABRICATION
(Continued)

TABLE 3.1 WELDING CONDITIONS DURING EACH PASS OF THE SEAM AND BUTT WELDS.

	SEAM WELD PASSES			BUTT WELD PASSES		
WELD PASS NO.	I	V	v	I	V	v
1.	320	26	0.20	270	26	0.20
2.	320	25	0.20	290	25.5	0.20
3.	320	25	0.20	270	26	0.20
4.	300	26	0.27	285	25.5	0.20
5.	285	25	0.20	280	26	0.20
6.	280	25	0.20	290	26	0.20
7.	290	25	0.40	-	-	-

I = Welding Current in Amperes

V = arc voltage in Volts

v = arc travel speed in inches/sec

Note: Heat input, $Q = \frac{VI}{v}$, for each pass was held below 40,000 Joules/inch.

positioning the cylinder on the welding table, the two cylinder halves were tack welded at positions 6" from either end and at the center with 1" welds on the inside of each mating edge.

Although the main objective of the experiment was, as stated above, the measurement of temperature, strains and distortion during butt welding two unstiffened cylinders, it was decided to measure these variables during the seam welding operation as well. Figure 3.2 provides the location of the electric resistance strain gages and the Chromel/Alumel thermocouples used. Note that the arrangement depicted is such so as to allow the use of the same strain gages and thermocouples for both the seam and butt welds.

After completion of the seam weld, the 60 inch long, 18 inch OD HY-130 cylinder was transported to the Army Materials and Mechanics Research Center in Watertown, Massachusetts, where it was sawn into three sections, each 20 inches in length--laboratory limitations could not allow the joining of longer cylinders. The two sections to be joined were then prepared for welding by machining a 60° single Vee groove (see Fig. 3.3).

The actual butt welding of the two cylinders was performed at the M.I.T. laboratory. A supporting structure that would allow uniform cylinder rotation at a controlled speed with respect to the fixed position of the GMAW torch was designed and manufactured. This structure supported the two cylinders from within and was bolted to the base of a tilting turntable to allow for constant clearance between the stationary GMAW torch and cylinder outer wall during rotation.

The butt welding was performed under similar to the seam welding conditions. Six passes were required (see Fig. 3.4). Table 3.1 provides welding current, arc voltage, and arc travel speed data for each pass.

Temperature changes and transient strains were measured using the instrumentation described above. To measure radial distortion during welding, two Bourns Linear Motion Potentiometers were placed at the inner surface of one of the two cylinders.

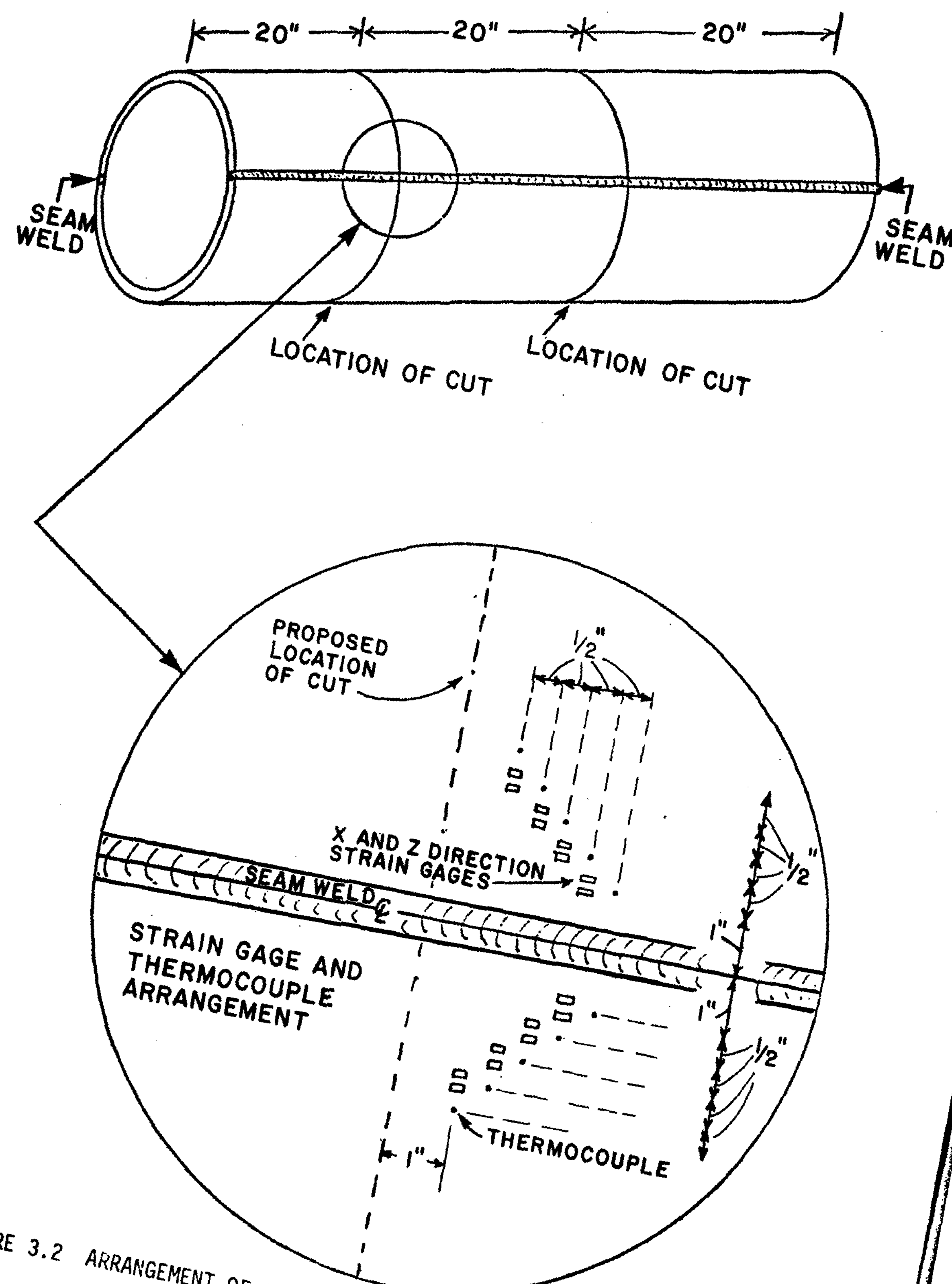

FIGURE 3.2 ARRANGEMENT OF STRAIN GAGES AND THERMOCOUPLES

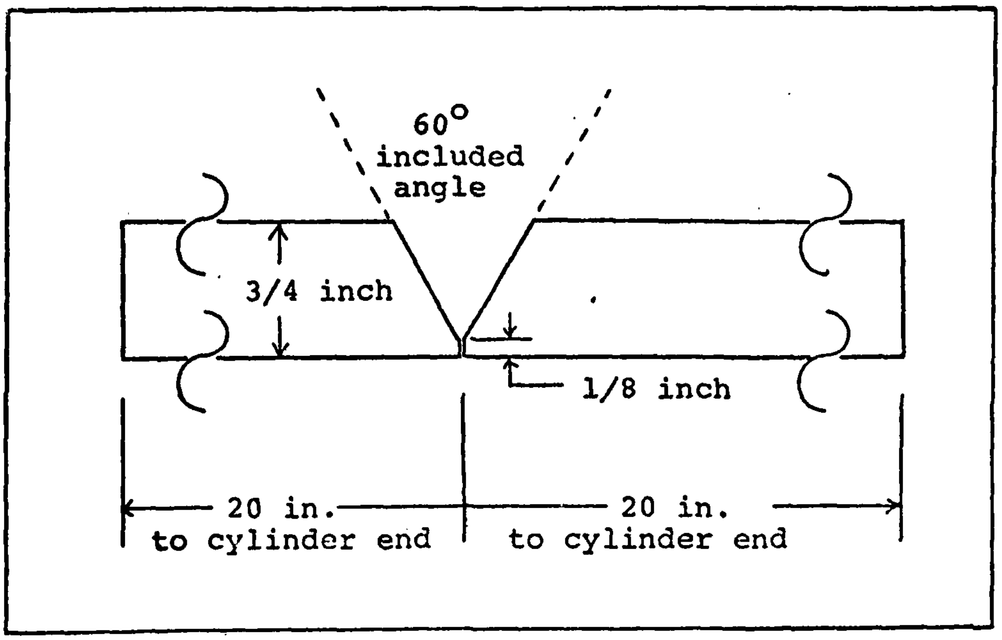

FIGURE 3.3 WELD JOINT GEOMETRY FOR THE BUTT WELDING OF THE TWO CYLINDERS

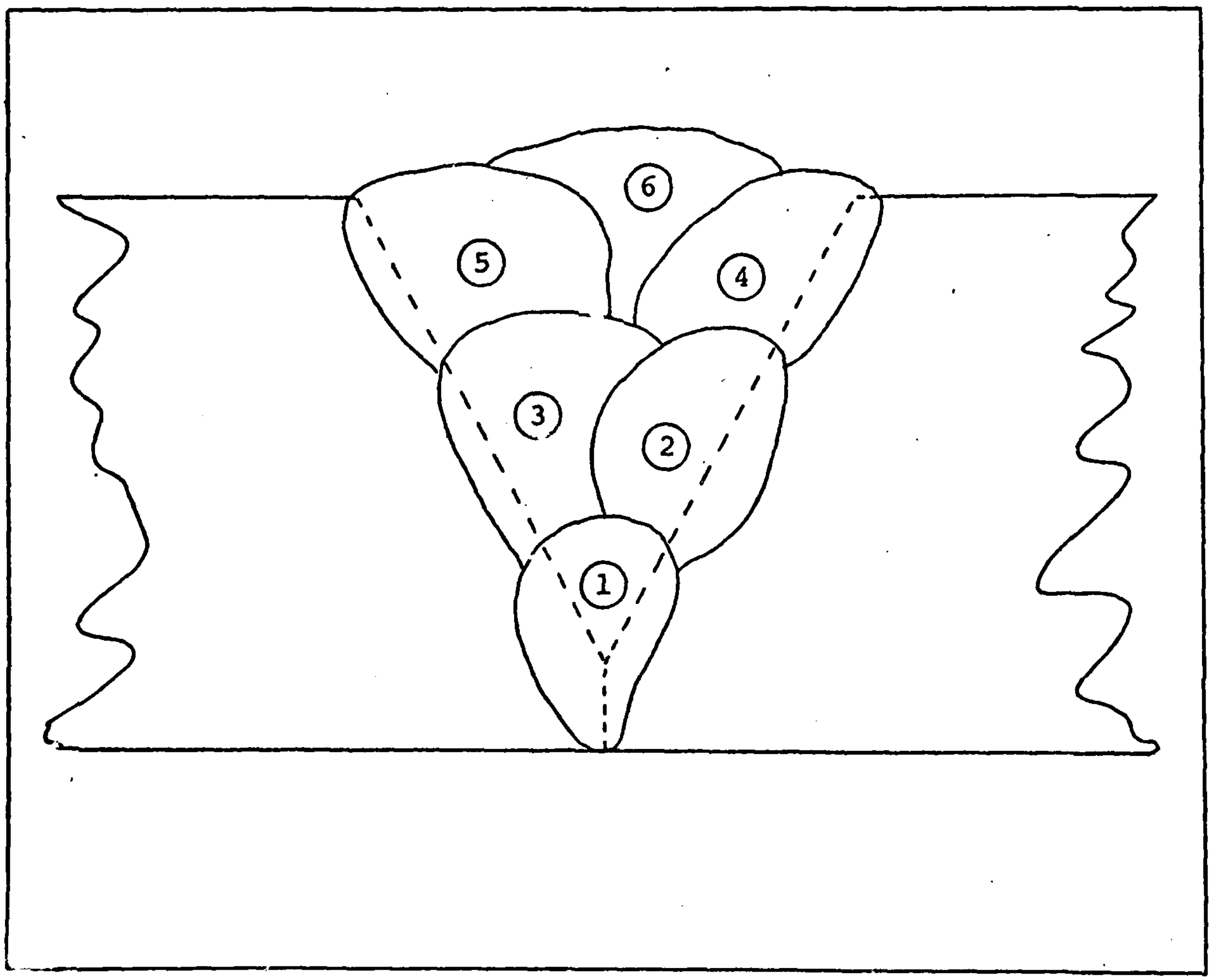

FIGURE 3.4 APPROXIMATE SHAPE OF WELDING PASSES PERFORMED FOR THE JOINING OF THE TWO CYLINDERS

3.3.2 Experimental Results

Four types of results were obtained from the performed experiment, as follows:

a. After the 60 inch cylinder was formed by seam welding, a 1/2 inch ring was cut for metallurgical examination. 500X photo-micrographs, and 1200X and 6000X electron scan micrographs of the weld metal, the fusion zone, the heat affected zone, and the parent metal were taken. These micrographs are currently under examination.

b. Temperature changes were measured during each welding pass, between passes, and during the final cooling stage of both the seam and butt welds. Figure 3.5 shows the temperature distribution obtained during the first pass of the butt welding.

c. Transient strains in two directions were similarly measured for both the seam and butt welds. For the case of the butt welds, strains were measured in the direction along the cylinder length (herein called longitudinal or x-direction) and in the circumferential direction or else the one of welding arc travel (herein called transverse or z-direction). Figures 3.6 through 3.9 provide curves of experimentally determined transient strain distributions at 1, 1.5, 2, and 2.5 inches from the weld line (the analytically obtained curves shown will be referred to later). The distributions shown are for the first welding pass. Positive values of strain denote tension and negative ones compression.

d. Radial distortion was measured at two points, 1/2 and 1 inch away from the weld centerline, during the butt welding of the two cylinders. Figure 3.10 shows the data obtained for the first welding pass (the analytical curves shown will be referred to later). Positive values of radial distortion correspond to displacements in the outward direction from the cylinder center, i.e., expansion.

3.4 Analysis of Data Obtained When Butt-Welding Unstiffened Cylindrical Shells (Step 2.7)

An analysis of the problem of welding two unstiffened cylindrical shells was performed using existing computer programs developed at M.I.T.

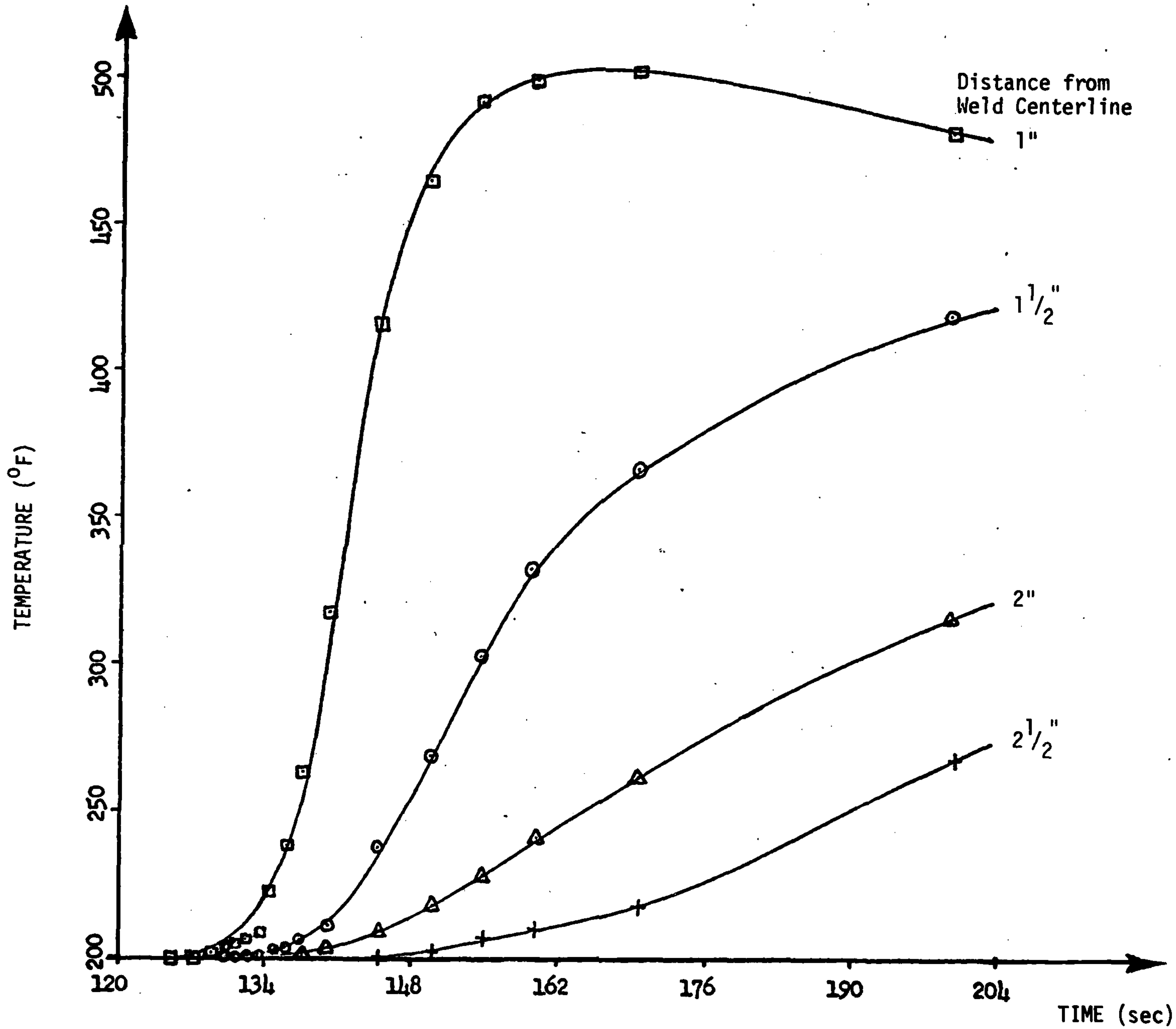

FIGURE 3.5 EXPERIMENTAL TEMPERATURE DISTRIBUTION FOR THE FIRST PASS OF THE BUTT WELD

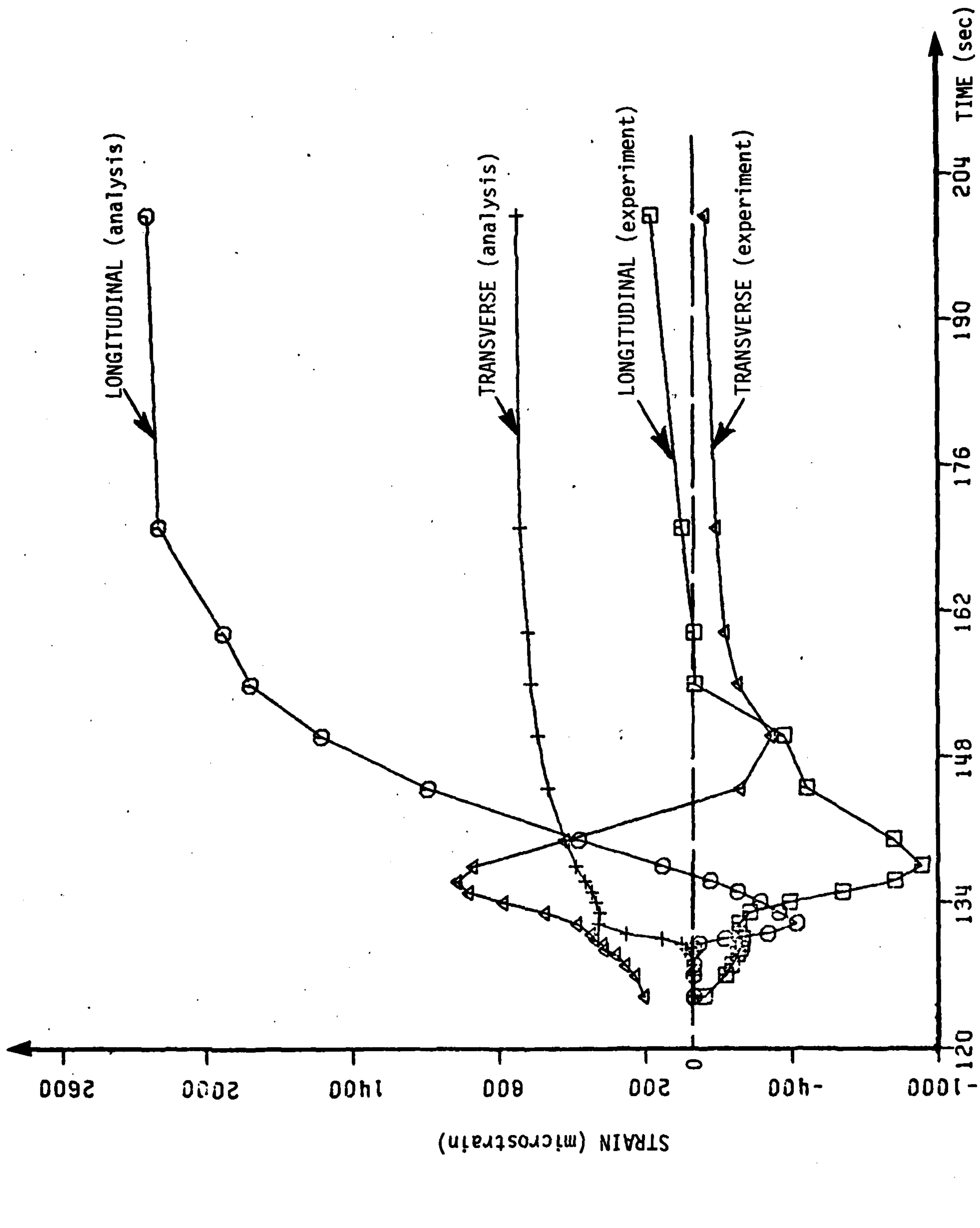

FIGURE 3.6 COMPARATIVE PLOT OF EXPERIMENTAL AND ANALYTICAL STRAIN 1.0 IN. FROM WELD CENTERLINE (First Pass)

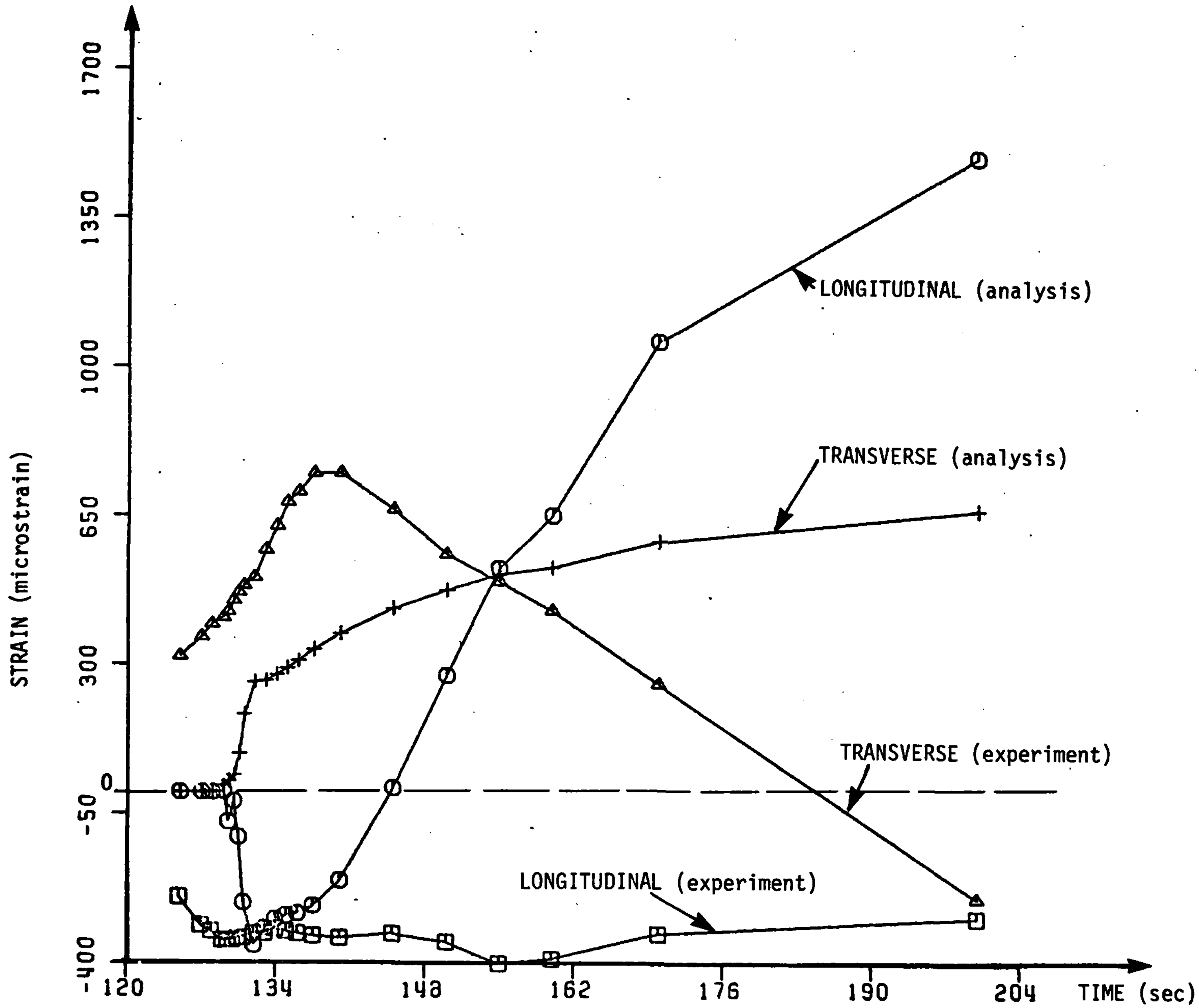

FIGURE 3.7 COMPARATIVE PLOT OF EXPERIMENTAL AND ANALYTICAL STRAIN 1.5 IN. FROM WELD CENTERLINE (First Pass)

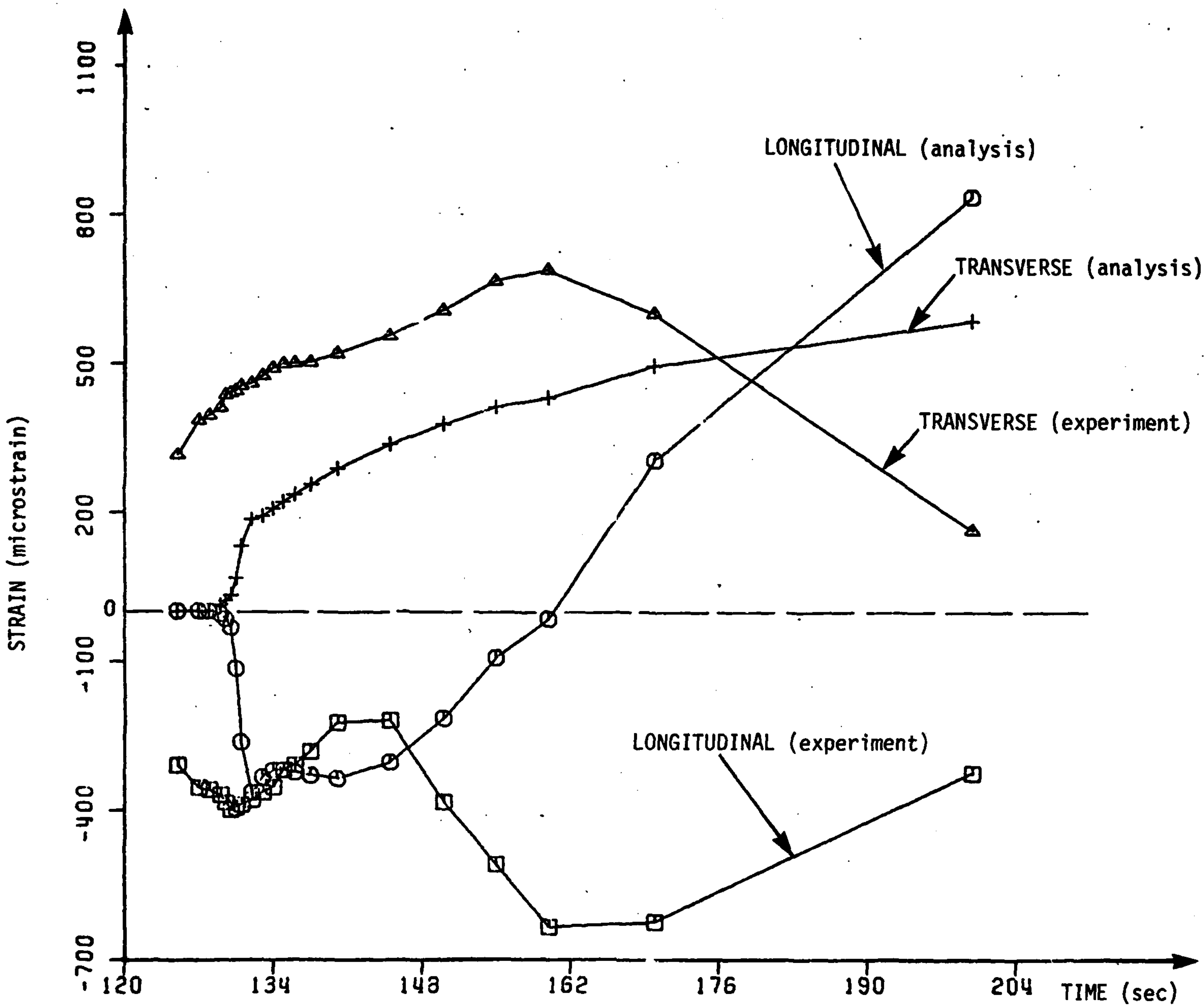

FIGURE 3.8 COMPARATIVE PLOT OF EXPERIMENTAL AND ANALYTICAL STRAIN 2.0 IN. FROM WELD CENTERLINE (First Pass)

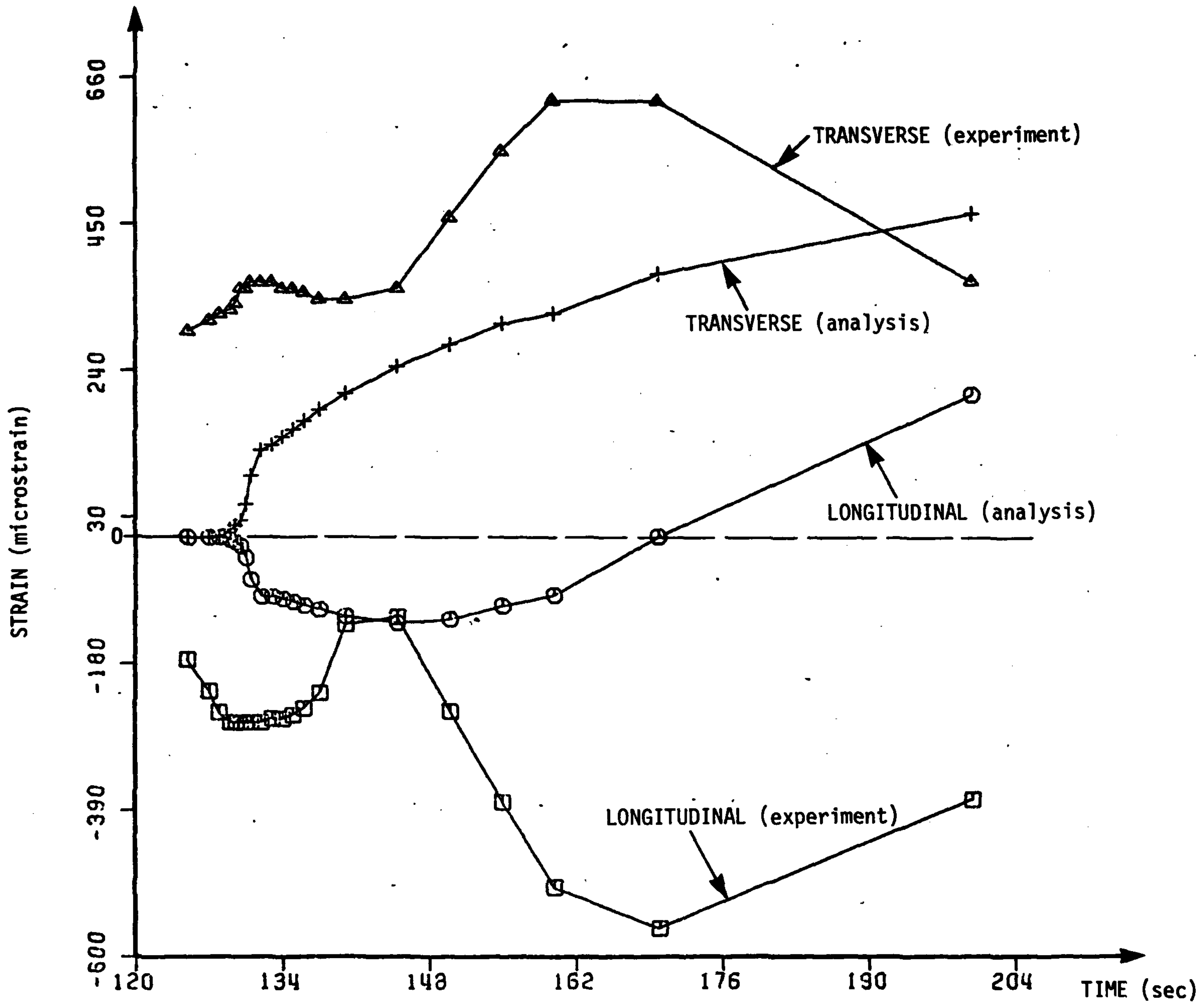

FIGURE 3.9 COMPARATIVE PLOT OF EXPERIMENTAL AND ANALYTICAL STRAIN 2.5 IN. FROM WELD CENTERLINE (First Pass)

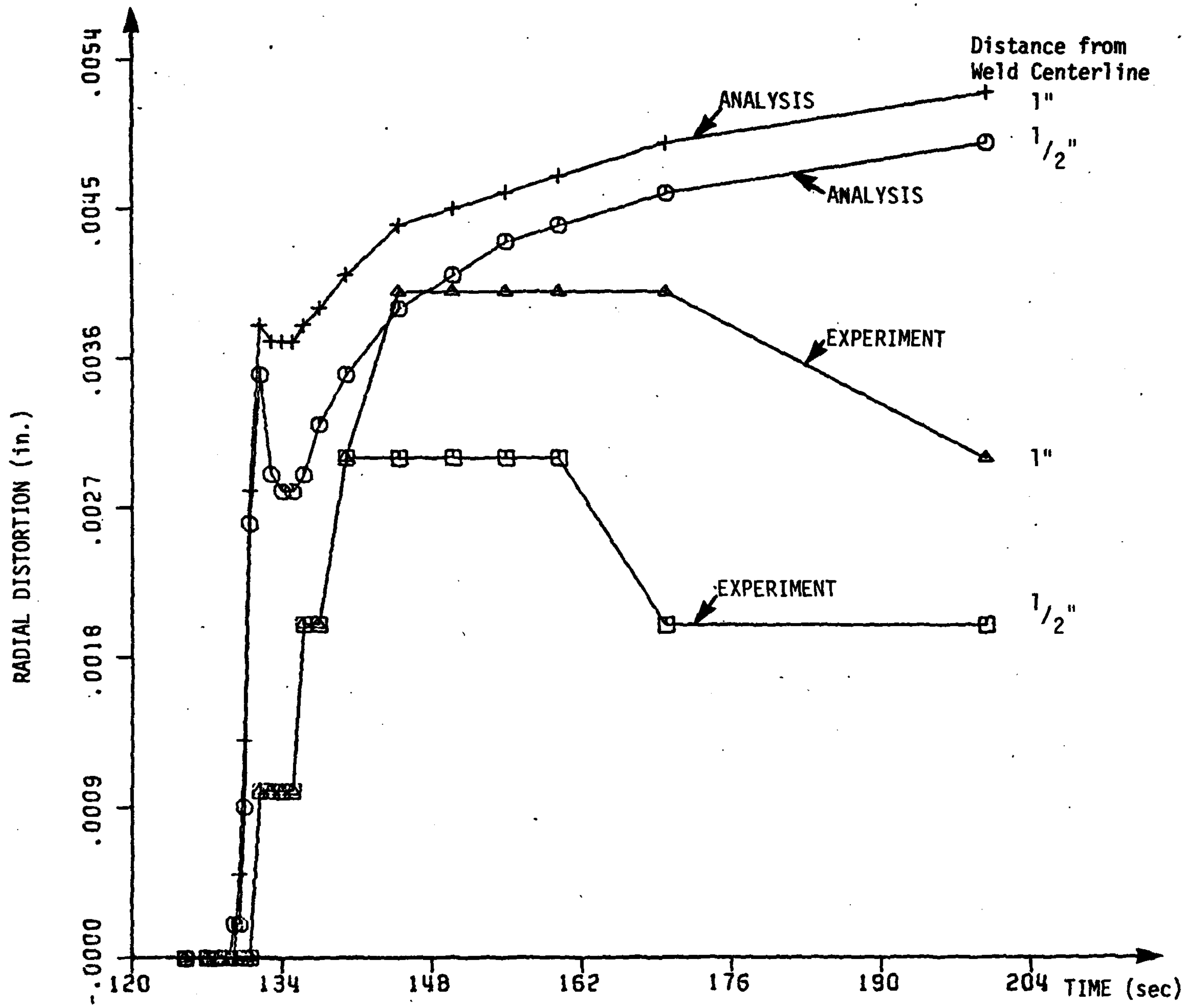

FIGURE 3.10 COMPARATIVE PLOT OF EXPERIMENTAL AND ANALYTICAL RADIAL DISTORTION 0.5 IN AND 1.0 IN FROM WELD CENTERLINE (First Pass)

in previous years. The analysis was divided into two parts. First, a heat flow analysis was conducted. The results of this analysis were then used as an input for the stress analysis.

A more detailed discussion of the tools used and the results obtained follows.

3.4.1 Heat Flow Analysis

A computer program[10] capable of predicting temperature distributions during welding was used. This program is based on the analytical solution of the heat conduction problem as developed from a moving point heat source on the surface of a plate of finite thickness and assuming a quasi-stationary state. Furthermore, the solution assumes:

a. A small heat source as compared to the body under consideration.

b. Instantaneous supply of heat.

c. Radiation and convection heat losses are negligible.

d. Thermophysical properties do not depend on temperature.

The program is capable of computing the temperature history during welding at any point on the surface and within the thickness of a cylinder. Since the output of the program would be used later on as input to the stress analysis program, the points at which temperatures were to be calculated were chosen so as to coincide with the nodes of the finite element mesh shown in Fig. 3.11.

Moreover, the following parameters, pertaining to the first welding pass, were used as input to the heat flow program:

Welding arc velocity (v) = 0.2 in./sec.

---

[10] This program, coded B-4, is explained in detail in: Muraki, T., and Masubuchi, K., "Computer Programs Useful for the Analysis of Heat Flow in Weldments", M.I.T. OSP #81499 and #22016, June 30, 1974.

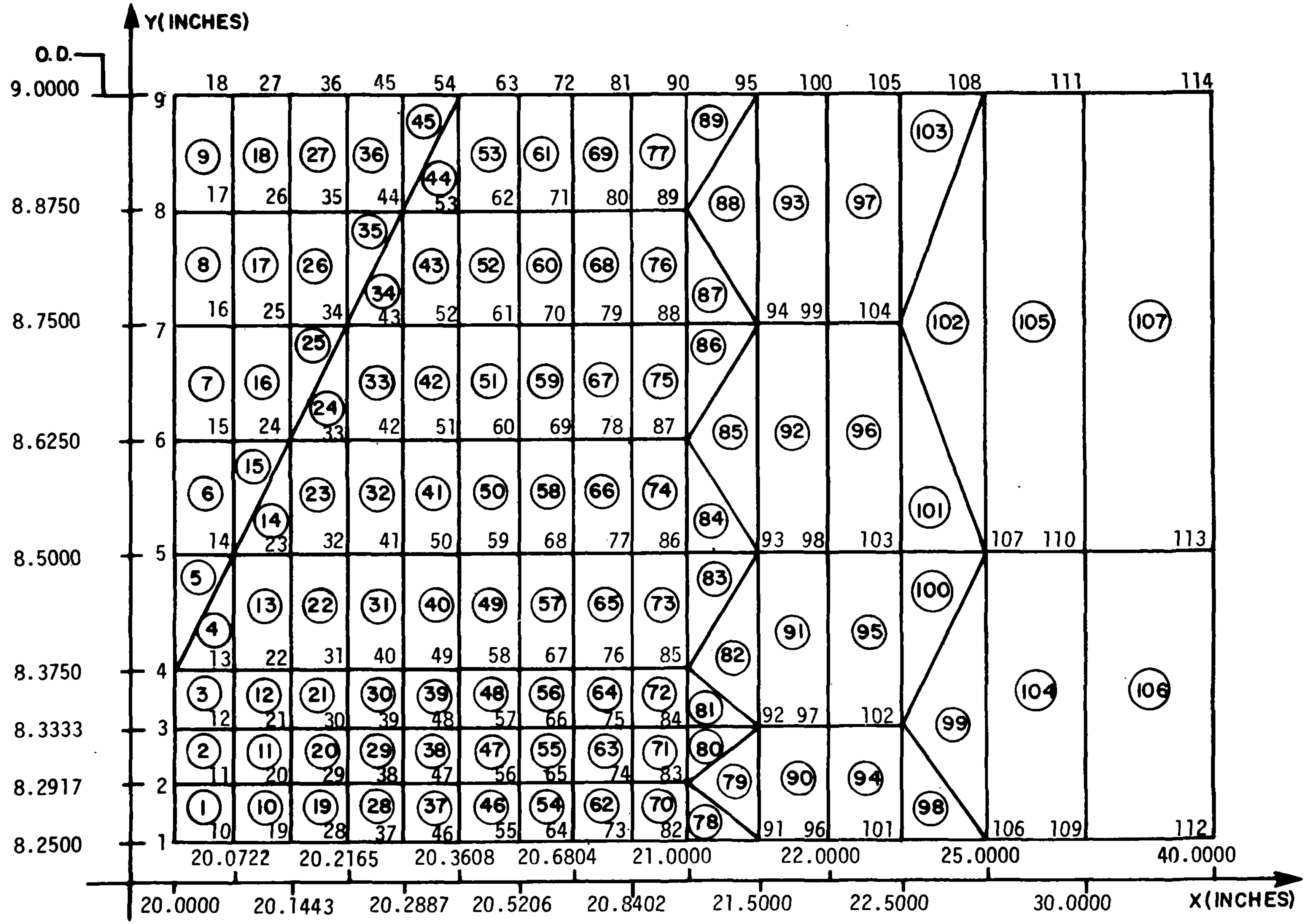

FIGURE 3.11 FINITE ELEMENT MESH USED FOR THE STRAIN, STRESS, AND DISTORTION ANALYSIS

Heat intensity[11] (q) = 6,084 Joules/sec. in.
Density (ρ) = 0.282 lb/in^3
Specific heat (c) = 124.5 Joules/lb.°F
Thermal conductivity (k) = 0.525 Joules/sec. in °F

Figure 3.12 presents the temperature distribution predicted by the computer program at the same four points for which experimental measurements were taken.

Qualitative comparison of the analytical (Fig. 3.12) and measured (Fig. 3.5) temperature distributions shows remarkable coincidence. The slightly higher overall values of the analytically generated values may be explained by the assumed welding arc efficiency of 0.65. No efforts were made to use different arc efficiencies since the obtained results were thought to be adequate for the purposes of the present research stage.

3.4.2 Strain, Stress, and Distortion Analysis

The analysis of strains, stresses, and distortion during butt welding two unstiffened cylindrical shells was performed using a finite element computer program capable of making thermo-plastic analyses of axis-symmetric structural components.[12]

Figure 3.11 depicts the finite element mesh used for the analysis. Note that due to the symmetry of the problem--since only the first welding pass was analyzed--one of two joined cylinders was analyzed. Furthermore, it should be noted that the x-axis is along the cylinder length, the y-axis

---

[11] Heat intensity is defined as:

$$q = \frac{IV\eta_a}{h}$$

where I = arc current
V = arc voltage
h = plate thickness
η_a = arc efficiency (assumed equal to 0.65 for the case under consideration)

[12] *Details about this computer program can be found in* T. Muraki's, "Manual on Axisymmetric Finite Element Program for Analysis of Thermal Stress and Metal Movement During Welding", M.I.T., Cambridge, Mass., January, 1978.

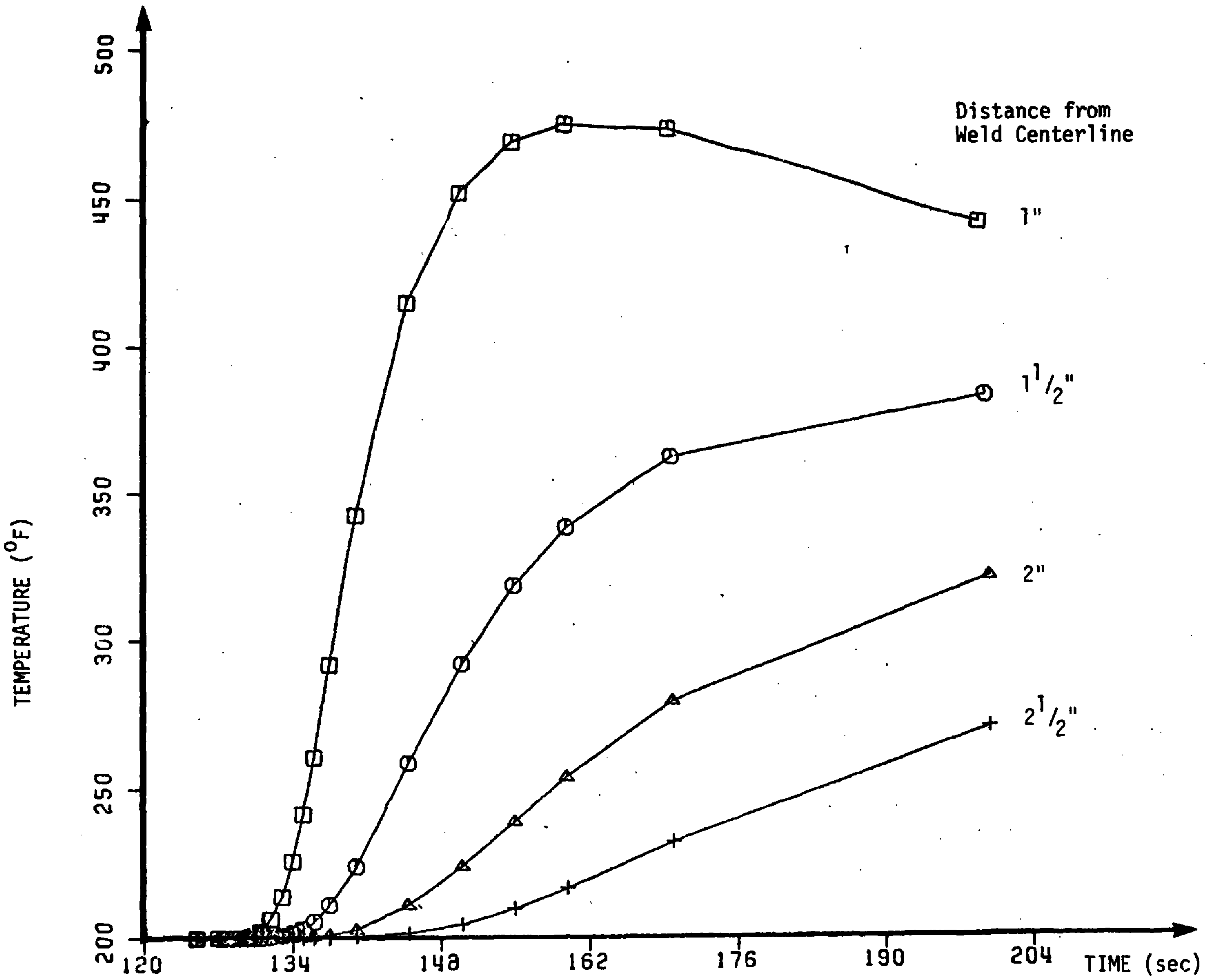

FIGURE 3.12 ANALYTICAL TEMPERATURE DISTRIBUTION FOR THE FIRST PASS OF THE BUTT WELD

along the radial direction, and the origin (x = y = 0) of the axes is located at the center of the cylinder end.

The computer program required as input the temperature history of each nodal point. This information was provided by the heat flow analysis. Other required inputs were the thermophysical and mechanical material properties as a function of temperature (provided by the ONR) and welding parameters (given in Section 3.4.1).

Finally, referring to Fig. 3.11, it should be noted that not all elements in the half-V welding groove were active during the solution. More specifically, and since the first welding pass was analyzed, only element #5 participated in the solution--elements #6, 7, 8, 9, 15, 16, 17, 18, 25, 26, 27, 35, 36, and 45 were absent.

Figures 3.6 through 3.9 present analytically determined longitudinal and transverse transient strain histories at four points (1, 1.5, 2, and 2.5 inches from the weld centerline) and compare them with the measured values. As it can be seen, the comparisons are not favorable. In most cases not only the magnitude but also the sign of the strain differ. Similar observations can be made regarding distortion comparisons (see Fig. 3.10).

The above facts lead to the conclusion that more needs to be done towards refining the computer programs. Such an effort is currently under way.

4. RESEARCH PLAN FOR THE THIRD YEAR

4.1 Task 1 - Thick Plates

It is expected that the work to be carried out during the third and last year of this research contract will conclude all steps originally proposed under Task 1. More specifically, the following steps are reaching conclusion or have started being executed:

a. The measurement of through thickness residual stresses of the rest of the welded specimens are nearing completion (Step 1.5). In addition, a new 1 in. thick HY-130 specimen is in the process of being electron beam welded because the one welded in Step 1.2 has had some undercutting that made it unsuitable for residual stress measurements on the weld line. Upon completion of the welding operation measurements of residual stresses will take place. It is expected that the whole operation will be finished early in the spring of 1980.

b. Experiments on simple restrained butt welds (Step 1.6) are to be completed by the end of January. During these experiments measurements of temperatures and transient strains are being taken.

c. Upon receiving the appropriate plates from NSRDC, something that is expected to happen in early January, experiments will be carried out on restrained cracking test specimens (Step 1.9). All the necessary preliminary work for these experiments has already been completed (choice of geometry, welding parameters, locations of strain gages and thermocouples, etc.).

d. Regarding the analytical part that pertains to temperatures, transient strains, and residual stresses (Step 1.7), it is expected that the final version of the computer program under development will be available in mid-spring 1980. At the same time all the experiments conducted will have been analyzed.

e. Efforts will be made towards analyzing the restrained cracking test using the computer program referred to above and a new one based on the fracture mechanics theory (utilizing the finite element method).

AD-A079 920 MASSACHUSETTS INST OF TECH CAMBRIDGE DEPT OF OCEAN E--ETC F/G 13/5
STUDY OF RESIDUAL STRESSES AND DISTORTION IN STRUCTURAL WELDMEN--ETC(U)
NOV 79 V J PAPAZOGLOU, K MASUBUCHI N00014-75-C-0459
UNCLASSIFIED 82558 NL

2 OF 2
AD A
079920

END
DATE
FILMED
2 -- 80
DDC

4.2 Task 2 - Cylindrical Shell

The residual stresses in the cylindrical specimen welded during the second year and described in Section 3.3 will be measured as planned (Step 2.10). If necessary a second cylindrical shell specimen will be prepared and tested in the same manner.

The residual stresses measured will then be compared with predictions using computer programs. Although no final decision has yet been made on which program should be used, efforts will be undertaken to use the computer program that will have been developed under Task 1, making the required modifications for axisymmetric analysis.

5. PUBLICATIONS AND DEGREES GRANTED

5.1 Publications

Work based on Office of Naval Research sponsored research has resulted in the following publications during the previous two years:

- Masubuchi, K., "Analysis of Design and Fabrication of Welded Structures", Pergamon Press, 1980.
- Papazoglou, V.J., and Masubuchi, K., "Analysis and Control of Distortion in Welded Aluminum Structures", The Welding Journal, Vol. 57, 1978, pp. 251s-262s.
- Masubuchi, K., and Papazoglou, V.J., "Analysis and Control of Distortion in Welded Aluminum Structures", Transactions S.N.A.M.E., Vol. 86, 1978, pp. 77-100.

It is expected that several other publications will appear after the completion of the current research program.

5.2 Degrees Granted

The following degrees have been granted to students working on this project:[13]

Lipsey, M.D.: Ocean Engineer and Master of Science in Naval Architecture and Marine Engineering.

Coneybear, G.W.: Master of Science in Naval Architecture and Marine Engineering.

Mylonas, G.A.: Master of Science in Naval Architecture and Marine Engineering and Master of Science in Mechanical Engineering.

Rogalski, W.J.: Ocean Engineer and Master of Science in Naval Architecture and Marine Engineering.

Mabry, J.P.: Ocean Engineer and Master of Science in Naval Architecture and Marine Engineering.

---

[13] Note that most of these students were U.S. Navy Officers and so their services were furnished at no cost to the project.

5.3 Theses Completed

The following theses, containing information included in this technical progress report, have been completed:

1. Lipsey, M.D., "Investigation of Welding Thermal Strains in High Strength Quenched and Tempered Steel", Ocean Engineer Thesis, M.I.T., June 1978.

2. Coneybear, G.W., "Analysis of Thermal Stresses and Metal Movement During Welding", S.M. Thesis, M.I.T., May 1978.

3. Mylonas, G.A., "Experimental Investigation of Residual Stress Distributions in Thick Welded Plates", S.M. Thesis, M.I.T., July 1979.

4. Rogalski, W.J., "An Economic and Technical Study on the Feasibility of Using Advanced Joining Techniques in Constructing Critical Naval Marine Structures", Ocean Engineer Thesis, M.I.T., May 1979.

5. Mabry, J.P., "Prediction and Control of Residual Stresses and Distortion in HY-130 Thick Pipe Weldments", Ocean Engineer Thesis, M.I.T., May 1979.